INFORMATION TO USERS

This manuscript has been reproduced from the microfilm master. UMI films the text directly from the original or copy submitted. Thus, some thesis and dissertation copies are in typewriter face, while others may be from any type of computer printer.

The quality of this reproduction is dependent upon the quality of the copy submitted. Broken or indistinct print, colored or poor quality illustrations and photographs, print bleedthrough, substandard margins, and improper alignment can adversely affect reproduction.

In the unlikely event that the author did not send UMI a complete manuscript and there are missing pages, these will be noted. Also, if unauthorized copyright material had to be removed, a note will indicate the deletion.

Oversize materials (e.g., maps, drawings, charts) are reproduced by sectioning the original, beginning at the upper left-hand corner and continuing from left to right in equal sections with small overlaps. Each original is also photographed in one exposure and is included in reduced form at the back of the book.

Photographs included in the original manuscript have been reproduced xerographically in this copy. Higher quality 6" x 9" black and white photographic prints are available for any photographs or illustrations appearing in this copy for an additional charge. Contact UMI directly to order.

UMI

A Bell & Howell Information Company
300 North Zeeb Road, Ann Arbor MI 48106-1346 USA
313/761-4700 800/521-0600

Downloaded from SHAREOK. Persistent Handle URL: https://hdl.handle.net/11244/5741

UNIVERSITY OF OKLAHOMA

GRADUATE COLLEGE

DETERMINATION OF LEAKAGE FROM SUBSURFACE CONTAINMENT SYSTEMS USING INFORMATIONAL ENTROPY AND HYDRAULIC SIGNATURE ASSESSMENT METHODS

A Dissertation

SUBMITTED TO THE GRADUATE FACULTY

in partial fulfillment of the requirements for the

degree of

DOCTOR OF PHILOSOPHY

By

RANDALL R. ROSS

Norman, Oklahoma

1998

UMI Number: 9911874

UMI Microform 9911874
Copyright 1999, by UMI Company. All rights reserved.

This microform edition is protected against unauthorized
copying under Title 17, United States Code.

UMI
300 North Zeeb Road
Ann Arbor, MI 48103

© Copyright by Randall R. Ross 1998

All Rights Reserved

DETERMINATION OF LEAKAGE FROM SUBSURFACE CONTAINMENT SYSTEMS USING INFORMATIONAL ENTROPY AND HYDRAULIC SIGNATURE ASSESSMENT METHODS

A DISSERTATION APPROVED FOR THE SCHOOL OF
CIVIL ENGINEERING AND ENVIRONMENTAL SCIENCE

BY

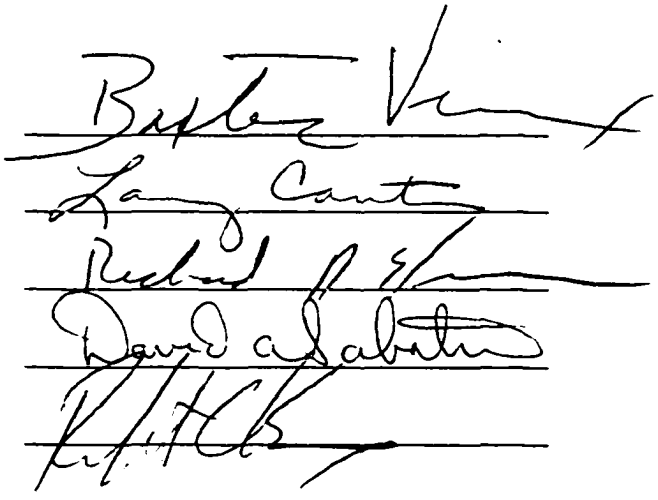

ACKNOWLEDGMENTS

I am grateful to my committee chairman, Dr. Baxter Vieux for his support, encouragement and patience during this endeavor. I would also like to thank the other committee members Dr. Larry Canter, Dr. Douglas Elmore, Dr. Robert Knox and Dr. David Sabatini for their time and insights.

Dr. Jack Keeley deserves special recognition for his guidance, encouragement and medicinal libations. I also wish to thank Dick Scalf for encouraging me to participate in the EPA's Office of Research and Development Long-term Training Program, as well as Clint Hall and Jerry Jones for allowing me to finish what I started a mere decade ago. Special thanks go to Dr. Milovan Beljin for his helpful insight, constructive comments, and especially for helping me keep things in perspective and reminding me that this too shall pass.

Most special thanks go to my father and mother, Richard and Lois Ross, to whom I am immeasurably indebted; without their love and compassion, none of this would have come to pass. To them I am grateful for instilling within me an understanding of the importance and worth of continued learning throughout life.

Finally, to my loving wife, Debra and our wonderful sons, Rylan and Hunter, I owe a special debt of gratitude for their unwaivering support and unconditional love.

You were there when the nights were long and the weekends were nothing more than extra work days. I know that I cannot make up for time that was lost, but I can make the best of the times to come. My precious family is a constant reminder of the infinite joys of life. I love you very much.

This dissertation is dedicated to my late grandmother, Esther Ross, who said "Randy, your education is the one thing that no one can ever take away from you."

TABLE OF CONTENTS

Page

ACKNOWLEDGMENTS iv

TABLE OF CONTENTS vi

LIST OF TABLES ix

LIST OF FIGURES x

ABSTRACT xiii

CHAPTER 1 DISSERTATION OVERVIEW 1

1.1 INTRODUCTION 1

1.2 DISSERTATION ORGANIZATION 2

CHAPTER 2 EVALUATION OF CONTAINMENT SYSTEMS USING HYDRAULIC HEAD DATA 5

2.1 ABSTRACT 5

2.2 INTRODUCTION 6

2.3 PERFORMANCE EVALUATION OF SUBSURFACE BARRIERS 7

2.4 METHODOLOGIES 8

2.5 DISCUSSIONS AND CONCLUSIONS 14

2.6 REFERENCES 16

CHAPTER 3 ESTIMATION OF MONITORING POINT DENSITY CONTAINMENT SYSTEM LEAK DETECTION 18

3.1 ABSTRACT 18

3.2 INTRODUCTION 19
3.2.1 Subsurface Containment Systems 20
3.2.2 Current Monitoring Practices 21
3.2.3 Alternative Approach to Leakage Assessment 27

3.3 METHODOLOGY 28
3.3.1 Conceptual Model 29
3.3.2 Mathematical Model 31
3.3.3 Model Setup 34
3.3.4 General Simulation Scenarios 36
3.3.5 Hydraulic Signature Assessment Method 39

3.4 RESULTS AND DISCUSSION 45

3.5 CONCLUSIONS 52

3.6 REFERENCES 55

CHAPTER 4 INFORMATIONAL ENTROPY AS A LEAK DETECTION INDEX IN THE PRESENCE OF NOISE AND TREND SURFACES 60

4.1 ABSTRACT 60

4.2 INTRODUCTION 61
4.2.1 Informational Entropy 63

4.3 METHODOLOGY 66
4.3.1 Ground Water Flow Modeling 66
4.3.2 Spatial Analysis 69
4.3.2.1 Random Noise and Trend Surfaces 70
4.3.2.2 Quantification of Noise and Trend Data 72
4.3.2.3 Sampling 73
4.3.3 Information Content and Entropy 76
4.3.3.1 Selection of Bin Width 79

4.4 RESULTS AND DISCUSSION 80
4.4.1 Simulated Containment System Leakage 84
4.4.2 Application of Noise and Trend Data To Simulation Results 85
4.4.3 Effects of Noise and Trend Data on Entropy 95

4.4.4 Discrimination of Different Magnitudes of Leakage Without Noise 97
4.4.5 Discrimination of Model Results and Noise of Similar Magnitude 97
4.4.6 Discrimination of Hydraulic Signatures with Varying Magnitudes of Noise 98
4.4.7 Signal to Noise Ratio 103
4.4.8 Entropy Threshold Number 109

4.5 CONCLUSIONS 121

4.6 REFERENCES 123

CHAPTER 5 SUMMARY, CONCLUSIONS AND RECOMMENDATIONS .. 129

5.1 SUMMARY AND CONCLUSIONS 129

5.2 RECOMMENDATIONS FOR FURTHER RESEARCH 133

CHAPTER 6 BIBLIOGRAPHY 135

LIST OF TABLES

Page

Table 3.1 Potential hypothesis testing errors 26

Table 3.2 General method for determining monitoring point grid spacing ... 42

Table 3.3 Simulated flux through windows of varying hydraulic conductivity 48

Table 3.4 Parameters and results obtained from hydraulic assessment method 53

Table 4.1 General outline of steps used in study 67

Table 4.2 Statistics for overlay images 71

Table 4.3 IDRISI modules 74

Table 4.4 Flux through high K window 87

Table 4.5 Total entropy (I_T) values for model results 96

Table 4.6 Total entropy values and root mean square error (RMSE) for model results with noise and trend surface added 102

Table 4.7 Signal to noise ratio for model and derived surfaces 107

Table 4.8 Entropy threshold Numbers 115

Table 4.9 Box ratio (r) numbers derived from N_{ET} values 117

LIST OF FIGURES

Page

Fig. 2.1 Flowchart of potential actions relating to hydraulic head relationships 10

Fig. 2.2 Possible hydraulic head relationships 12

Fig. 3.1 Conceptual model domain 35

Fig. 3.2 Hydraulic signature variations due to changes in conceptual hydrogeologic settings 43

Fig. 3.3 Nomograph relating ratio of semi-major axis of elliptical target and grid size to β for different target shapes using a square grid sampling pattern 44

Fig. 3.4 Nomograph relating radius of circular hydraulic signature to β probability of non-detection given different grid spacings 46

Fig. 3.5 Approximate boundaries of hydraulic signature defined by critical values and variations in the signature due to anisotropy ($K_{aq}=1\times10^{-2}$ cm/s, $K_{win}=1\times10^{-2}$ cm/s) 50

Fig. 3.6 Approximate boundaries of hydraulic signature defined by critical values and variations in the signature due to anisotropy ($K_{aq}=1\times10^{-2}$ cm/s, $K_{win}=1\times10^{-3}$ cm/s) 51

Fig. 4.1 Bin width vs. entropy 81

Fig. 4.2 Entropy diagram and histograms for model results ($K_{win}=1\times10^{-2}$ cm/s) 83

Fig. 4.3 Entropy diagrams and hydraulic head distribution for model results with variable K_{win} 86

Fig. 4.4 Entropy diagrams and hydraulic head distributions for model results ($K_{win}=1\times10^{-2}$ cm/s) with uniform random noise (0-0.05 m) and trend surface 88

Fig. 4.5 Entropy diagrams and hydraulic head distributions for model results (K_{win}=1×10^{-2} cm/s) with uniform random noise (0-0.1 m) and trend surface 90

Fig. 4.6 Entropy diagrams and hydraulic head distributions for model results (K_{win}=1×10^{-2} cm/s) with Gaussian random noise and trend surface 91

Fig. 4.7 Entropy diagram and hydraulic head distributions for model results (K_{win}=1E-2 cm/s, 1E-3 cm/s and 1E-4 cm/s) with uniform random noise (0-0.05 m) and trend surface 92

Fig. 4.8 Entropy diagram and hydraulic head distributions for model results (K_{win}=1×10^{-2} cm/s, 1×10^{-3} cm/s and 1×10^{-4} cm/s) with uniform random noise (0-0.1 m) and trend surface 93

Fig. 4.9 Entropy diagram and hydraulic head distributions for model results (K_{win}=1×10^{-2} cm/s, 1×10^{-3} cm/s and 1×10^{-4} cm/s) with Gaussian random noise and trend surface 94

Fig. 4.10 Entropy diagram for model results (K_{win}=1×10^{-2} cm/s) and Gaussian noise with similar RMS (RMSN=4.12×10^{-2}) 99

Fig. 4.11 Entropy diagram for model results (K_{win}=1×10^{-3} cm/s) and Gaussian noise with similar RMS (RMSN=9.2×10^{-3}) 100

Fig. 4.12 Entropy diagram for model results (K_{win}=1×10^{-4} cm/s) and Gaussian noise with similar RMS (RMSN=2.2×10^{-3}) 101

Fig. 4.13 Discriminator numbers versus RMSS for model results with noise and trend data 104

Fig. 4.14 Entropy versus RMS of hydraulic signature and noise 105

Fig. 4.15 Total entropy versus SNR 108

Fig. 4.16 Entropy diagram illustrating method for determining N_{ET} using intersection of (0.9×I_T) and upper entropy envelope 110

Fig. 4.17 Entropy diagram illustrating method for determining N_{ET} using intersection of (0.9×I_T) and maximum entropy line 111

Fig. 4.18 Entropy threshold numbers versus RMS for hydraulic signatures of model results and noise 113

Fig. 4.19 Entropy threshold numbers versus SNR for hydraulic signatures of model results and noise 114

Fig. 4.20 Hydraulic signatures of leakage through windows with hydraulic conductivities of K_{win}=1×10^{-2} cm/s, 1×10^{-3} cm/s, and 1×10^{-3} cm/s and applications of uniform random noise (0-0.05 m) and trend data 118

Fig. 4.21 Hydraulic signatures of leakage through windows with hydraulic conductivities of K_{win}=1×10^{-2} cm/s, 1×10^{-3} cm/s, and 1×10^{-3} cm/s and applications of uniform random noise (0-0.1 m) and trend data 119

Fig. 4.22 Hydraulic signatures of leakage through windows with hydraulic conductivities of K_{win}=1×10^{-2} cm/s, 1×10^{-3} cm/s, and 1×10^{-3} cm/s and applications of Gaussian noise and trend data 120

ABSTRACT

The use of physical and hydraulic containment systems for the isolation of contaminated ground water and aquifer materials associated with hazardous waste sites has increased during the last decade. The existing methodologies for monitoring and evaluating leakage from hazardous waste containment systems rely primarily on limited hydraulic head data. The number of hydraulic head monitoring points available at most sites employing physical containment systems may be insufficient to identify significant leakage from the systems. A general approach for evaluating the performance of containment systems, based on relative spatial and temporal hydraulic head distributions is used to introduce two methodologies for estimating the minimum number of monitoring points necessary to identify the hydraulic signature of leakage from a containment system. The first method is a probabilistic approach, based on the principles of geometric probability. Three-dimensional ground-water flow modeling results are used to illustrate the utility of the method. Leakage from a vertical barrier containment system is simulated using a variety of hydrogeologic conditions ranging from homogeneous to heterogeneous and isotropic to anisotropic. The second method utilizes informational entropy to quantify the spatial variability of hydraulic signatures associated with containment system leakage in the presence of background noise and trend surfaces.

CHAPTER 1

DISSERTATION OVERVIEW

1.1 INTRODUCTION

Physical containment systems are being used as components of ground-water remedies at a growing number of hazardous waste sites. Their primary purpose is to prevent or reduce the impact of contaminant sources on ground-water, thereby reducing the risks to human health and the environment from exposure to hazardous compounds. Unfortunately, all containment systems leak to some extent. Advective leakage may occur over, under or through a barrier. Contaminated ground water may also leak through the underlying strata into which the vertical barrier is supposedly keyed. Diffusion may serve as another mechanism for the release of contaminants into the environment. This dissertation focuses primarily on identifying leakage through discrete zones of high hydraulic conductivity (windows), in otherwise low hydraulic conductivity vertical barriers. The range of leakage rates varies from negligible to significant. The severity of a leak with respect to potential impacts on human health and the environment is dependent not only on the rate of leakage, but also on the concentration of contaminants being introduced into the environment.

There are currently no uniform methods to reliably measure and document the hydrologic performance of existing and proposed hazardous waste containment systems. The overall integrity of a containment system can be evaluated based on estimating the rate of leakage using well hydrographs from inside and outside the system and appropriate assumptions (e.g., dimensions of the containment system and average porosity, etc.). If the observed leakage rate greatly exceeds the predicted leakage rate based on design criteria, it may be desirable to further evaluate potential avenues of leakage. This dissertation presents several methods for evaluating containment system leakage using existing or proposed monitoring systems by 1) identifying whether the systems are functioning as designed with respect to leakage rates, 2) determining the probability of detecting the hydraulic signature of a leak from a containment system, given specified constraints, and 3) discriminating hydraulic signatures of leaks from different background noises using informational entropy.

1.2 DISSERTATION ORGANIZATION

This dissertation discusses research results of into methods for evaluating the leakage from subsurface vertical barrier containment systems is discussed in this dissertation. Three of the chapters are a series of papers that have either been published or will be submitted for publication. The format follows the requirements of the journals to which the papers are submitted. However, the headings, subheadings, tables and figures have been numbered to be congruous with the context of the dissertation.

Chapter 2 presents an introduction to the potential problems related to evaluating the performance of hazardous waste containment systems. The chapter presents a general method for determining if a containment system is leaking, and if so, whether the leakage exceeds the rate deemed permissible under the constraints of the design criteria.

Chapter 3 presents the results of a three-dimensional ground-water flow model of a leaking subsurface vertical barrier and discusses a method for identifying the hydraulic signature associated with the simulated leakage. The methodology is used to determine the minimum number of monitoring points necessary to identify the hydraulic mound created under different hydrogeologic conditions ranging from homogeneous to heterogeneous, and isotropic to anisotropic settings, given specific constraints. The methodology is a variant of an approach used to determine the number of sampling points required to locate a localized area of high contaminant concentrations or hot spot.

Chapter 4 focuses on the application of entropy or information content to quantify the spatial variability of model-predicted hydraulic head distributions (as described in Chapter 3). A methodology is presented that allows estimation of the number of monitoring or sampling points necessary to discriminate the hydraulic signatures of different magnitudes of leakage from a containment system from those of random noise and trend surfaces. Chapter 5 summarizes the significant findings of the research and presents recommendations for additional research. Chapter 6 is a bibliography of all citations in this dissertation.

The research presented in this dissertation provides two independent methods for evaluating the adequacy of existing and proposed monitoring strategies for identifying discrete leakage from hazardous waste containment systems. The overall objective of this research is to advance the fundamental and applied understanding of the detection of leakage from subsurface vertical barrier containment systems using relatively low cost hydraulic head data. The concepts presented may also be applicable to a better understanding of the hydraulic signature associated with interaquifer leakage via improperly abandoned wells.

As of December 2, 1998 Chapter 2 has been published as:

Ross, R.R. and M.S. Beljin (1998). "Evaluation of Containment Systems Using Hydraulic Head Data". J. Envir. Engin., 124(6):575-578.

Chapters 3 and 4 have been submitted to the Journal of Environmental Geology and the Journal of Mathematical Geology, respectively, for review and consideration.

CHAPTER 2

EVALUATION OF CONTAINMENT SYSTEMS USING HYDRAULIC HEAD DATA

2.1 ABSTRACT

Subsurface vertical barriers have been used as components of containment systems to prevent or reduce the impact of contaminant sources on ground-water resources. A better understanding of the hydraulic head distribution associated with vertical barriers can enhance the ability of existing performance monitoring systems to detect breaches in physical containment systems and may aid in the design of new performance monitoring systems. Given the current regulatory interest in containment systems as either supplemental or stand-alone remedial alternatives, and the lack of adequate performance monitoring strategies at most existing hazardous waste sites utilizing vertical barrier technologies, there is an immediate need for general guidelines for determining whether a containment system is functioning as intended. This chapter describes an approach for evaluating the performance of containment systems, based on relative spatial and temporal hydraulic head distributions.

2.2 INTRODUCTION

Subsurface vertical barriers have been used to control ground-water seepage in the construction industry for many years. More recently, such barriers have been incorporated as components of containment systems to prevent or reduce the impact of contaminant sources on ground-water resources. Canter and Knox (1986) classify containment systems as active (e.g., ground-water extraction to control hydraulic gradient) or passive (e.g., physical barriers only). Frequently, containment systems employ a combination of active and passive components, depending on the remedial objectives and complexity of the hydrogeologic setting. Such systems commonly incorporate low permeability vertical barriers (walls) keyed into an underlying low permeability aquitard (floor), a low permeability cover (cap) to prevent the infiltration of precipitation, extraction wells, and a monitoring network.

Soil-bentonite slurry trench cutoff walls (slurry walls) are the most common types of vertical barriers used at hazardous waste sites (Rumer and Ryan, eds., 1995). Potential failure mechanisms of vertical barriers can be classified as design errors, construction defects, and post-construction property changes. Proper design will reduce the potential for errors associated with wall configuration (e.g., depth and thickness), materials incompatibility and other factors leading to system failure (Evans, 1991). Construction defects generally form high hydraulic conductivity "windows" in a low hydraulic

conductivity slurry wall. These windows may result from several mechanisms including (U.S.EPA, 1987):

- Emplacement of improperly mixed backfill materials
- Sloughing/spalling of *in situ* soils from sides of trench; and
- Failure to excavate all *in situ* material when keying a wall to the underlying low permeability unit.

Post-construction property changes may result from wet-dry cycles due to water table fluctuations, freeze-thaw degradation or chemical incompatibility between the slurry wall components and NAPLs (Evans, 1991).

2.3 PERFORMANCE EVALUATION OF SUBSURFACE BARRIERS

Recently, much attention has been focused on the use of containment technologies as supplemental and stand-alone remedial options for hazardous waste sites by the industrial and regulatory communities (Rumer and Ryan, eds., 1995). The U.S. EPA recently sponsored a project to evaluate the adequacy of performance monitoring systems associated with selected hazardous waste sites (Mills, 1996).

The performance of hazardous waste containment systems has generally been evaluated on the basis of construction specifications. Specifically, most systems are required to maintain hydraulic conductivity of a vertical barrier below a specified value, typically less than 1×10^{-7} cm/s. During construction, the use of appropriate field quality assurance (QA) and quality control (QC) testing is essential to ensure that the design performance

specifications are satisfied. Despite rigorous field QA/QC procedures, the unintentional formation of preferential pathways within a vertical barrier is still possible. Consequently, the regulatory community identified the need to develop procedures to verify post-construction performance and identify unsatisfactory zones in containment systems (U.S. EPA, 1987). Whereas the success of a construction dewatering vertical barrier system may be judged by the ability of the barrier to limit ground-water leakage to quantities that can reasonably be extracted, there are no uniform methods to reliably measure and document the hydrologic performance of existing and proposed hazardous waste containment systems (Grube, 1992).

2.4 METHODOLOGY

To determine whether a containment system is protective of human health and the environment, leakage from the system into the environment must be evaluated. Several geophysical techniques have been identified as potentially applicable for the indirect detection of defects associated with vertical barriers. These techniques include ground penetrating radar, electrical resistivity and continuous-wave microwave technologies. Ground penetrating radar is capable of providing continuous spatial measurements of the elevation of the water table in granular soils (Shih and others, 1986). This may allow the identification of abrupt changes in the water table surface which may be indicative of gross failures of a vertical barrier. Electrical resistivity and continuous-wave microwave technologies may be used to identify similar water table anomalies (Koerner and Lord,

1985). Unfortunately, the resolution necessary to identify small scale, yet potentially significant breaches in a containment system may be beyond the ability of much of the instrumentation currently available. Additionally, the high costs of data acquisition and difficulties associated with data interpretation are among some of the problems which plague many of the high-tech geophysical techniques.

Hydrogeological techniques may be used to determine whether leakage is occurring, and if so, estimate the rate of loss from the system (Day, 1995). If it is determined that a significant volume of ground water is exiting the system, the location and magnitude of the leak(s) must be established to ascertain whether major repair efforts are necessary to maintain a protective remedy. The hydraulic signature associated with a containment system leak is dependent on the magnitude of the difference in hydraulic head across the barrier wall, the areal extent of the leakage, and the hydraulic conductivities of the vertical barrier, window and surrounding aquifer materials (Bodocsi and others, 1990). Although spatial variations in water levels have been used to identify gross construction defects in ground-water containment systems, no specific protocols/methodologies have been developed to evaluate whether or not ground-water containment systems are operating as designed.

The water level elevation within a containment system may be higher, lower, or approximately equal to that in the adjacent aquifer. By analyzing the relationship of the hydraulic head distribution inside and outside the containment system (Fig. 2.1a and 2.1b),

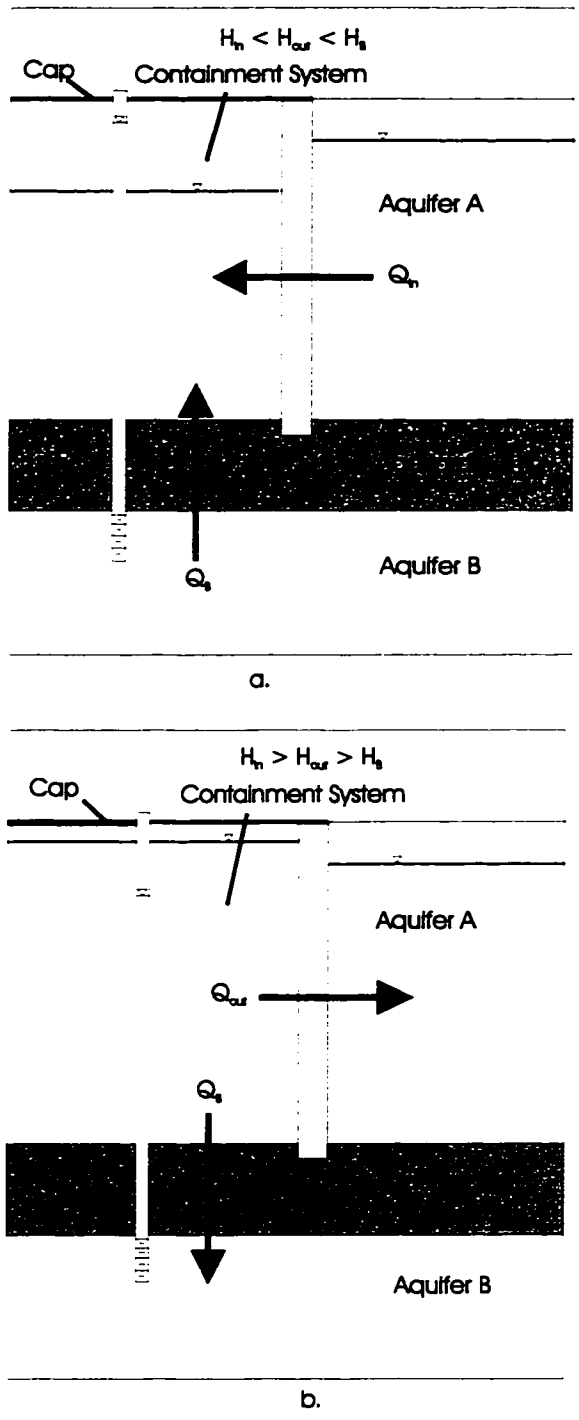

H_{in} = Hydraulic Head Inside Containment System
H_{out} = Hydraulic Head Outside Containment System
H_s = Hydraulic Head In Underlying Aquifer B
Q_{in} = Leakage Into Containment System
Q_{out} = Leakage Out of Containment System
Q_s = Leakage Through Aquitard

Fig. 2.1 Hydraulic heads associated with a containment system.

it is possible to assess whether or not the system is operating as designed and which potential transport mechanisms are most significant and require further evaluation.

Under ideal conditions, the hydraulic head will be lower inside a containment system relative to that outside the system, within the same and underlying aquifers (Fig. 2.1a). This will ensure that any advective transport through the vertical barrier is inward, rather than outward into the environment. Under such conditions, diffusion may be the dominant transport mechanism of dissolved contaminants from the system (Mott and Weber, 1991). Relatively small differences in hydraulic heads, inside and outside a containment system indicate the lack of significant active hydraulic forces for advective transport of contaminants. However, due to the concentration gradient across the barrier, diffusive flux from the system is still possible. Containment systems characterized by higher hydraulic heads inside the confines of a vertical barrier system are susceptible to diffusive and advective losses (Fig. 2.1b).

While the hydraulic heads inside and outside a containment system have been used to identify gross system failures (Day, 1995), little attention has been given to monitoring the changes in hydraulic heads with time. Temporal water level fluctuations should be evaluated in conjunction with spatial head variations to assess whether or not containment is effective. A general flow-chart for evaluating the effectiveness of a vertical barrier containment system is offered by Fig. 2.2. Significant fluctuations of water levels within a fully encapsulating passive containment system indicate the failure of one or more of its

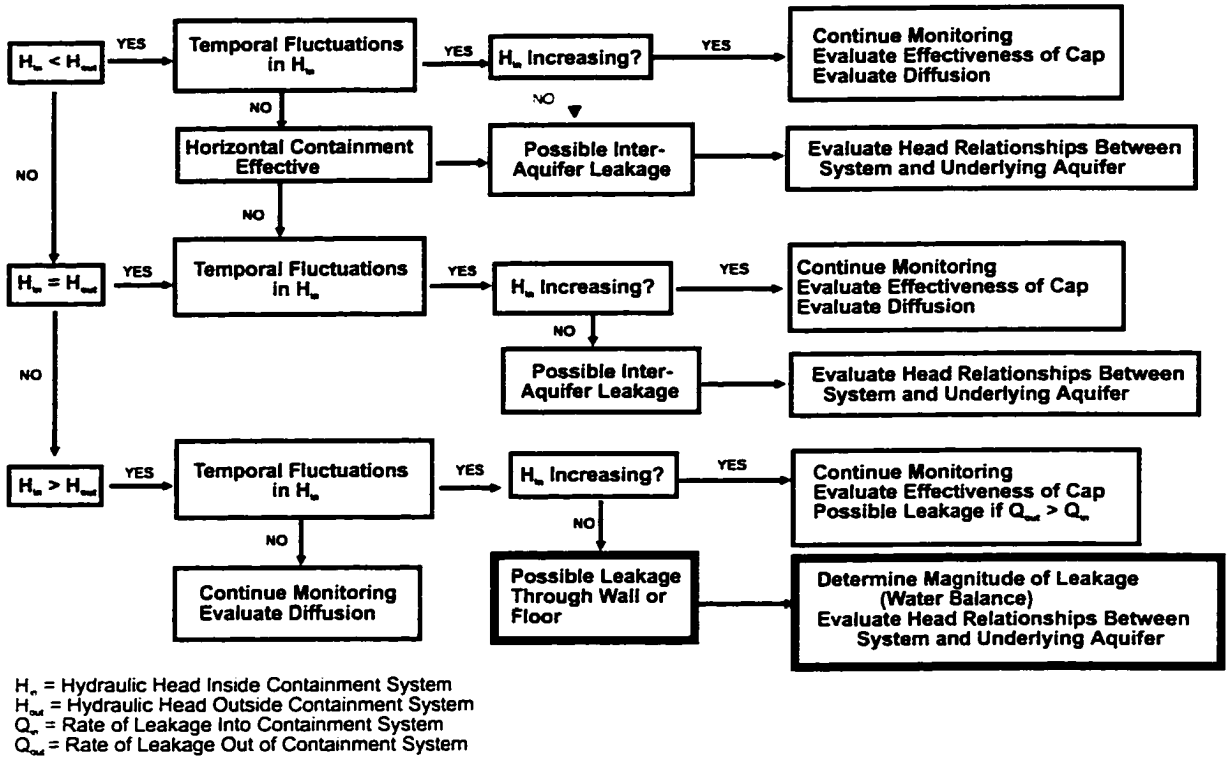

Fig. 2.2 Flow chart illustrating potential actions necessary to evaluate the performance of a containment system, based on relative spatial and temporal hydraulic head relationships.

components (e.g., cap, floor or walls). Under ideal conditions, the water level inside the system will be stable, whereas water levels outside the system may fluctuate significantly in response to hydraulic stresses such as precipitation events, surface water fluctuations and local ground-water extraction. A rise in water levels in response to precipitation events may indicate leakage through the cap, floor, or walls. Declining water levels in systems with hydraulic heads greater than or equal to exterior water levels may indicate leakage through the floor or walls, requiring an evaluation of hydraulic head distributions of an underlying water-bearing unit with respect to heads in the containment system, or evaluation of the wall integrity. The volume and rate of leakage from such a system may be estimated with minimal monitoring data. However, determining the location of specific breaches may require significantly more information.

Analysis of sufficiently detailed piezometric head data may allow the identification of subtle changes in the hydraulic head distribution, thereby indicating the general locations of potential leaks in a vertical barrier. Until recently, such an undertaking would be prohibitively expensive due to the high cost of installing the large number of monitoring wells necessary to adequately define the hydraulic head distribution around a barrier wall. However, with the development of several relatively inexpensive small diameter piezometer installation technologies (e.g., Pro-Terra VibraDrill®, GeoProbe®,etc.) it may now be possible to install sufficient numbers of small diameter monitoring points to identify the hydraulic signatures associated with containment system leaks. Similarly, information

obtained from cone penetrometer surveys may be useful for identifying similar hydraulic signatures.

2.5 DISCUSSION AND CONCLUSIONS

Analysis of hydraulic head relationships between a containment system and adjacent and/or underlying aquifers can indicate whether or not the potential exists for advective losses of contaminants from the system. Figures. 2.1a and 2.1b represent the most and least desirable end members, respectively, of a continuum of possible relationships between the hydraulic head inside and outside a containment system. Ideally, the hydraulic gradient across system boundaries will be inward (Fig. 2.1a). However, regardless of the hydraulic head relationships, as long as a concentration gradient exists across the slurry wall, it may still be possible for contaminants to exit the confines of the system by the process of diffusion.

Analysis of spatial and temporal hydraulic head fluctuations (Fig. 2.2) can indicate whether or not problems exist with integral components of a containment system. Rapid fluctuations which correlate positively with precipitation events may indicate failure of one or more components of the system. Rising water levels inside a containment system with higher hydraulic heads relative to the adjacent or underlying aquifer, suggest failure of the cap to prevent the infiltration of precipitation. Such a system may still discharge

contaminated ground water to the environment if the rate of leakage out of the system is less than the rate of leakage into the system.

It may be possible to identify the general location of suspected leaks indicated by spatial and temporal water level fluctuations using existing monitoring systems. However, the hydraulic signature associated with a containment system leak is a function of the hydraulic gradient across the barrier, the areal extent of the leak, and the hydraulic conductivities of the vertical barrier, window, and surrounding aquifer materials. Therefore, the identification of specific leak locations and discharge rates may require an additional three-dimensional hydraulic characterization and the installation of additional piezometer clusters.

Additional research will provide a better understanding of the complex hydraulics associated with leaky containment systems. Such insight could be used to enhance existing performance monitoring systems and aid in the design of new monitoring systems, and allow estimation of monitoring point spacing requirements (vertically and horizontally) necessary to detect containment system breaches. Given the current interest in containment systems, as either supplemental or stand-alone remedial alternatives, and the lack of adequate performance monitoring strategies at most existing hazardous waste sites utilizing containment technologies, there is an immediate need for a general protocol to determine whether or not a containment system is operating as designed.

2.6 REFERENCES

Bodocsi, A., McCandless, R.M., and Ling, K.W. (1990). "Detection of Macro Defects in Soil-Bentonite Cutoff Walls," *Remedial Action, Treatment and Disposal of Hazardous Waste, Proceedings of the Fifteenth Annual Research Symposium*, Cincinnati, OH, April 10-12, 1989. EPA/600/9-90/006.

Canter, L.W. and Knox, R.C. (1986). *Ground Water Pollution Control*, Lewis Publishers, Boca Raton, FL.

Day, S.R. (1995). personal communication.

Evans, J.C. (1991). "Geotechnics of Hazardous Waste Control Systems," Chapter 20, *Foundation Engineering Handbook*, 2nd ed., H.Y. Fang, ed., Van Nostrad-Reinhold Company, New York.

Grube, W.E., Jr. (1992). "Slurry Trench Cut-Off Walls for Environmental Pollution Control," *Slurry Walls: Design, Construction and Quality Control*. ASTM STP 1129, David B. Paul, Richard R. Davidson, and Nicholas J. Cavalli, Eds., American Society for Testing and Materials, Philadelphia.

Koerner, R.M. and Lord, A.E. (1985). "Microwave System for Locating Faults in Hazardous Material Dikes," U.S. Environmental Protection Agency, Hazardous Waste Engineering Research Laboratory, Cincinnati, OH, EPA/600/2-85/014.

Mills, A. (1996). personal communication.

Mott, H.V., and Weber, W.J., Jr. (1991). "Diffusion of organic contaminants through soil-bentonite cut-off barriers," *Res. J. Water Pollut. Control Fed.*, Vol. 63, pp. 166-176.

Rumer, R.R. and Ryan, M.E., eds. (1995). *Barrier Containment Technologies For Environmental Remediation Applications*, John Wiley & Sons, Inc., New York.

Shih, S.R., Doolittle, J.A., Myhre, D.L. and Schellentrager, G.W. (1986). "Using Radar for Groundwater Investigation," *Journal of Irrigation and Drainage Engineering*, Vol.112, No.2, pp. 110-118, May, 1986.

U.S. EPA (1987). "Construction Quality Control and Post-Construction Performance Verification for the Gilson Road Hazardous Waste Site Cutoff Wall," Hazardous Waste Engineering Research Laboratory, Office of Research and Development, Cincinnati, OH, EPA/600/2-87/065.

CHAPTER 3

ESTIMATION OF MONITORING POINT DENSITY FOR CONTAINMENT SYSTEM LEAK DETECTION

3.1 ABSTRACT

The use of physical and hydraulic containment systems for the isolation of contaminated ground water and aquifer materials associated with hazardous waste sites has increased during the last decade. The existing methodologies for monitoring and evaluating leakage from hazardous waste containment systems rely primarily on limited hydraulic head data. The number of hydraulic head monitoring points available at most sites employing physical containment systems may be insufficient to identify significant leakage from the systems. A general approach for evaluating the performance of containment systems, based on estimations of apparent leakage rates, is used to introduce a methodology for determining the minimum number of monitoring points necessary to identify the hydraulic signature of leakage from a containment system. The probabilistic method is based on the principles of geometric probability. The method is demonstrated using three-dimensional ground-water flow modeling results of leakage from a vertical barrier containment system under a variety of hydrogeologic conditions.

3.2 INTRODUCTION

Recently, much attention has focused on the use of containment technologies as supplemental or stand-alone remedial alternatives for hazardous waste sites by the industrial and regulatory communities. Subsurface vertical barriers have been used to control ground-water seepage in the construction industry for many years (D'Appolonia, 1980). More recently, such barriers have been employed as components of hazardous waste containment systems to prevent or reduce the impact of contaminants on ground-water resources (Rumer and Ryan, 1995). While subsurface vertical barriers appear to be useful for isolating long-term sources of ground-water contamination at many sites, the potential exists for leakage of contaminants through high hydraulic conductivity zones or windows. Such windows may form during construction or result from post-construction changes in barrier properties (Evans, 1991). Consequently, there is concern that the performance of numerous hazardous waste containment systems has not been adequately evaluated or demonstrated.

This paper describes a general approach for evaluating the required number of monitoring points necessary to identify leakage through discrete zones of high hydraulic conductivity within a subsurface vertical barrier. Hydraulic head distributions are generated by a numerical ground-water flow model simulating leakage through a subsurface vertical barrier under a range of conceptual conditions. The model data are used to illustrate the utility of the proposed method. The resulting techniques will be useful for evaluating existing containment systems by providing insight as to how many monitoring points are

necessary to determine the approximate locations of discrete leaks, given specified confidence and constraints.

3.2.1 Subsurface Containment Systems

Depending on the remedial objectives and complexity of the hydrogeologic setting, subsurface containment systems may be active (e.g., ground-water extraction to manage hydraulic gradient), or passive (e.g., physical barriers) (Canter and Knox, 1986). Frequently, containment systems employ a combination of active and passive components, which commonly incorporate low permeability vertical barriers (walls) keyed into underlying low permeability units. Many containment systems also include a low permeability cover to prevent or reduce the infiltration of precipitation, extraction and/or injection wells and/or trenches for ground-water management and a monitoring network.

Soil-bentonite slurry trench cutoff walls (slurry walls) are the most common type of subsurface vertical barriers used at hazardous waste sites and are generally installed circumferentially around the suspected source areas within a site (U.S. EPA, 1984). Slurry walls are typically constructed in a two-step process consisting of trench excavation and backfilling with appropriate materials. During excavation, a bentonite slurry is used to maintain trench stability and form a low permeability filter cake on the sides of the excavation. The excavated materials are appropriately amended and replaced in the trench (D'Appolonia, 1980). Cement-bentonite slurry cutoff walls have been widely used in Europe

and are gaining wider acceptance in the United States. Other types of vertical barriers include plastic cement cutoff walls, vibrating beam cutoff walls, deep soil mixing walls, composite cutoff walls, steel sheet pile walls and grout barriers (Rumer and Ryan, 1995).

Construction defects or post-construction property changes are potential failure mechanisms of subsurface vertical barriers (Evans, 1991). Construction defects may result in the formation of high hydraulic conductivity "windows" in a low hydraulic conductivity barrier. Some of the mechanisms responsible for the formation of such windows include emplacement of improperly mixed backfill materials, sloughing or spalling of *in situ* soils from sides of trench, and failure to excavate all *in situ* material when keying wall to the underlying low permeability unit (U.S. EPA, 1987). Post-construction property changes may result from wet-dry cycles due to water table fluctuations, freeze-thaw degradation or chemical incompatibility between the slurry wall components and nonaqueous phase liquids (Evans, 1991).

3.2.2 Current Monitoring Practices

The performance of hazardous waste containment systems has generally been evaluated based on construction specifications. Most subsurface vertical barriers are required to maintain a hydraulic conductivity of $1x10^{-7}$ cm/s, or less. The use of appropriate construction quality assurance (CQA) and quality control (CQC) testing during installation is essential to ensure that the design performance specifications are achieved (U.S. EPA,

1987) . However, preferential pathways may develop in spite of rigorous field CQA and CQC procedures.

The regulatory community recognized the need to develop procedures to verify post-construction performance and identify unsatisfactory zones in containment systems (U.S. EPA, 1987). While construction dewatering systems are deemed successful if the barriers limit ground-water leakage to reasonably extracted quantities, there are no uniform methods to reliably measure and document the hydrologic performance of existing and proposed hazardous waste containment systems (Grube, 1992).

The minimum number of monitoring points necessary to determine whether a containment system is functioning as designed may be relatively small (Ross and Beljin, 1998). For example, in some cases it may be possible to determine if leakage is occurring by analyzing the water level trends of two monitoring wells - one located within the confines of the system and one located outside the system. It may also be possible to estimate the volume and rate of leakage based on water level trend data. The approximate volume of leakage (V_L) into or out of a containment system may be estimated by

$$V_L = \Delta h \, A_{cs} \, S_y \qquad (1)$$

where Δh is the average change in hydraulic head within the containment system determined from well hydrographs, A_{cs} is the total area of the containment system and S_y is the specific yield of the aquifer within the confines of the system.

The average rate of leakage (Q_L)from the system may be calculated by dividing the volume of leakage (V_L) by the amount of time (t) over which the change in hydraulic head occurred, or

$$Q_L = V_L/t \qquad (2)$$

The average rate of leakage from the containment system may be compared to the design leakage rate (Q_{DL}), calculated by

$$Q_{DL} = K_w A_w i_w + K_f A_f i_f + Q_i \qquad (3)$$

where K_w and K_f are the assumed design hydraulic conductivity values for the vertical containment barrier and floor of the system, respectively; A_w and A_f are the approximate surface areas of the vertical barrier walls and floor, respectively; i_w and i_f are the hydraulic gradients across the vertical barrier and floor, respectively, and Q_i is the infiltration rate through the cap.

Apparent leakage rates that are greater than design criteria ($Q_L >> Q_{DL}$) indicate leakage from the containment system. Significant leakage from the containment system may require an assessment of the potential risks to human health and the environment posed by

the leakage. While estimating the rates of leakage from a system may be relatively straightforward, determining the locations of specific leaks will require significantly more information.

The risks associated with leakage from a containment system must be evaluated with respect to human health and the environment. Inyang and Tumay (1995) relate the risks to human health from exposure to ground-water contaminants in terms of the probability of a toxic response (P(r)) of an individual to a hazardous contaminant by

$$P(r) = 1 - \exp\left[-B\int_0^t C(t)dt\right] \tag{4}$$

where B is a constant, dependent on human physiology and contaminant toxicity, and C(t) is the individual contaminant exposure concentration as a function of time.

The risk associated with leakage from a containment system may also be related to a hypotheses test in which the null hypothesis (H_o) states that no detectable leakage is occurring from the containment system. Conversely, the alternate hypothesis (H_1) states that the containment system has detectable leakage. There are two ways of making an incorrect decision with respect to the stated hypotheses (Conover, 1980). First, if the null hypothesis is true (i.e., no detectable leakage) and is mistakenly rejected, a type I error occurs (Table

3.1). The risks associated with such an error are minimal, since no discharge of contaminants to the environment occurs. However, if the null hypothesis is false (e.g., the system leaks) and is mistakenly accepted, a type II error occurs. The probability of making a type II error is defined as β, and is referred to by Gilbert (1987) as the consumer's risk. A consumer's risk of β=0.1 indicates that there is 10 percent probability of not detecting a leak when one is present.

The potential health risks associated with a type II error will depend on the mass flux of contaminants out of the system. Contaminant mass flux is a function of contaminant concentration and ground-water discharge rates from the system. A significant leak with a high discharge rate but low concentrations may pose a less significant health hazard than a small leak of highly contaminated ground water.

Subtle variations in the hydraulic head distribution associated with leakage through a subsurface barrier may be identifiable if sufficient hydraulic head data are available for analysis. Such an undertaking would generally be considered prohibitively expensive due to the high cost of installing a piezometer network capable of adequately defining the hydraulic head distribution. However, the recent development of relatively inexpensive installation techniques may make it feasible to install a sufficient number of small diameter piezometers to identify the hydraulic signatures associated with significant containment system leakage.

Table 3.1. Potential hypothesis testing errors (After Conover, 1980).

	Accept H_o	Reject H_o
H_o is True	Correct Decision Probability=1-α	**Type I Error** Probability=α (level of significance)
H_o is False	**Type II Error** Probability=β	Correct Decision Probability=1-β

3.2.3 Alternative Approach to Leakage Assessment

The process of locating a leak in a hazardous waste containment system can be analogous to mineralogical prospecting where a compromise is sought between the cost of exploration and the thoroughness of the search. For mineral exploration applications, the expected benefit of a search is the sum of the value of each target multiplied by the probability of finding it, assuming that the target exists in the search area (Singer, 1972). For containment system leak detection, the expected benefit of a search is the potential reduction in risks to human health and the environment associated with the detection and abatement of significant leaks. An increase in the number of monitoring points will result in increased costs, but may also result in the reduction in risks associated with potential hazardous waste discharge to the environment if leakage is occurring through a barrier.

Gilbert (1987) presents a methodology that can be used to (1) determine the grid spacing required to detect highly contaminated local areas or hot spots at a given level of confidence, or (2) estimate the probability of finding a hot spot of specified dimensions, given a specified grid spacing. The methodology is based on the work of Singer (1972), Singer and Wickman (1969) and Savinskii (1965), who developed statistical tables to calculate the probability of success in locating circular and elliptical targets using grid configurations. The probability of detecting a target using a specific grid spacing is determined by the method of geometric probability, which is a function of the ratio of the area of the target to the area of one cell of the grid.

Gilbert's (1987) method utilizes the following assumptions: (1) the highly contaminated areas are circular or elliptical in shape; (2) the boundaries of the hot spot are clearly identifiable based on contamination levels; (3) hot spot orientation is random with respect to the sampling grid; and (4) the distance between grid points is much larger than the area sampled.

The methodology presented below is based on the work of Singer and Wickman (1969) and Gilbert (1987). The assumptions have been modified to address variations in the distribution of hydraulic head, rather than contaminant concentrations. The assumptions and specific details relating to the applications of the proposed method for hydraulic signature detection are discussed after the modeling section. The methodology section is followed by a discussion of the results of the application of the proposed method to the model data.

3.3 METHODOLOGY

A model may be defined as a simplified version of a real system that approximates the stimulus-response relationships of that system. By definition, the use of a model requires the application of simplifying assumptions to describe the pertinent features, conditions, and significant processes that control how the system reacts to stimuli. One of the primary objectives of the modeling portion of this study is to predict the hydraulic head distribution associated with leakage through discrete portions of a vertical barrier under different hydrogeologic conditions.

The hydraulic signature associated with leakage from a containment system is simulated for a variety of hydrogeological settings. The modeling results provide the data on which the new method is demonstrated. The proposed method is evaluated under conditions ranging from relatively simple homogeneous, isotropic conditions to more complex heterogeneous, anisotropic conditions.

3.3.1 Conceptual Model

The first step in developing a model involves the formulation of a conceptual model consisting of a set of assumptions that describes the characteristics and components of the system, and the relevant mechanisms and processes that affect the behavior of the system. These assumptions include the geometry, properties, and nature of the boundaries of the system. The next step is to express the conceptual model in the form of a mathematical model. Once a mathematical model has been constructed, a method of solution may be employed, using either analytical or numerical methods (Bear et al., 1992). The solution of the mathematical model yields a predicted response of the system to the stated stimuli. The method of solution used in this study is the numerical model.

The conceptual model presented in this paper is based on characteristics of several specific hazardous waste sites which incorporate physical containment as a major component of the selected remedy. The specific sites which influenced the development of the model used in this study include the Gilson Road Superfund site (Nashua, New Hampshire), the

G.E. Superfund site (Moreau, New York), and the Velsicol/Michigan Chemical Company Superfund site (St. Louis, Michigan). The simulation results are used as input for the hydraulic signature assessment methodology. The conceptual model for the containment system consists of a soil-bentonite slurry wall fully penetrating an unconsolidated surficial aquifer, keyed in to an underlying, low permeability aquitard. The hypothetical aquifer is discretized into 25 one-meter thick layers. It is assumed that no recharge is added to the upper surface of the aquifer due to the presence of a low permeability cap over the containment system.

Hydraulic head values are assumed to be higher in the interior of the containment system, simulating a "worst-case" scenario for potential contaminant losses from the system. The elevated water levels in the containment system are derived from deficiencies in the upgradient portion of the system (i.e., leakage under or through the upgradient wall) and water levels are assumed to be relatively stable over time. Ground-water flow is assumed to be horizontal, except in the immediate vicinity of the vertical barrier. Given the long-term nature of most hazardous waste containment systems, the hydraulic heads are averaged over long time periods. Consequently, steady-state flow conditions are assumed for all simulations used in this study.

Three routes of containment system leakage have been reported, including flow through the vertical barrier (e.g., high hydraulic conductivity window), flow between the cap and wall, and flow under the wall. Flow through the barrier may occur via high hydraulic

conductivity windows formed by the entrapment of sloughed aquifer material from the trench walls. In many containment systems, the seal between the cap and barrier is constructed by overlaying the wall with a low permeability cap. Such designs are not intended to prevent the flow of ground water and contaminants beyond the confines of the containment system, but rather to divert surface runoff away from the containment system. Flow between the cap and vertical barrier is possible if the water level within the containment system rises above the interface between the cap and barrier. Flow between the barrier and the underlying low permeability unit may result from incomplete removal of higher hydraulic conductivity aquifer material during trench excavation, thereby failing to create an adequate key between the barrier wall and the underlying aquitard (Evans, 1991). For the purposes of this study, the primary focus is on leakage through high hydraulic conductivity windows within the wall.

Scenario variations evaluated through sensitivity analyses include the location, dimensions and hydraulic conductivity of the window; the ratio of the hydraulic conductivity of the window and wall (K_{win}:K_{wall}); the ratio hydraulic conductivity of the aquifer and wall (K_{aq}:K_{wall}); and the magnitude of the hydraulic gradient across the wall.

3.3.2 Mathematical Model

Mathematical models generally consist of a set(s) of differential equations known to govern ground-water flow through porous media, and definitions of the initial and boundary

conditions that describe the state of a system and the interactions of the system with its surrounding environment (Bear et al., 1992). The equation governing ground-water flow through porous media under steady-state conditions results from a component by component substitution of Darcy's law into the continuity equation, resulting in:

$$\frac{\partial}{\partial x}\left(K_x \frac{\partial}{\partial x}\right) + \frac{\partial}{\partial y}\left(K_y \frac{\partial}{\partial y}\right) + \frac{\partial}{\partial z}\left(K_z \frac{\partial}{\partial z}\right) = 0 \qquad (5)$$

If the system in question is assumed to be homogeneous and isotropic, where $K_x=K_y=K_z$, the equation may be rewritten as Laplace's equation:

$$\frac{\partial^2 h}{\partial x^2}+\frac{\partial^2 h}{\partial y^2}+\frac{\partial^2 h}{\partial z^2}=0 \qquad (6)$$

The above equations, in combination with specified initial and boundary conditions, constitute a mathematical model for the flow of ground water through the porous media.

The boundary conditions assumed for the conceptual model include constant head boundaries for the upgradient and downgradient sides of the model and no-flow boundaries for the sides and bottom of the model oriented parallel to ground-water flow. The appropriate equations for constant head and no-flow boundaries, respectively, are:

$$h = h(x, y, z)$$
$$\frac{\partial h}{\partial x} = 0 \qquad (7)$$
$$\frac{\partial h}{\partial z} = 0$$

The hydraulic head distribution associated with a linear segment of a conceptual vertical barrier was simulated using Visual MODFLOW® (Guiger and Franz, 1995), a commercial version of the three-dimensional, finite difference ground-water flow model MODFLOW, developed by the U.S. Geological Survey (McDonald and Harbuagh, 1988). MODFLOW is one of the most widely used ground-water flow models and has been extensively verified and validated.

The hydraulic head data generated by the numerical simulations are extracted, visualized, sampled, analyzed, and appropriately manipulated using several software packages. Hydraulic head data from a vertical cross-section parallel to and immediately down-gradient from the simulated vertical barrier (i.e., row 26) are used throughout this study. The data are extracted from MODFLOW output files and reformatted as image files for analysis using MODRISI (Ross and Beljin, 1995). The GIS software used in this study is IDRISI, a raster GIS that provides numerous analytical capabilities that are directly applicable to this and other hydrogeologic studies (Eastman, 1995). The uniform grid spacing facilitates the transfer of data from one software package to another. The raster

format allows importation and exportation of uniform grid model data and also provides a robust platform for the analysis, visualization and data manipulation.

3.3.3 Model Setup

The model domain consists of 51 rows, 51 columns, and 25 layers (Fig. 3.1) and is discretized into uniform 1 m^3 blocks ($\Delta x_j = \Delta y_i = \Delta z_k = 1$ m). This configuration is sufficiently large to reduce boundary effects and provides sufficient resolution to allow identification of subtle variations in hydraulic heads associated with leakage through a vertical barrier. The uniform grid size allows consistent precision over the entire model domain and simplifies data management and transfer between software packages.

The conceptual soil-bentonite slurry wall is simulated as a one meter thick barrier with uniform properties ($K_{wall} = 1 \times 10^{-7}$ cm/s), except for the window. The hydraulic conductivity values for the aquifer and window are scenario dependent. Leakage through the wall is simulated as a window with dimensions of 2 x 3 nodes (6 m^2), located in the approximate center of the vertical barrier (row 25, columns 24-26, layers 12 and 13). The dimensions of the windows were selected to represent the suspected dimensions of confirmed leaks associated with subsurface containment systems.

Boundary conditions are depicted in Fig. 3.1. The upgradient and downgradient sides of the model are constant-head boundaries. The up and down gradient constant head

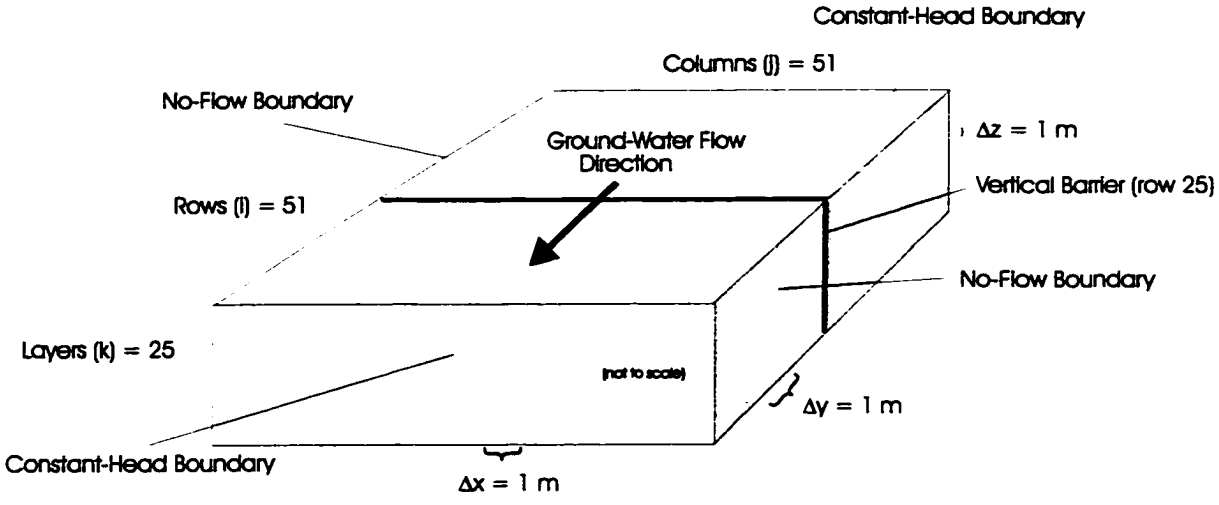

Fig. 3.1 Conceptual model domain and boundary conditions.

boundary values are set at 24.99 m and 24.01 m, respectively, resulting in a horizontal hydraulic gradient across the model domain of 0.0196. This value falls within the range of hydraulic gradients commonly observed in the field. The sides and lower surface of the model oriented parallel to ground-water flow are simulated as no-flow boundaries.

The primary objective of model validation is defined as determining how well a model's theoretical foundation and computer implementation describe actual system behavior in terms of the degree of correlation between calculated and independently observed cause-and-effect responses of the real-world ground-water system for which the model has been developed (van der Heijde, 1987). The applicability of the numerical model for simulating the hydraulic head distribution associated with leakage from a containment system was demonstrated by comparing model results to data generated from a laboratory bench scale model of a soil-bentonite cutoff wall (Ling, 1995). Simulation results agreed favorably with the physical model results, indicating that the approach described in this study is appropriate for simulating the hydraulic head distribution associated with leaking vertical barriers.

3.3.4 General Simulation Scenarios

Several hypothetical hydrogeologic conditions are evaluated in this study. Different scenarios are used to better understand the potential variability of the hydraulic signatures

associated with different subsurface conditions and to account for potential uncertainties associated with predictive modeling (Bear et al., 1992). The general scenarios include:

1) uniform K, where K_h:K_v = 1 (homogeneous and isotropic);
2) uniform K with variable K_h:K_v (homogeneous and anisotropic);
3) log normally distributed K, K_h:K_v = 1 (heterogeneous and isotropic); and
4) lognormally distributed K with variable K_h:K_v (heterogeneous and anisotropic).

A range of homogeneous and isotropic conditions were simulated in an effort to provide a reference case for evaluating the effects of varying average aquifer hydraulic conductivity values on the hydraulic signature of a simulated leak. The scenarios spanned a wide range of K values with respect to the aquifer material and zone of leakage. The hydraulic conductivity values for the aquifer (K_{aq}) range from 1×10^{-2} cm/s to 1×10^{-5} cm/s. These values fall within the range of medium sand to silty sand, respectively.

The hydraulic conductivity of the vertical barrier (K_{wall}) is maintained throughout the study at 1×10^{-7} cm/s. This corresponds to the design hydraulic conductivity of most soil-bentonite slurry walls (LaGrega and others, 1994). The hydraulic conductivity values for the window (K_{win}) ranged from 1×10^{-2} cm/s to 1×10^{-5} cm/s. The hydraulic conductivity value for the window is assumed to be less than or equal to that of the adjacent aquifer materials.

Several of the homogeneous scenarios were modified to simulate anisotropic conditions, where the horizontal hydraulic conductivity (K_h) differs from the vertical hydraulic conductivity (K_v). The homogeneous and anisotropic scenarios simulate the general effects of layering by varying the horizontal to vertical hydraulic conductivity ratios of aquifer materials. Small-scale anisotropy has been attributed to the preferential orientation of fine-grained materials, especially in sediments of fluvial or alluvial origin (Todd, 1980). The K_h:K_v ratios were increased by one and two orders of magnitude (K_h:K_v = 10 and 100) relative to the isotropic simulations (K_h:K_v = 1). These values fall within the range of values reported in the literature (e.g., Freeze and Cherry, 1979).

The horizontal hydraulic conductivity remained constant throughout the simulations ($K_h = 10^{-2}$ cm/s). The hydraulic conductivity of the window varied from 10^{-2} cm/s to 10^{-5} cm/s. The window configuration for the homogeneous anisotropic simulations was identical to those used in the homogeneous isotropic simulations .

One of the primary limitations of using ground-water flow models as predictive tools results from the uncertainty associated with input parameters. This uncertainty is directly related to the spatial variability of hydrogeologic properties of the porous medium (i.e., aquifer material). To account for some of the spatial variability and uncertainties associated with three-dimensional predictive flow modeling, several scenarios utilizing heterogeneous distributions of hydraulic conductivity were assessed.

A lognormal distribution of the hydraulic conductivity of aquifer materials has been reported in the literature (Freeze, 1975; Bakr, 1976). The assumption of lognormal distributed hydraulic conductivity is used for the heterogeneous isotropic and heterogeneous anisotropic simulations. Unique lognormal hydraulic conductivity distributions were generated for each of the 25 layers. This approach resulted in the generation of approximately 63,000 unique K values within the model domain. The mean and standard deviation for the hydraulic conductivity for each layer is approximately 1.6×10^{-2} cm/s and 2×10^{-2} cm/s, respectively. The location of the vertical barrier and configuration of the window for the heterogeneous simulations is similar to that of the homogeneous simulations.

The heterogeneous and anisotropic simulations utilize the same lognormal hydraulic conductivity distribution used for the heterogeneous and isotropic simulations. However, the horizontal to vertical hydraulic conductivity ratios were changed from 1. to 10 and 100.

3.3.5 Hydraulic Signature Assessment Method

The methodology used to address the hydraulic head distribution associated with leakage from a containment system was developed based on the work of Singer and Wickman (1969) and Gilbert (1987). The proposed method is directly applicable to determining the grid spacing necessary to detect the hydraulic signature associated with a discrete leak in a subsurface vertical barrier. The methodology requires the following assumptions:

- the hydraulic signature of the leak is circular or elliptical;
- hydraulic head data are acquired on a square grid;
- the criteria delineating the hydraulic signature are defined;
- there are no measurement misclassification errors.

The model results indicate that the hydraulic signatures associated with the simulated leaks range in shape from approximately circular to elliptical when viewed in vertical cross-section. An increase in the anisotropy results in the elongation of the leak signatures in the horizontal directions. Generally, the greater the K_h:K_v ratio, the more elliptical the hydraulic signature of the leak.

The criteria for delineating the hydraulic signature of a leak from background noise are based on the average hydraulic head value ($\bar{x}_h$) of the model cross-sectional surface. For this study, hydraulic head values of $\bar{x}_h$+0.05 m and $\bar{x}_h$+0.1 m were identified as critical values (C_v), indicating the presence of a hydraulic anomaly associated with containment system leakage. This follows the assumption that any background noise associated with the hydraulic head measurements is significantly less than 0.05 m. The dimensions of the hydraulic anomalies are determined using GIS software by image reclassification to delineate nodes exceeding the average hydraulic head by the specified critical values.

The dimensions of the hydraulic signatures delineated by the two values for C_v are expressed as shape factors (S), defined as the ratio of the length short axis to the length of

the long axis of the hydraulic signature. The shape factor for a circular feature is 1. An increase in K_h:K_v results in the elongation of the feature and a decrease in S, where $0 < S \leq 1$.

The probability tables of Singer and Wickman (1969) were used to generate the nomographs relating the probability of not detecting a leak when a leak is present (β) to the ratio of the semi-major axis to grid size (L/G). The semi-major axis is defined as one-half the length of the long axis of an elliptical feature. As indicated, different curves are used for hydraulic features characterized by different shape factors. The general procedure for determining monitoring point spacing necessary to detect a hydraulic anomaly of given dimensions and specified confidence is outlined in Table 3.2, and in the following example.

In order to determine the minimum grid spacing necessary to identify a hydraulic feature of specified dimensions, an acceptable probability of not detecting the feature must be established. For this example, a value of β=0.1 is assumed for a leak signature with dimensions of 5 m by 4 m, as delineated by C_v=0.1 in Fig. 3.2a. From Fig. 3.3, a value of approximately 0.8 is indicated for the ratio of the length of the semi-major axis to grid size (L/G), given β=0.1 and S=0.8. Therefore, solving for G using L=2.5, it is determined that a minimum grid spacing of approximately 3.12 m is necessary to identify the specified feature with a 90% probability of success. The resulting grid spacing (G) may be used to determine the minimum number of block-centered monitoring points required to detect the feature for a specified area by dividing the total area by the area of one square grid (G^2).

Table 3.2. General steps for determining monitoring point grid spacing.

1.	Specify the radius or one half the length of the long semi-major axis (L) of the hydraulic signature (mound) associated with the leak;
2.	Assuming a circular hydraulic signature, let the shape factor (S) equal one; for elliptical features, S may be calculated using equation (9);
3.	Specify the maximum acceptable probability (β) of not detecting the hydraulic feature (β=0.1);
4.	Knowing L, S and assuming a value for β, determine L/G from Fig. 3.3. and solve for G (minimum grid spacing required to detect the hydraulic anomaly associated with the leak, given the specified constraints).

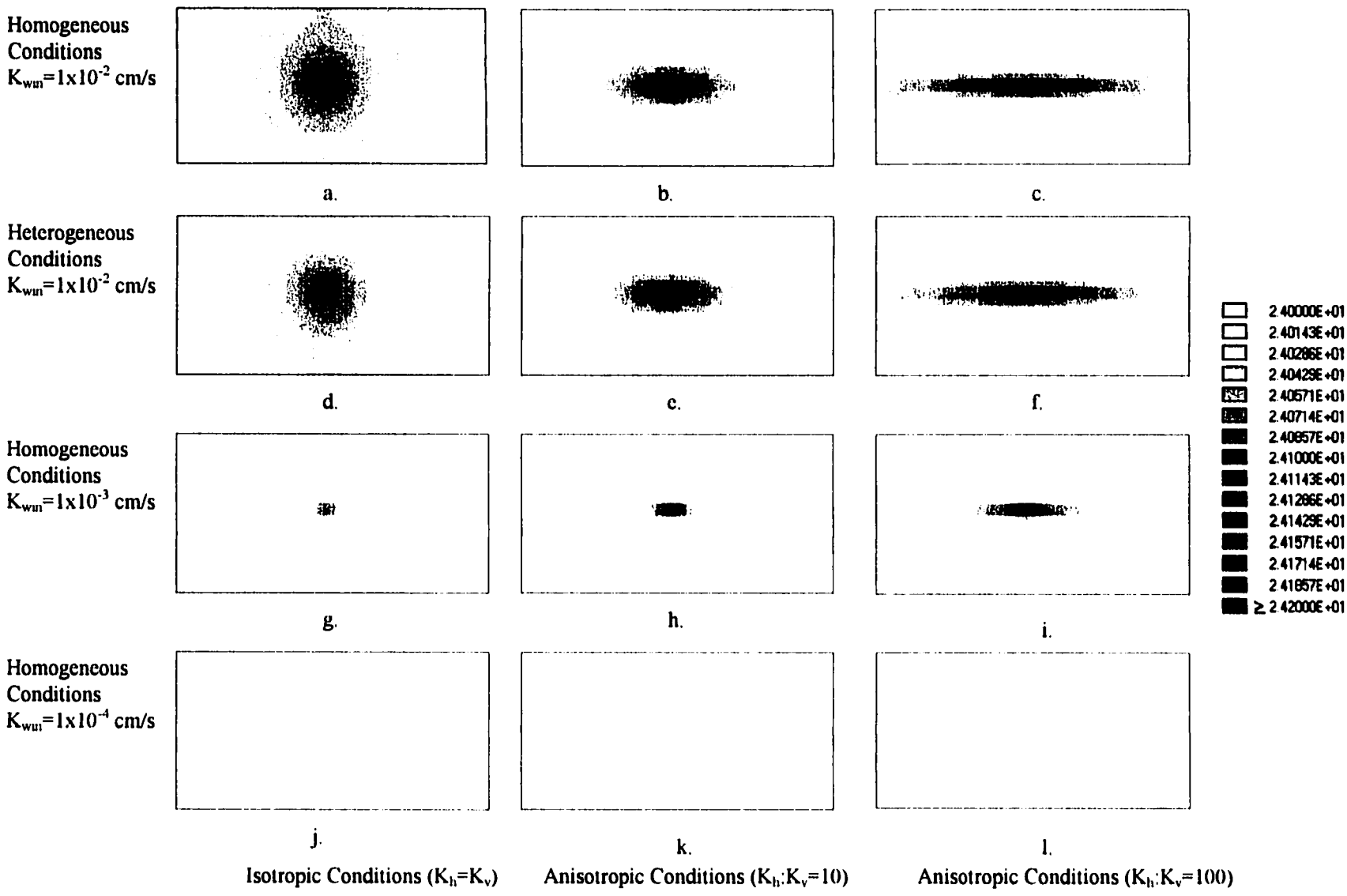

Figure 3.2. Hydraulic signature variations due to changes in conceptual hydrogeologic setting, ranging from homogeneous and isotropic to heterogeneous and anisotropic conditions.

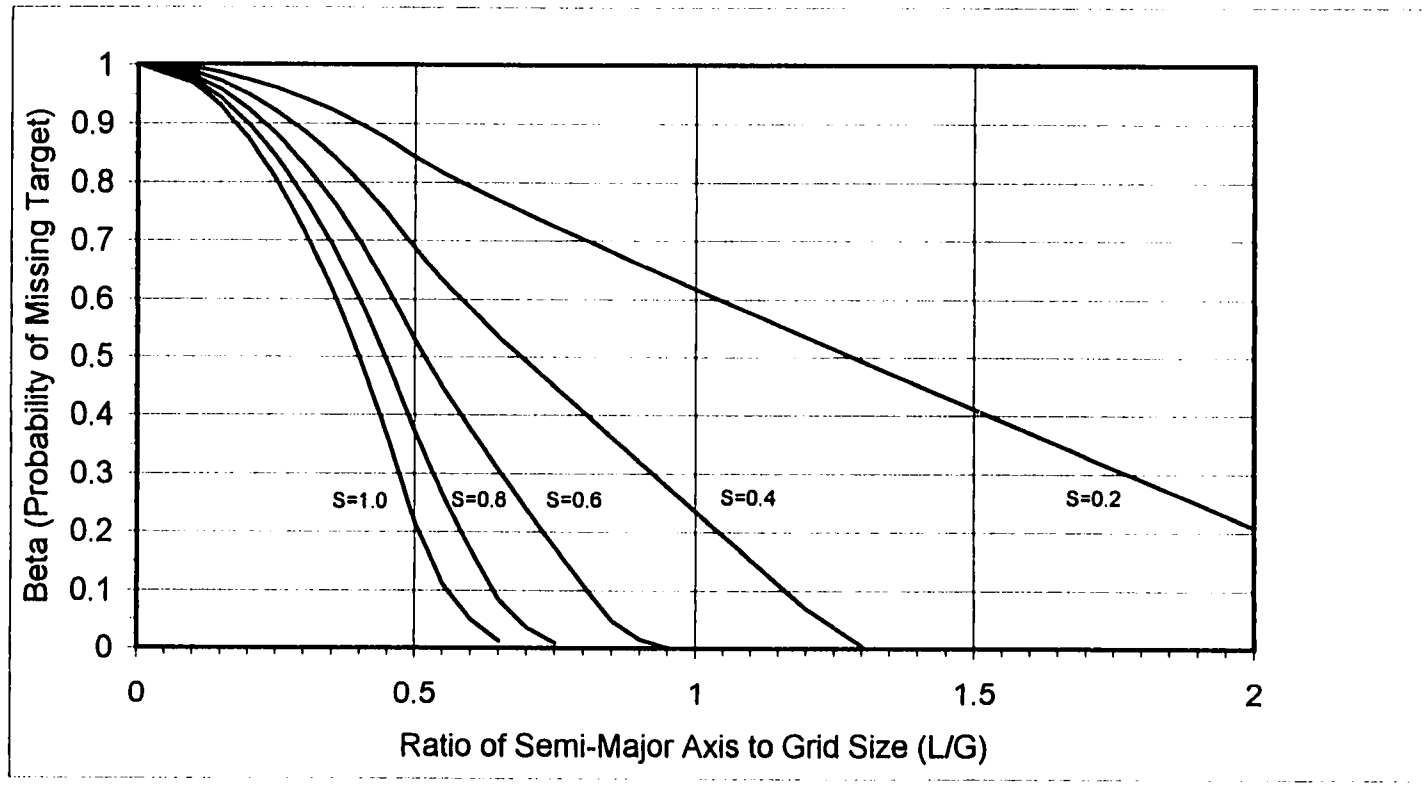

Fig. 3.3 Nomograph relating ratio of semi-major axis of elliptical target and grid size to probability of missing target (Beta) for different shape factors using a square sampling grid.

The probability tables of Singer and Wickman (1969) were also used to generate nomographs relating the probability of not detecting a leak (β) of specified dimensions (L), for different grid dimensions (G). Figure 3.4 illustrates this relationship for circular hydraulic signature (S=1.0). These nomographs may be used to estimate the dimensions of the smallest hydraulic signature capable of being identified by a monitoring network of known dimensions within an acceptable level of confidence (β). For example, given a monitoring point spacing of 20 m, what is the smallest circular hydraulic anomaly that can be detected with 80% probability of success (β=0.2)? From Fig. 3.4, it is noted that a circular feature with a radius of approximately 10.1 m can be detected with the specified probability and grid spacing. The probability of not detecting the anomaly will increase as the radius of the hydraulic signature decreases.

3.4 RESULTS AND DISCUSSION

The dimensions of the hydraulic signatures associated with leakage through a subsurface vertical barrier are a function of the hydrogeologic properties of the aquifer, vertical barrier and zone of leakage. The evaluated parameters include variations in the hydraulic conductivity of the window (K_{win}), hydraulic conductivity distribution within the aquifer and the horizontal-to-vertical hydraulic conductivity ratio (K_h:K_v).

Assuming all other variables remain constant, the magnitude of the hydraulic signature diminishes significantly as the hydraulic conductivity of the window decreases

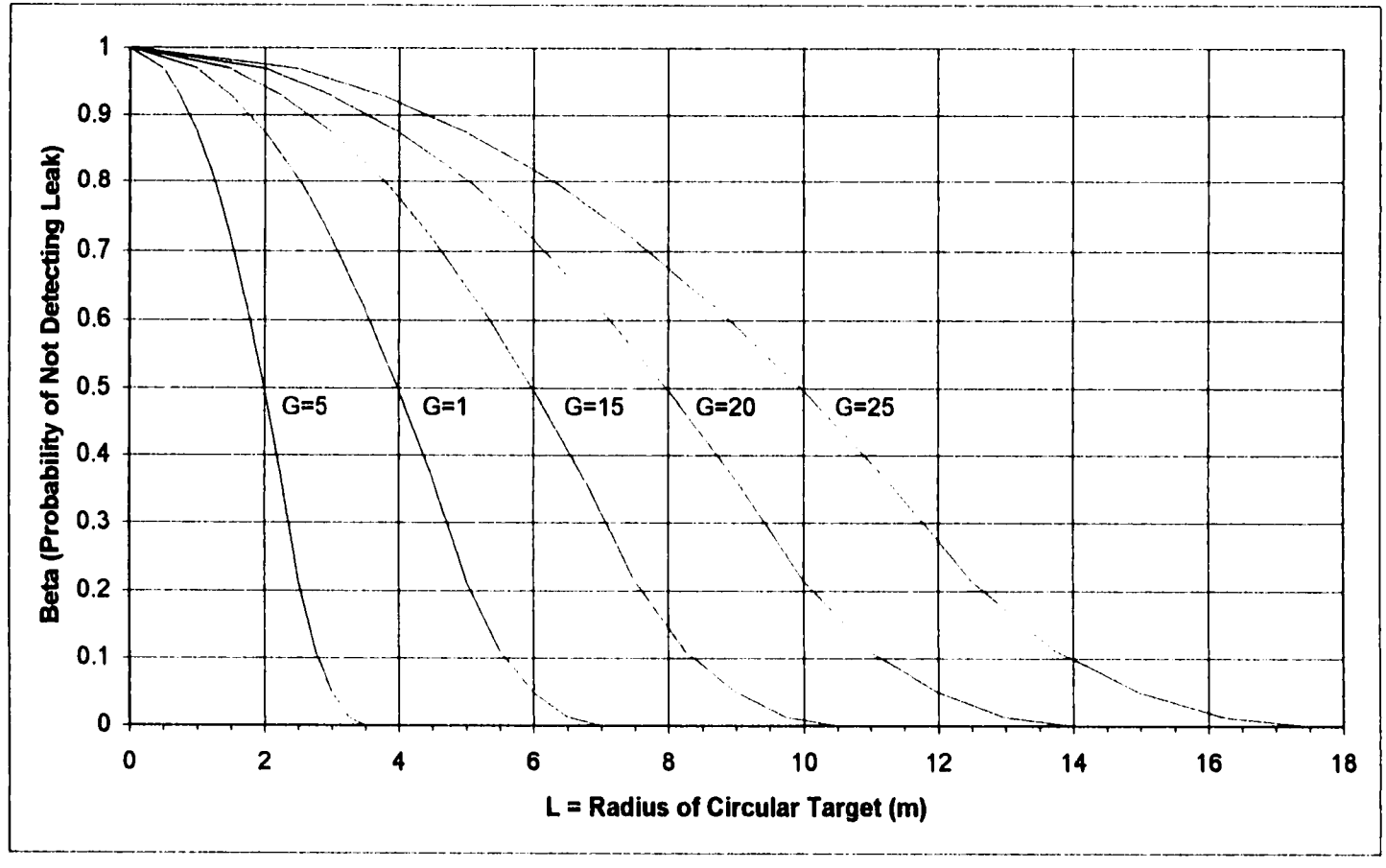

Fig. 3.4 Nomograph relating radius of circular hydraulic signature to Beta for different grid spacings.

(Fig. 3.2). The hydraulic signature of leakage through the 1×10^{-2} cm/s hydraulic conductivity window (Fig. 3.2a) becomes less prominent as K_{win} is reduced to 1×10^{-3} cm/s (Fig. 3.2g). As K_{win} is further reduced to 1×10^{-4} cm/s, the hydraulic signature becomes discernable only immediately adjacent to the window (Fig. 3.2j). All head values for the simulations of ground-water flow through the 1×10^{-5} cm/s window are within a range of approximately 0.002 m. The decrease in hydraulic signature corresponds to a decrease in flux through the window, as the window hydraulic conductivity is reduced (Table 3.3).

The effect of varying the horizontal-to-vertical hydraulic conductivity values is illustrated in Fig. 3.2. For example, the hydraulic signature from leakage through a window with a hydraulic conductivity of 1×10^{-2} cm/s under homogeneous and isotropic ($K_h=K_v$) conditions forms an approximately circular feature (Fig. 3.2a). However, as the horizontal-to-vertical hydraulic conductivity ratio increases one order of magnitude ($K_h:K_v=10$), the hydraulic signature of the leak becomes elliptical (Fig. 3.2b). As the ratio increases to $K_h:K_v=100$, the hydraulic signature of the leak becomes highly elongated (Fig. 3.2c). Similar trends are observed with respect to increasing the horizontal-to-vertical hydraulic conductivity ratio for the heterogeneous simulations (Fig. 3.2d, e and f) and other homogeneous simulations with smaller hydraulic conductivity values for the windows (Fig. 3.2g-l).

The method described above was applied to different hydraulic signatures developed from three-dimensional ground-water flow simulations of leakage through a vertical barrier.

Table 3.3. Simulated flux through windows of varying hydraulic conductivity.

Window Hydraulic Conductivity (cm/s)	Minimum Head Value (m)	Maximum Head Value (m)	Range (m)	Flux Through Window (m^3/d)
1×10^{-2}	24.0293	24.2627	0.2334	1.31×10^{1}
1×10^{-3}	24.0117	24.0826	0.0709	3.98×10^{0}
1×10^{-4}	24.0071	24.0165	0.0094	4.96×10^{-1}
1×10^{-5}	24.0063	24.008	0.0017	5.09×10^{-2}

Delineation of the hydraulic signature of leakage through a window (K_{win} = 1×10^{-2} cm/s) is illustrated in Fig. 3.5a. This figure depicts the hydraulic head distribution associated with leakage through a window located in the approximate center of a vertical barrier in a homogeneous, isotropic aquifer (K_{aq}=1×10^{-2} cm/s, K_h=K_v). The approximate dimensions of the vertical hydraulic mound as defined by C_v=$\bar{x}$+0.05 and $\bar{x}$+0.1 are 5 m by 4 m, and 7 m by 6 m, respectively.

An increase in the anisotropy of the simulated aquifer by one order of magnitude (K_h:K_v=10) produces a vertically compressed and horizontally elongated hydraulic signature (Fig. 3.5b). Similarly, increasing the anisotropy of the simulated aquifer by two orders of magnitude (K_h:K_v=100) results in even greater compression and elongation of the hydraulic signature in the vertical and horizontal directions, respectively (Fig. 3.5c).

Hydraulic signatures for leakage through a window with a hydraulic conductivity value of 1×10^{-3} cm/s exhibits similar trends in response to increases in anisotropy (Fig. 3.6a, b and c). However, the overall hydraulic signature of the window is decreased significantly relative to that of the base case. This results in a lack of head values greater than the elevation threshold for C_v=0.1 for the homogeneous isotropic simulations. The hydraulic head values associated with leakage through windows with hydraulic conductivities < 1×10^{-3} cm/s were all less than C_v=0.05 and, therefore, could not be evaluated as described above.

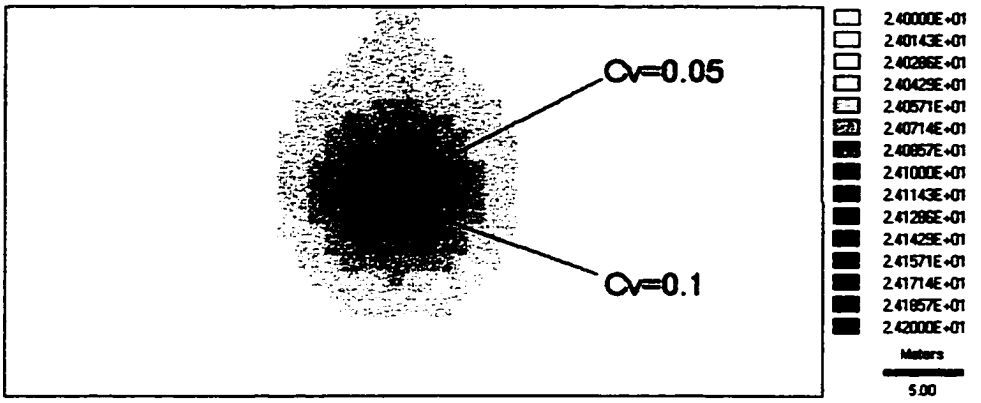

a. Homogeneous and Isotropic (Kh=Kv)

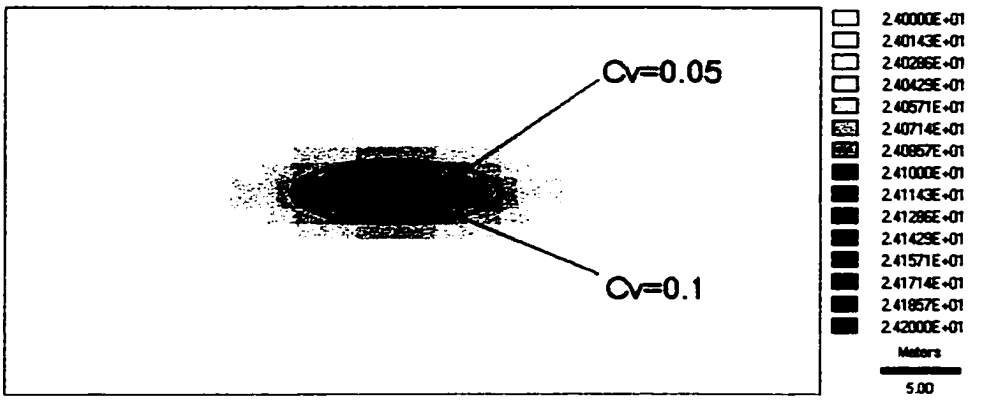

b. Homogeneous and Anisotropic (Kh:Kv=10)

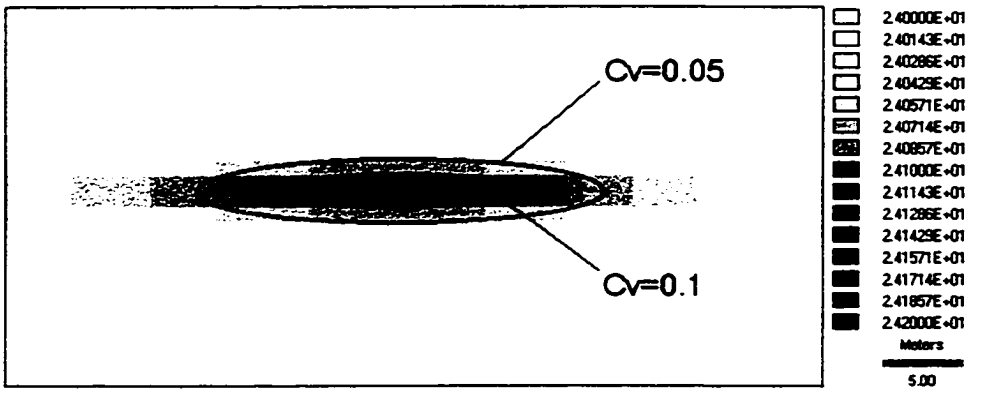

c. Homogeneous and Anisotropic (Kh:Kv=100)

Figure 3.5 Hydraulic signature variations due to changes in anisotropy (K_{aq}=1x10^{-2} cm/s, K_{win}=1x10^{-2} cm/s). The ellipses define the approximate boundaries of the hydraulic features defined by specified critical values (C_v=0.1 and 0.05).

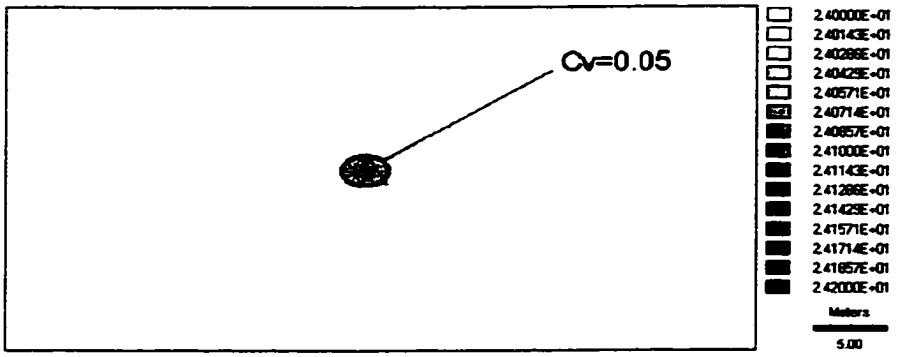

a. Homogeneous and Isotropic (Kh=Kv)

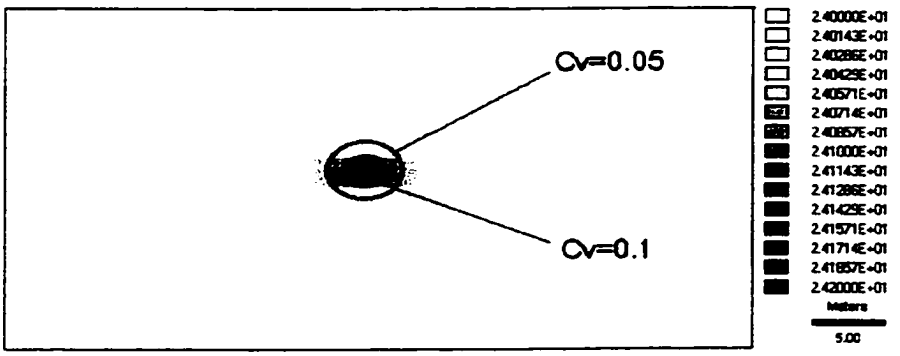

b. Homogeneous and Anisotropic (Kh:Kv=10)

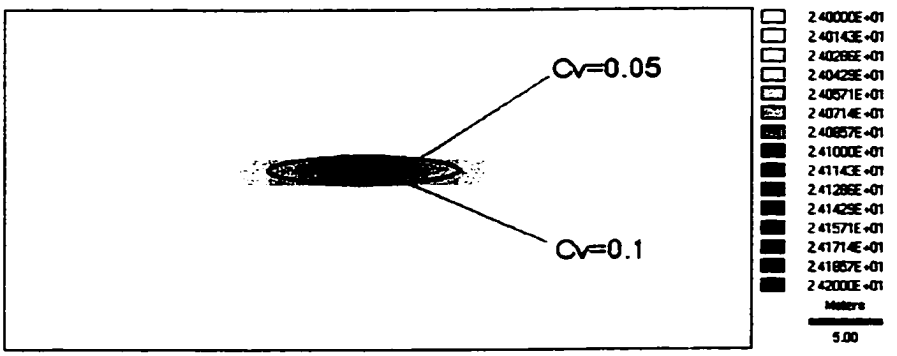

c. Homogeneous and Anisotropic (Kh:Kv=100)

Figure 3.6 Hydraulic signature variations due to changes in anisotropy (K_{aq}=1x10^{-2} cm/s, K_{win}=1x10^{-3} cm/s). The ellipses define the approximate boundaries of the hydraulic features defined by specified critical values (C_v=0.1 and 0.05).

The grid sizes necessary to identify the hydraulic features described above with a 90% probability of success (β=0.1) were obtained using the nomograph in Fig. 3.3. The number of sampling points (N_s) necessary to identify the hydraulic features within the domain of the model cross-section is determined by dividing the cross-sectional area of the model (1275 m^2) by the area of one square grid spacing (G^2). The results are listed in Table 3.4.

The number of monitoring points required to identify the hydraulic signatures of the simulated leaks using the prescribed constraints and confidence ranged from approximately 40 to over 300 over a 1275 m^2 area. The wide range of values is a function of the variability in the size and shape of the hydraulic features. This variability results from the use of different critical values to define the hydraulic signatures of the leaks and the wide range of shape factors resulting from the three orders of magnitude range of K_h:K_v values used to simulate aquifer anisotropy.

3.5 CONCLUSIONS

Numerical modeling of ground-water flow through high hydraulic conductivity windows in subsurface vertical barriers was conducted to provide data sets for use with a probabilistic method for determining the grid spacing necessary to identify the hydraulic signature associated with the leaks. The proposed method represents a potential tool that may be used by the regulatory community and others to evaluate the adequacy of existing

Table 3.4 Parameters and Results Obtained from Hydraulic Assessment Method

K_{win} (cm/s)	K_h:K_v	C_v	S	L	L/G	G	N_s
1×10^{-2}	1	0.1	0.8	2.5	0.64	3.91	84
1×10^{-2}	1	0.05	0.85	3.5	0.62	5.65	40
1×10^{-2}	10	0.1	0.28	3.5	1.64	2.13	280
1×10^{-2}	10	0.05	0.31	6.5	1.51	4.3	69
1×10^{-2}	100	0.1	0.13	7.5	3.5	2.14	278
1×10^{-2}	100	0.05	0.16	12.5	2.9	4.3	69
1×10^{-3}	1	0.1	BCL	BCL	BCL	BCL	BCL
1×10^{-3}	1	0.05	0.67	1.5	0.74	2.03	311
1×10^{-3}	10	0.1	0.67	1.5	0.74	2.03	311
1×10^{-3}	10	0.05	0.4	2.5	1.17	2.14	280
1×10^{-3}	100	0.1	0.4	2.5	1.17	2.14	280
1×10^{-3}	100	0.05	0.15	6.5	3.05	2.13	281
1×10^{-2}*	1	0.1	0.8	2.5	0.64	3.91	84
1×10^{-2}*	1	0.05	0.85	3.5	0.62	5.65	40
1×10^{-2}*	10	0.1	0.28	3.5	1.64	2.13	280
1×10^{-2}*	10	0.01	0.31	6.5	1.51	4.3	69
1×10^{-2}*	100	0.1	0.13	7.5	3.5	2.14	278
1×10^{-2}*	100	0.05	0.16	12.5	2.9	4.31	69

BCL = All head values below critical value threshold.

*Heterogeneous simulations; all other simulations homogeneous

and proposed hazardous waste containment systems for identifying containment system leakage. The utility of the proposed method is demonstrated using simulated data. Based on the application of the method presented above using the simulation results, the following conclusions are made:

- The number of points necessary to identify the hydraulic signature of a discrete leak within prescribed constraints is a function of the criteria used to delineate the feature;
- By using the nomographs described above, the probability of failing to detect the hydraulic signature of a leak can be estimated for a given monitoring well spacing and specified confidence;
- The dimensions of the smallest hydraulic signature detectable with a given monitoring point spacing can be estimated, given the appropriate constraints and specified confidence;
- The monitoring point spacing used at many hazardous waste sites is likely inadequate to detect the hydraulic signatures of all but the largest leaks;
- The method for delineating the hydraulic signature of a leak using the average hydraulic head plus specified values does not appear to be sensitive to the heterogeneity of the aquifer. However, the method is sensitive to changes in anisotropy; and
- The method provides no means for assessing the increase in the number of sampling points necessary due to noise.

3.6 REFERENCES

Bakr, A.A.M (1976). Stochastic Analysis of the Effect of Spatial Variations of Hydraulic Conductivity on Groundwater Flow, Ph.D. Dissertation, New Mexico Institute of Mining and Technology, 243 pp.

Bear, J., Beljin, M.S., and Ross, R., (1992). *Fundamentals of Ground-Water Modeling, Ground Water Issue*, U.S. Environmental Protection Agency, Office of Research and Development, R.S. Kerr Environmental Research Laboratory, Ada, OK, EPA/540/S-92/005.

Canter, L.W., and Knox, R.C. (1986). *Ground Water Pollution Control*, Lewis Publishers, Boca Raton, FL. 526 pp.

D'Appolonia, D.J. (1980). "Soil-bentonite slurry trench cutoff," Journal of Geotechnical Engineering, ASCE, 106(4):399-417.

Conover, W.J. (1980). *Practical Nonparametric Statistics*, John Wiley & Sons, New York, pp. 493.

Eastman, J.R. (1995). *IDRISI for Windows: User's Guide*, Version 1.0, Clark University, Worchester, MA.

Evans, J.C. (1991).,"Geotechnics of Hazardous Waste Control Systems," Chapter 20. Foundation Engineering Handbook, 2nd ed., (H.Y. Fang, Ed.), Van Nostrand Reinhold, New York..

Freeze, R.A. (1975). "A Stochastic-Conceptual Analysis of One-Dimensional Groundwater Flow in Nonuniform Homogeneous Media," Water Resour. Res. Vol. 11, No. 5, pp. 725-741.

Freeze, R.A. and Cherry, J.A. (1979). Groundwater. Prentice-Hall. 604 p.

Geraghty and Miller, Inc. 1994. *MODFLOW 386 Manual*, Reston, VA, 113 pp.

Gilbert, R.O. (1987). *Statistical Methods for Environmental Pollution Monitoring*, Van Nostrand Reinhold, New York.

Grube, W.E., Jr. (1992). "Slurry Trench Cut-Off Walls for Environmental Pollution Control," Slurry Walls: Design, Construction and Quality Control. ASTM STP 1129, David B. Paul, Richard R. Davidson, and Nicholas J. Cavalli, Eds., American Society for Testing and Materials, Philadelphia.

Guiger, N., and Franz, T. (1995). "VISUAL MODFLOW, The Integrated Modeling Environment for MODFLOW and MODPATH, Version 1.1," Waterloo Hydrogeologic, Ontario, Canada.

Inyang, H. I., and Tumay, M.T. (1995). "Containment Systems for Contaminants in the Subsurface", Chapter 5 in Encyclopedia of Environmental Control Technology, Gulf Publishing, Houston, TX, pp. 175-215.

LaGrega, M., Buchingham, P. and Evans, J. (1994). *Hazardous Waste Management*. McGraw-Hill, Inc. New York..

Ling, K., (1995b). *Windows Development and Detection in Soil-Bentonite Cutoff Walls*, Ph.D. Dissertation, University of Cincinnati.

McDonald, M.G., and Harbuagh, A.W. (1988). "A Modular Three-Dimensional Finite-Difference Ground-Water Flow Model (MODFLOW)," U.S. Geological Survey Techniques of Water-Resources Investigation, Book 6, Chapter A1.

Ross, R.R., and Beljin, M.S. (1995). "MODRISI: A PC Approach to GIS and Ground-Water Modeling," Proceedings, National Conference on Environmental Problem-Solving with Geographic Information Systems, Cincinnati, OH, September 21-23, 1994. EPA/625/R-95/004.

Ross, R.R., and Beljin, M.S. (1998). "Evaluation of Containment Systems Using Hydraulic Head Data," J. Envir. Eng., 124(6):575-578.

Rumer, R.R., and Ryan, M.E., eds. (1995). *Barrier Containment Technologies For Environmental Remediation Applications*, John Wiley & Sons, New York., 170 pp.

Savinskii, J.D. (1965). *Probability Tables for Locating Elliptical Underground Masses with a Rectangular Grid*, Consultants Bureau, New York, 110 pp.

Singer, D.A., (1972). "ELIPGRID, a Fortran IV program for calculating the probability of success in locating elliptical targets with square, rectangular and hexagonal grids." Geocon Programs, 4(1):1-16.

Singer, D.A., and Wickman, F.E. (1969). "Probability Tables for Locating Elliptical Targets with Square, Rectangular and Hexagonal Point-Nets," Mineral Sciences Experiment Station Special Publication 1-69, Pennsylvania State University, University Park Pennsylvania, 100 pp.

Todd, D.K. (1980). Groundwater Hydrology. John Wiley & Sons, New York, 560 pp..

U.S. EPA (1984). "Slurry Trench Construction for Pollution Migration Control," Municipal Environmental Research Laboratory, Office of research and Development, Cincinnati, OH, EPA-540/2-84-001.

U.S. EPA (1987). "Construction Quality Control and Post-Construction Performance Verification for the Gilson Road Hazardous Waste Site Cutoff Wall," Hazardous Waste Engineering Research Laboratory, Office of Research and Development, Cincinnati, OH. EPA/600/2-87/065.

CHAPTER 4

INFORMATIONAL ENTROPY AS A LEAK DETECTION INDEX IN THE PRESENCE OF NOISE AND TREND SURFACES

4.1 ABSTRACT

The use of physical and hydraulic containment systems for isolation of contaminated ground water and aquifer materials associated with hazardous waste sites has increased during the last decade. Existing methodologies for monitoring and evaluating leakage from hazardous waste containment systems rely primarily on limited hydraulic head data. The number of hydraulic head monitoring points available at most sites using physical containment systems may be insufficient to identify significant leakage from the system. The methodology presented in this paper uses of informational entropy as a discriminator index to identify the hydraulic signature associated with leakage from hazardous waste containment systems in the presence of background noise and trend surfaces, based on limited hydraulic head data.

4.2 INTRODUCTION

Remedial strategies for contaminated ground water at hazardous waste sites have relied extensively on conventional ground-water extraction and *ex situ* treatment (pump-and-treat) systems in an effort to meet stringent remedial objectives. Numerous reports have identified specific reasons why conventional pump-and-treat systems have failed to reach clean-up goals at many sites (American Petroleum Institute, 1993; U.S. EPA, 1994; National Research Council, 1994). These reasons include the heterogeneous nature of the subsurface, the presence of nonaqueous phase liquids (NAPLs), sorption of contaminants by aquifer materials and uncertainties associated with subsurface characterization.

Other demonstrated and developing remedial technologies (e.g., in situ bioremediation, steam-enhanced extraction, and in situ reactive barriers) are currently being applied and evaluated as alternatives to pump-and-treat remediation. Many of these technologies have been successfully used to remove contaminants from ground water. However, most of these suffer from the same limitations that impact pump-and-treat systems (Gilham and Burris, 1992).

Until recently, most ground-water remediation technologies have focused on restoration of the dissolved contaminant plume(s), rather than removal of contaminant sources (e.g., residual and/or free product NAPL). This has resulted in the apparent failure to meet the remedial objectives at many sites. However, if contaminant sources are isolated,

such that minimal contaminant mass is dissolved into passing ground water, the potential for restoring dissolved plumes may be significantly increased. Physical containment using subsurface vertical barriers is a potential mechanism of contaminant source isolation. Much attention has focused on the use of containment technologies as supplemental or stand-alone remedial alternatives for hazardous waste sites by the industrial and regulatory communities. Subsurface vertical barriers have been used to control ground-water seepage in the construction industry for many years. More recently, such barriers have been employed as components of containment systems to prevent or reduce the impact of contaminant sources on ground-water. While vertical barriers may be useful for isolating sources of ground-water contamination, there is growing concern that containment system performance has not been adequately evaluated.

A recent study concluded that out of 130 sites investigated subsurface engineered barriers to isolate hazardous waste, only 36 had sufficient monitoring data to enable a detailed analysis of field performance (Tetra Tech, 1997). The study further concluded that only 27 of the sites had monitoring systems capable of providing sufficient data to evaluate the system with respect to established site-specific performance criteria.

Ross and Beljin (1998) discuss a method for evaluating the overall performance of subsurface vertical barrier containment systems using temporal and spatial variations of hydraulic head data. They conclude that, while head data from existing wells can be used

to assess leakage, the identification of specific leak locations will require the characterization of the three-dimensional hydraulic head distribution associated with the leakage.

This paper describes a new technique which utilizes the concept of informational entropy or information content to identify the minimum number of monitoring points necessary to distinguish between different magnitudes of containment system leakage in the presence of trend surfaces and background noise. The method uses informational entropy to quantify changes in the spatial variability of the hydraulic signature of simulations of leakage through a subsurface vertical barriers as the number of sampling points increases.

4.2.1 Informational Entropy

According to Papoulis (1984), the term entropy, as a thermodynamic concept, was introduced by Clausius (1850), and the probabilistic interpretation in the context of statistical mechanics was first described by Boltzmann (1877). Planck (1906) presented the explicit relationship between entropy and probability. Shannon (1948) described the concept of information content, a mathematical equivalent to thermodynamic entropy, to quantify the amount of information contained in messages conveyed as binary codes with respect to digital signal processing. In communication theory, entropy is a measure used to determine the channel bandwidth necessary for the transmission of signals of varying information content. Jaynes (1957) related the work of Shannon (1948) to statistical mechanics and applied the maximum entropy method to problems involving the determination of unknown

parameters from incomplete data. Johnson (1992) states that, according to Jaynes (1957), the information measure described by Shannon is true only for discrete probability distributions, but can be applied to discrete approximations to continuous functions. The hydraulic head distributions used in this study represent a discrete approximation to a continuous function, and should therefore be suitable for applications of Shannon's entropy measure.

In hydrology, Leopold and Langbein (1962) were the first to use the concept of entropy to describe the degree of order or disorder in a system in terms of the probability or improbability of the observed state with respect to the hydraulic geometry of river channels. They stated that the entropy of a fluvial system is a function of the distribution or availability of energy within the system, and not a function of the total energy of the system. In this sense, entropy is a measure of the complexity of the drainage network. Amorocho and Espildora (1973) used entropy associated with streamflow and model predictions to evaluate model performance.

Barrtels, and others (1985) stated that a series of sample results may approximate the probability distribution function (PDF) of a variable (i.e., hydraulic head). If a sufficiently large number of samples are obtained, the PDF will be approached. An approximate PDF may be compared with a reference distribution function that represents the total information obtainable from a system. If the distribution function of the samples approximates the reference PDF, the loss in information content is minimal. However, if all the sample values

occupy one histogram interval, the loss in information content is maximal. Chapman (1986) extended the work of Amorocho and Espildora (1973) by using proportional class intervals, rather than fixed intervals, in calculating entropy as a measure of data uncertainty.

Chiu (1987) used entropy functions to estimate the parameters needed to model transport of sediments in open channels. Englehardt and Lund (1992) described the use of entropy in risk analysis to estimate conditional probability distributions where no data were available, but one or two statistics were known. Krstanovic and Singh (1992) developed an entropy-based approach for evaluating whether to keep or eliminate rain gauges depending entirely on reductions or gains in information content at specific rain gauges. Woodbury and Ulrych (1993) and Woodbury and others (1995) used the principle of minimum relative entropy to determine the prior probability distribution function of a set of model parameters based on limited information.

Vieux (1993) used entropy to evaluate information loss associated with the effects of aggregating and smoothing on raster surfaces of digital elevation models and the resulting error associated with predicted surface runoff values. Information content was used to determine the largest grid size which captures the spatial variability of infiltration parameters on a watershed scale by Vieux and Farajalla (1994) and Farajalla and Vieux (1995). They also described the spatial variability measure (SVM) coefficient to normalize entropy values by the logarithm of the number of cells. The use of informational entropy as a measure of spatial variability permits quantification of the number of grid cells (sampling points)

necessary to capture the variability of a spatially distributed parameter. In this sense, entropy is a statistical measure that can be used to assess the grid cell resolution supported by the data for modeling distributed processes.

4.3. METHODOLOGY

The hydraulic head distribution, or hydraulic signature, associated with a linear segment of a conceptual leaking vertical barrier is simulated using a three dimensional, finite difference ground-water flow model. The hydraulic signatures of the leaks are evaluated using informational entropy to measure the spatial variability of leaks of different magnitudes. The effects of applying regional or local hydraulic gradients or trend surfaces and uncertainty in the form of different statistical distributions of noise to the model results are also investigated. The general steps used in the study are outlined in Table 4.1, and discussed in detail in the following sections.

4.3.1 Ground-Water Flow Modeling

Visual MODFLOW® (Guiger and Franz, 1995), a commercial version of the three dimensional, finite difference ground-water flow model (MODFLOW) developed by the U.S. Geological Survey (McDonald and Harbuagh, 1988) was used to simulate the hydraulic head distribution associated discrete leakage through a vertical subsurface barrier. The ground-water flow domain consists of 51 rows, 51 columns and 25 layers discretized into uniform

Table 4.1. General Outline of Steps Used In Study.

1.	Simulate leakage using three-dimensional ground-water flow model;
2.	Extract hydraulic head data from model and save as vertical cross-section image file using MODRISI;
3.	Randomly sample with replacement hydraulic head image file 80 times each, for n_s=5, 10, 15, 20, 25, 30, 35, 40, 45, 50, 60, 70, 80, 90, 100, 150, 200, 300, 400, 500, 600, 700, 800, 900 and 1000 points using IDRISI;
4.	Calculate Entropy for each realization (n_r=2000);
5.	Apply noise and trend surfaces overlays to model results using IDRISI;
6.	Repeat steps 3 and 4;
7.	Modify model parameters and repeat steps 1-6

1 m^3 blocks ($\Delta x = \Delta y = \Delta z = 1$ m) (for additional details regarding the development of the conceptual model and application of the numerical model, refer to Chapter 3) . This configuration is sufficiently large to reduce boundary or edge effects and provides sufficient resolution to allow identification of subtle variations in hydraulic signature associated with leakage through a vertical barrier. The uniform grid size allows consistent precision over the entire model domain and simplifies data management and transfer between software packages. Leakage from the conceptual containment system occurs through a high hydraulic conductivity (K) zone or window with dimensions of 2 × 3 nodes (6 m^2), located approximately in the center of the vertical barrier. The vertical barrier is simulated as a one meter thick wall with uniform properties, bounded on either side by a homogeneous and isotropic aquifer.

The hydraulic conductivity of the conceptual aquifer (K_{aq}) is 1×10^{-2} cm/s. A horizontal hydraulic gradient of approximately 0.02 is simulated by the up-gradient and down-gradient constant head boundaries. The hydraulic conductivity of the window (K_{win}) is scenario dependant and varies from 1×10^{-2} cm/s to 1×10^{-5} cm/s. The vertical barrier hydraulic conductivity is 1×10^{-7} cm/s. The ratio of the hydraulic conductivity of the window relative to that of the vertical barrier may be expressed as K*. For example, the K* values for 1×10^{-2} cm/s, 1×10^{-3} cm/s, 1×10^{-4} cm/s and 1×10^{-5} cm/s window are 1×10^{5}, 1×10^{4}, 1×10^{3}, and 1×10^{2}, respectively.

Hydraulic head data from a vertical cross-section parallel to, and immediately down-gradient from, the vertical barrier are extracted from MODFLOW output files using MODRISI and reformatted as image files for analysis and visualization. MODRISI is a collection of utility programs that allows the extraction, manipulation, and transfer of data files between MODFLOW and numerous software packages (Ross and Beljin, 1995). A module within MODRISI reads the data array for each layer from a MODFLOW hydraulic head output file and extracts the specific head values for each row immediately down gradient of the vertical barrier. These values are then written as a vertical cross-sectional array and saved in the proper format for use with the geographical information system (GIS) software. The resulting hydraulic head image files provide the basic data for this study.

4.3.2 Spatial Analysis

The hydraulic head data extracted from the numerical simulations are visualized, sampled, analyzed and appropriately modified using GIS and other auxiliary software. The GIS software selected for this study is IDRISI, a raster-based system with numerous analytical capabilities that are directly applicable to hydrogeologic studies (Eastman, 1993 and 1995). The raster format allows the import and export of model data and provides a robust platform for data analysis, visualization, and modification. The GIS software was used to apply different "noise" overlays to vertical cross-sectional surfaces derived from the model results. After adding the noise overlays to model results, each surface was sampled and analyzed for information content.

4.3.2.1 Random Noise and Trend Surfaces

Three image files with different statistical distributions of noise were applied to the model results. The noise overlays were used to incorporate uncertainties associated with hydraulic head measurements and to help determine whether a leak, in the presence of such noise, can be discerned using informational entropy. Two types of random noise overlays were generated including, uniform (rectilinear) and normal (Gaussian). The rectilinear random overlays have approximately uniform distributions and ranges of 0 to 0.1 and 0 to 0.05. The latter range was selected to represent uncertainty at levels that are one order of magnitude greater than the histogram bin widths used in this study. Similarly, the 0 to 0.1 range of values represents twice the uncertainty and variability as the 0 to 0.05 range of values. A surface characterized by normally distributed random values with means of approximately 0.0 and standard deviation of 0.0136 is also applied as a noise overlay.

In addition to random noise, variations in head may result from hydraulic gradients, regionally or with depth, not related to containment system leakage. The key question is whether a leak detection measure is sufficiently robust to detect a leak in the presence of a trend surface. Two constant slope trend surfaces were applied to simulate vertical hydraulic gradients of 5×10^{-3} and -5×10^{-3}. These values fall within the range of vertical hydraulic gradients which the authors have observed at hazardous waste sites. The descriptive statistics for the noise and trend surface overlays are listed in Table 4.2.

Table 4.2. Statistics for Noise and Trend Surfaces

	Uniform/ Rectilinear		Normal/ Gaussian	Constant Slope
	R3	R4	N2	C3
Mean	0.0488	0.0244	0.0	0.061
Standard Deviation	0.0284	0.0142	0.0136	0.036
Variance	0.0008	0.0002	0.00018	0.0013
Minimum	0.0001	0.0001	-0.0364	0.001
Maximum	0.0999	0.0499	0.0408	0.121
RMSE	0.0564	0.0282	0.0136	0.0709

4.3.2.2 Quantification of Noise and Trend Data

In order to compare the relative strengths of the noise and trend data with the hydraulic signature of containment system leaks, a root-mean-square (RMS) measure is used. The root-mean-square noise (RMSN) strength is used to quantify the variability of the noise and trend data. The RMSN is calculated as

$$RMSN = \left(\sum_{i=1}^{N} (n_i)^2 / N_T\right)^{1/2} \qquad [1]$$

where n_i is the noise or trend value applied to each block and N_T is the total number of blocks in the model cross-section. The RMSN for the noise and trend data are included in Table 4.2.

The root mean square signal (RMSS) strength is used to quantify the spatial variability of the model cross-section and surfaces generated by the addition of noise and trend data to model results. The RMSS value is calculated by

$$RMSS = \left(\sum_{i=1}^{N_T} [h_n - (h_m + n_r)]^2 / N_T\right)^{1/2} \qquad [2]$$

where h_n is the hydraulic head value for the ith node for a non-leaking wall simulation (i.e., no window present), h_m is the head value for the ith node obtained from each simulation and n_r is the specified value for the noise and/or trend data applied to the ith node. The RMSS values quantify the variability of a surface (e.g., model results with or without the addition of noise and trend data), relative to the head distribution associated with the vertical cross-section immediately down gradient of a simulated non-leaky vertical barrier. The magnitude of the hydraulic signature of the model results, relative to the noise and/or trend data applied to the model, is measured by the signal (hydraulic signature) to noise ratio (SNR). The SNR is calculated by

$$SNR = RMSS/RMSN \qquad [3]$$

4.3.2.3 Sampling

The GIS software was used to randomly sample the hydraulic head data for each simulation. The random sampling scheme selects a specified number of points randomly with replacement. If a particular node is sampled more than once, only the last value is retained for analysis. This results in an effective sample size that may be smaller than the originally prescribed sample size, yet may allow an unbiased estimate of the population mean (Thompson, 1992). The procedure for sampling head values from the model data involves the successive application of several GIS modules described in Table 4.3.

Table 4.3. IDRISI Modules (Eastman, 1995).

SAMPLE	Produces a vector file of point locations from the image files created by MODRISI.
INITIAL	Creates an image file of proper dimensions;
POINTRAS	Converts point vector data obtained from SAMPLE module to raster representation.
EXTRACT	Distills values from image file created by POINTRAS module.

The cross-sectional surfaces derived from the model results and from the addition of noise and/or trend data to the model results were sampled by selecting the following number of points: 5, 10, 15, 20, 25, 30, 35, 40, 45, 50, 60, 70, 80, 90, 100, 150, 200, 300, 400, 500, 600, 700, 800, 900 and 1,000 points. The effective sample sizes were generally smaller than the specified number of points, especially for the larger sample sizes. This results from the fact that only the last value is retained for points that are selected more than once.

Two factors relating to the uncertainty of random sampling include the number of samples and the proximity of the samples to the leak. The closer the samples are to the hydraulic signature produced by a leak, the less uncertainty, and hence, the more confidence one has in detecting the leak. Other factors of importance include the spatial arrangement of the samples and the nature of the leak. For example, if the samples are located in close proximity to one another, one has less confidence in detecting the leak than if the if the samples are evenly distributed about the leak (Isaaks and Srivastava, 1989).

Each sampling event may be considered a single realization of the hydraulic head distribution. Because most random number generators are not truly random, and that different realizations can vary dramatically in terms of discrete probability distributions, 80 realizations were obtained for each sampling event, resulting in a total of 2,000 realizations for each surface. Multiple realizations are used to better define the boundaries of the entropy envelope, as discussed below. The use of fewer than 80 realizations per sampling event does not adequately define the entropy envelopes, and more than 80 realizations presented

significant file management problems, while not significantly improving the entropy quantification.

4.3.3 Information Content and Entropy

Each realization of the hydraulic head distribution is analyzed for information content using a variation of a method presented by Farajalla and Vieux (1995), who assessed the largest grid size necessary to capture the spatial variability of distributed hydrological modeling parameters. However, in the current work the number of sampling points is varied while maintaining a constant, uniform grid. This technique can determine the number of points necessary to quantify spatial variability of a surface without losing significant information content, while also developing a leak detection statistic.

The entropy or information content of a continuous function with the state variable X is generally expressed as (Chiu, 1987)

$$I(X) = -\int P(X) \log P(X)\, dX \qquad [4]$$

where P(X) is the probability density function. In such cases, P(X)dX is the probability of the state variable being between X and X + dX. However, for a discrete approximation of a continuous function (i.e., hydraulic head distribution generated by a three-dimensional

ground-water flow model), calculating information content requires the development of a histogram of the number of occurrences (n_i) of sampled hydraulic head values within discrete intervals (i). The width of the histogram intervals (bin width) is specified as 0.005 m. This is consistent with the precision of most water level measuring devices. Additional discussion regarding selection of appropriate bin widths are included in section 4.3.3.1. From the histogram data, information content or entropy is calculated by:

$$I = -\sum_{i=1}^{B} P_i \log(P_i) \qquad [5]$$

where B is the number of discrete intervals of the variate (hydraulic head) and P_i is the probability of occurrence of the variate within the discrete interval, calculated by:

$$P_i = n_i/N_s \qquad [6]$$

where N_s is the number of points sampled. By convention, a negative sign multiplies the summation in Equation [3], such that I is positive and increasing information content results in increasing entropy. The total entropy (I_T)of a surface is calculated using all nodal values ($N_s = N_T$=1275).

A maximum value for entropy (I_M) occurs when all values of the variate are equally probable and each histogram bin is occupied by a single variate value, where:

$$P_i = 1/N_s \quad [7]$$

The theoretical maximum entropy for a surface is calculated by:

$$I_M = \log(N_s) \quad [8]$$

A maximum entropy surface may be characterized by a uniformly sloping surface with a nodal width of one, or by a surface with highly variable elevations (Vieux, 1993). As specified, I_M requires that the data be distributed such that each histogram interval may contain only one value. For a uniformly sloping surface, characterized by a constant slope (e.g., vertical hydraulic gradient), each bin will be occupied by the same number of points. Consequently, the maximum entropy value calculated for such a surface will be less than I_M. The relative maximum entropy (I_{RM}) of a uniformly sloping surface is calculated by:

$$I_{RM} = \log(N_B) \quad [9]$$

where N_B is the number of uniformly filled histogram intervals. For this study, the relative maximum entropy value for the trend surface corresponds to the number of layers of the model (N_B=25), each layer characterized by a unique value, and is equal to log (25) = 1.398. Similarly, for a continuous random variable, a uniform probability distribution over the limits of X will result in maximum entropy (Chiu, 1987). A minimum entropy surface is

characterized by low spatial variability. Relatively flat surfaces with all values occupying one histogram bin have entropy values of zero, and consequently, zero information content.

The spatial variability of a surface may be quantified by calculating the spatial variability measure (SVM). The SVM is determined by normalizing the entropy of the surface by the logarithm of the number of points sampled (N_s) and subtracting from unity [$\log(N_s)/\log(N_s)$], as:

$$SVM = 1 - \frac{I}{\log(N_s)} \qquad [10]$$

The SVM represents the departure from a maximum entropy surface or equal probability plane (Farajalla and Vieux, 1994).

4.3.3.1 Selection of Bin Width

Selecting the appropriate bin width is important for studies involving the determination of information content. The effect of varying the bin width on information content values was evaluated by calculating the entropy for a data set using bin widths ranging from 0.0001 m to 0.5 m. For consistency purposes, the minimum and maximum head values are used for the lower and upper histogram bin boundaries, respectively. The number and distribution of empty histogram bins does not affect entropy values. The sensitivity of entropy calculations (Eq. 4) to changes in bin width is clearly illustrated in Fig.

4.1, which indicates a semi-log relationship between the bin width and entropy for most of the range of values. Information content decreases linearly as the log of the bin width increases over a wide range of values. However, as the bin widths increase to greater than approximately 0.025, the entropy approaches zero.

These results indicate that as the size of the bin width approaches the magnitude of the range of values for the surface, the information content decreases until all of the values fall within one histogram interval, resulting in zero information content. Consequently, if the specified bin width is too large (i.e., greater than the range of head values), the calculated entropy will not adequately capture the variability of the hydraulic head values of the surfaces. The bin width selected for this study (0.005 m) approximately corresponds with the advertised precision of many commercially available water-level measuring devices. Selection of a bin width significantly greater than 0.005 m would have resulted in the failure to adequately capture the information content of the hydraulic signatures.

4.4 RESULTS AND DISCUSSION

A graph of the number of points sampled versus entropy is characterized by a wide range of entropy values corresponding to small sample sizes. As the number of sampling points increases, the range of entropy values becomes progressively smaller, resulting in less uncertainty in the estimation of informational entropy. The range of entropy values for a given sample size approximately defines the upper and lower boundaries of the entropy

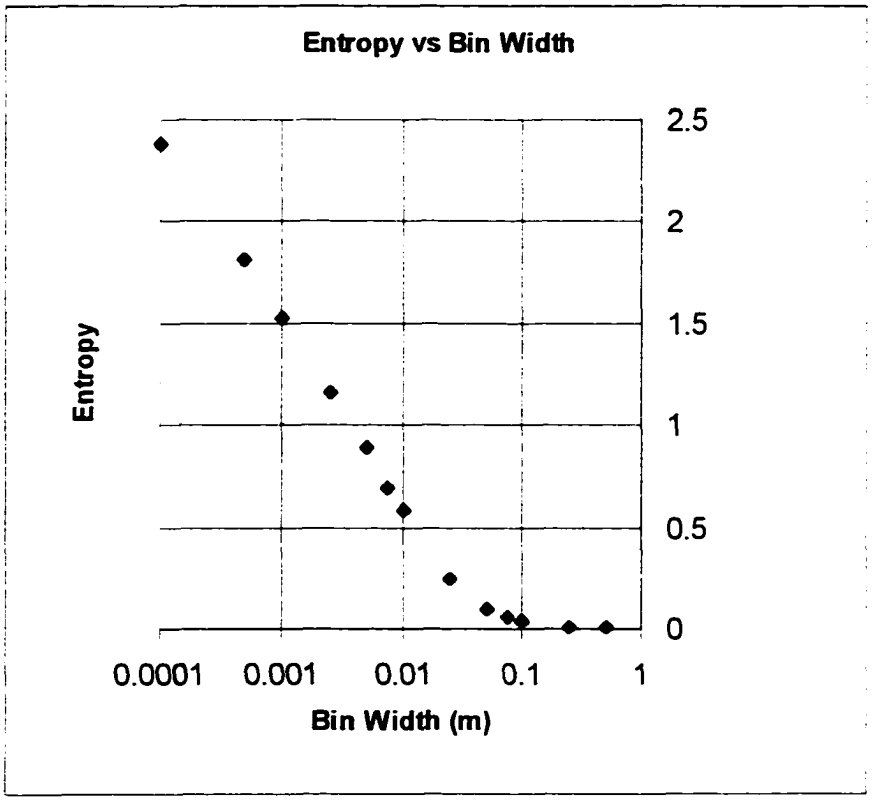

Fig. 4.1 The relationship between bin width and entropy.

envelope. The theoretical upper boundary for the entropy envelope corresponds to the maximum entropy value, I_M. For any N_s, if all occupied bins have one value, n_i, the entropy is maximum. This unlikely case forms a straight line equal to $\log(N_s)$ (Fig. 4.2a).

Figure 4.2i illustrates the general differences in the distribution of sampling points with respect to the upper and lower boundaries of the entropy envelope for leakage through a 1×10^{-2} cm/s window. Inspection of the histogram in Fig. 4.2h indicates that all 5 sampling points fall within one histogram bin, resulting in zero information content. Conversely, all five occupied bins of the histogram in Fig. 4.2b contain 1 sampling point, resulting in maximum information content, as previously defined. Histograms representing other points along the entropy envelope (Fig. 4.2c-h) illustrate that sets of sampling points associated with the upper boundary occupy more bins than sample sets with similar numbers of points associated with the lower entropy envelope boundary. This appears to be related to better geographic coverage associated with sampling points contained in data sets located near the upper boundary of the entropy envelope relative to the lower boundary data sets and the heteroscedasticity of the surface.

The effect of increasing the number of random sampling points to calculate the information content of vertical cross-sections of ground-water flow modeling results is dependant upon several factors, including the magnitude of the hydraulic signature and the nature and magnitude of noise applied to the model results. The information content of a surface characterized by a relatively strong hydraulic signature generally increases as the

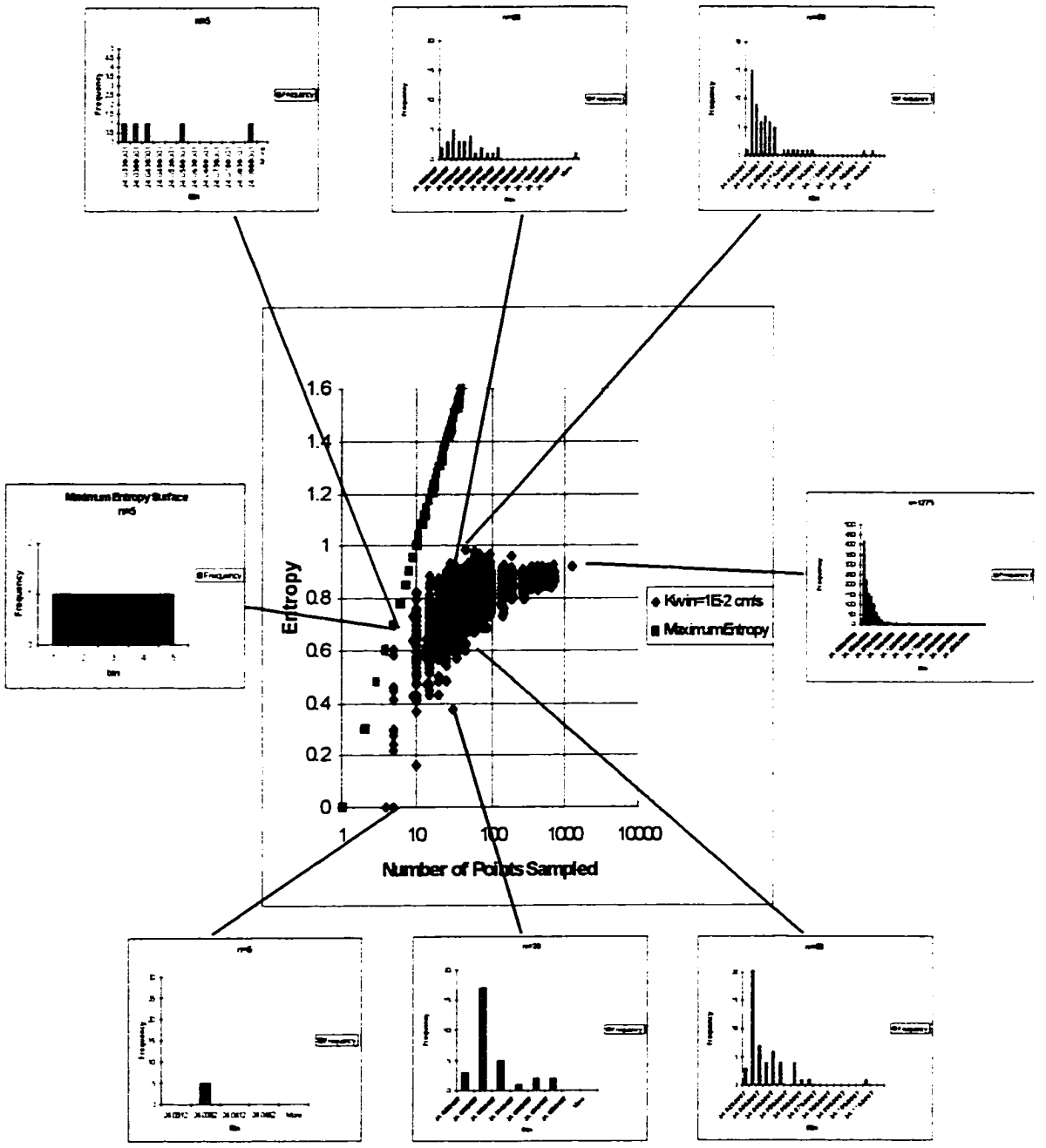

Fig. 4.2 Entropy envelope and related histograms.

number of sampling points increases. This is related to the fact that more histogram bins become occupied over the range of data as the magnitude of the hydraulic signature increases. This tendency is also noted when trend and noise data are added to hydraulic head surfaces, regardless of the magnitude of the hydraulic signature. However, the information content of relatively weak hydraulic signatures appear to decrease as the number of sampling points increases.

A leak detection index should be sufficiently robust to identify a leak in the presence of noise and trends. This is obviously dependent on the strength of the leak relative to that of the noise and trend surface variations. The number of sampling points needed to discriminate different magnitudes of leakage from background noise will depend on the hydraulic signature (signal) to noise ratio. The following section describes the results of the ground-water flow modeling, spatial analysis, and entropy calculations.

4.4.1 Simulated Containment System Leakage

The hydraulic signature associated with leakage through a subsurface vertical barrier is a function of the hydrogeologic properties of the aquifer, vertical barrier and zone of leakage. The dimensions of the signature will also be dependant on the hydraulic gradient across the vertical barrier, the area of leakage and other factors (Bodocsi and others, 1990). Assuming that all other variables remain constant, the magnitude of the hydraulic signature will diminish significantly as the hydraulic conductivity of the window decreases, as

illustrated in Figs. 4.3b, c and d. As expected, the decrease in hydraulic signature corresponds to a decrease in the calculated flux through the window (Table 4.4).

The hydraulic signature created by the flow of ground-water through the conductive (K_{win} = 1×10^{-2} cm/s) window is clearly visible in Fig. 4.3b. The signature becomes less prominent as the hydraulic conductivity of the window decreases (K_{win} = 1×10^{-3} cm/s, Fig. 4.3c, and K_{win} = 1×10^{-4} cm/s, Fig. 4.3d) resulting in a hydraulic signature that is discernable only immediately down gradient of the window. All hydraulic head values for the simulations with hydraulic conductivities $\leq 1\times10^{-5}$ cm/s are within a range of 0.002 m, which falls within one histogram bin interval and results in zero information content. Therefore, only the simulations of $K_{win} \geq 1\times10^{-4}$ cm/s are discussed in detail below.

4.4.2 Application of Noise and Trend Data To Simulation Results

The effects of applying noise to the hydraulic signature associated with ground-water flow through a relatively high hydraulic conductivity window (K_{win}=1×10^{-2} cm/s) are clearly visible in Figs. 4.4a-4.4d. The hydraulic signature is most pronounced for leakage through the window in the absence of noise (Fig. 4.4a). When uniformly distributed random noise is applied to model results, a less obvious hydraulic signature is produced (Fig. 4.4b). The effects of applying a trend surface to model data are clearly visible in Fig. 4.4c. Locating the window in the center of the vertical barrier resulted in a high degree of symmetry for the hydraulic signatures of leaks. Consequently, the application of upward and downward trend surface data (i.e., vertical hydraulic gradient) to model data resulted in the production of

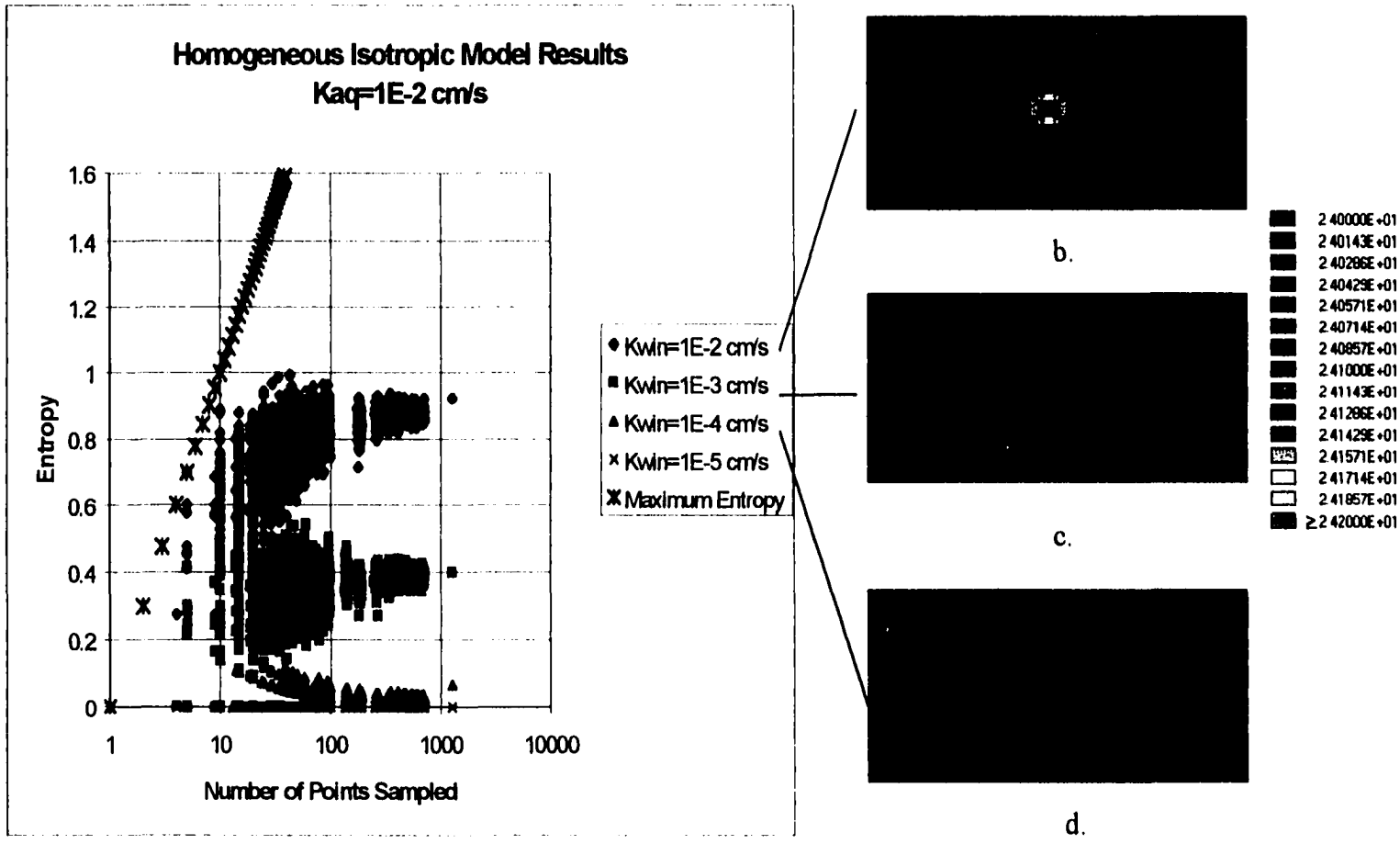

a.

Figure 4.3. Entropy diagrams and hydraulic signatures for homogeneous, isotropic simulation results.

Table 4.4. Simulated Flux Through High K Window.

Window K (cm/s)	Minimum Head Value (m)	Maximum Head Value (m)	Range (m)	Flux Through Window (m^3/d)
1E-2	24.0293	24.2627	0.2334	1.31×10^{1}
1E-3	24.0117	24.0826	0.0709	3.98×10^{0}
1E-4	24.0071	24.0165	0.0094	4.96×10^{-1}
1E-5	24.0063	24.008	0.0017	5.09×10^{-2}

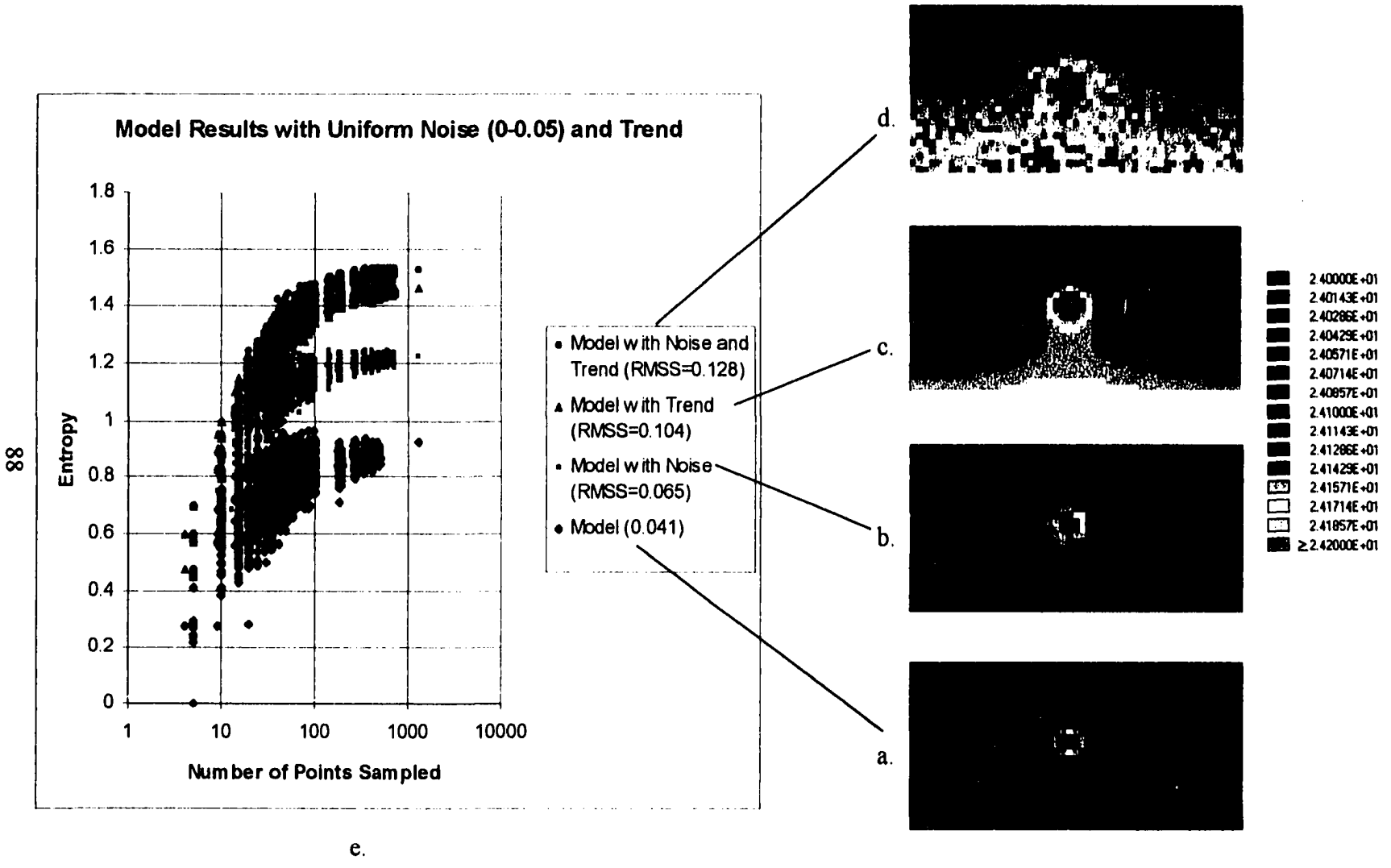

Fig. 4.4 Entropy diagram and hydraulic signatures of model results with uniform noise (0.0-0.05 m) and trend sur-

inverted and approximately mirror imaged data sets. The combined effects of uniformly distributed random noise and a trend surface produce an image that is more complex than the original model results, yet the hydraulic signature of the leak is still visible.

An increase in the level of uniform random noise applied to the model data results in a general degradation of the hydraulic signature (Figs. 4.5a - 4.5d). The addition of rectilinear random noise ranging from 0 to 0.1 m results in a slight decrease in the definition of the hydraulic signature (Fig. 4.5b). The signature of the leak impacted by the noise and trend surface (Fig. 4.5d) is weak, yet discernable from the background noise. Similar trends are observed in Figs. 4.6a - 4.6d, with respect to the effects of normally distributed noise and a trend surface on model results. The signature of the model results (Fig. 4.6a) is partially masked by the Gaussian noise (Fig. 4.6b). The addition of a trend surface further reduces the prominence of the signature (Fig. 4.6d).

The addition of noise and trend data to hydraulic signatures of leakage through windows with hydraulic conductivity values of 1×10^{-3} cm/s and 1×10^{-4} cm/s are presented in Figs. 4.7, 4.8 and 4.9. Generally, the reduction in hydraulic conductivity results in a lower flux of ground water through the window and a decrease in the magnitude of the hydraulic signature, as indicated by the decrease in the range of hydraulic head values in Table 4.4. Consequently, the hydraulic signatures of leakage through windows with $<1\times10^{-3}$ cm/s is almost indistinguishable from background noise (Figs. 4.7b, 4.8b and 4.9b).

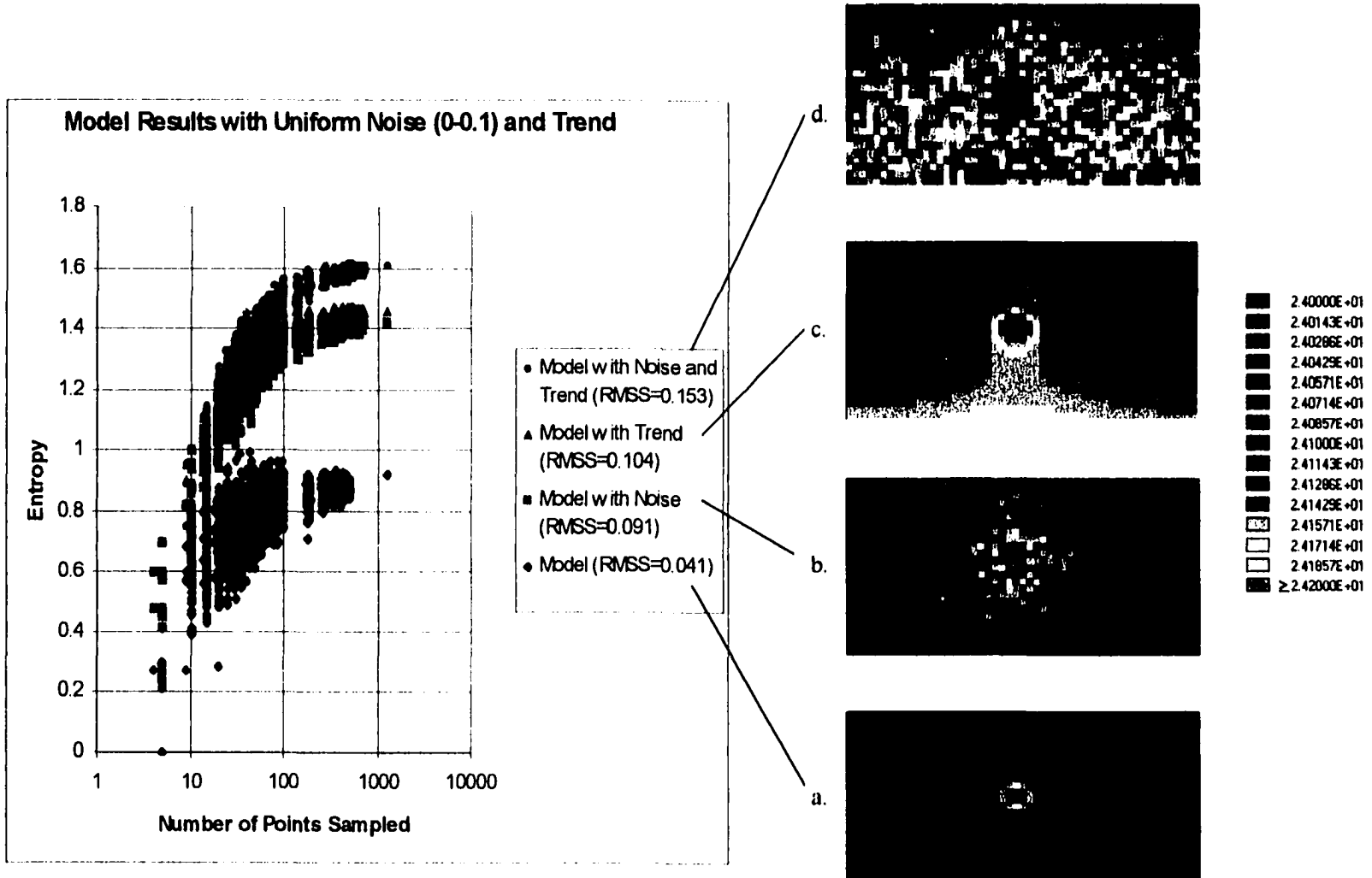

c.

Fig. 4.5 Entropy diagram and hydraulic signatures of model results with uniform noise (0.0-0.1 m) and trend surface.

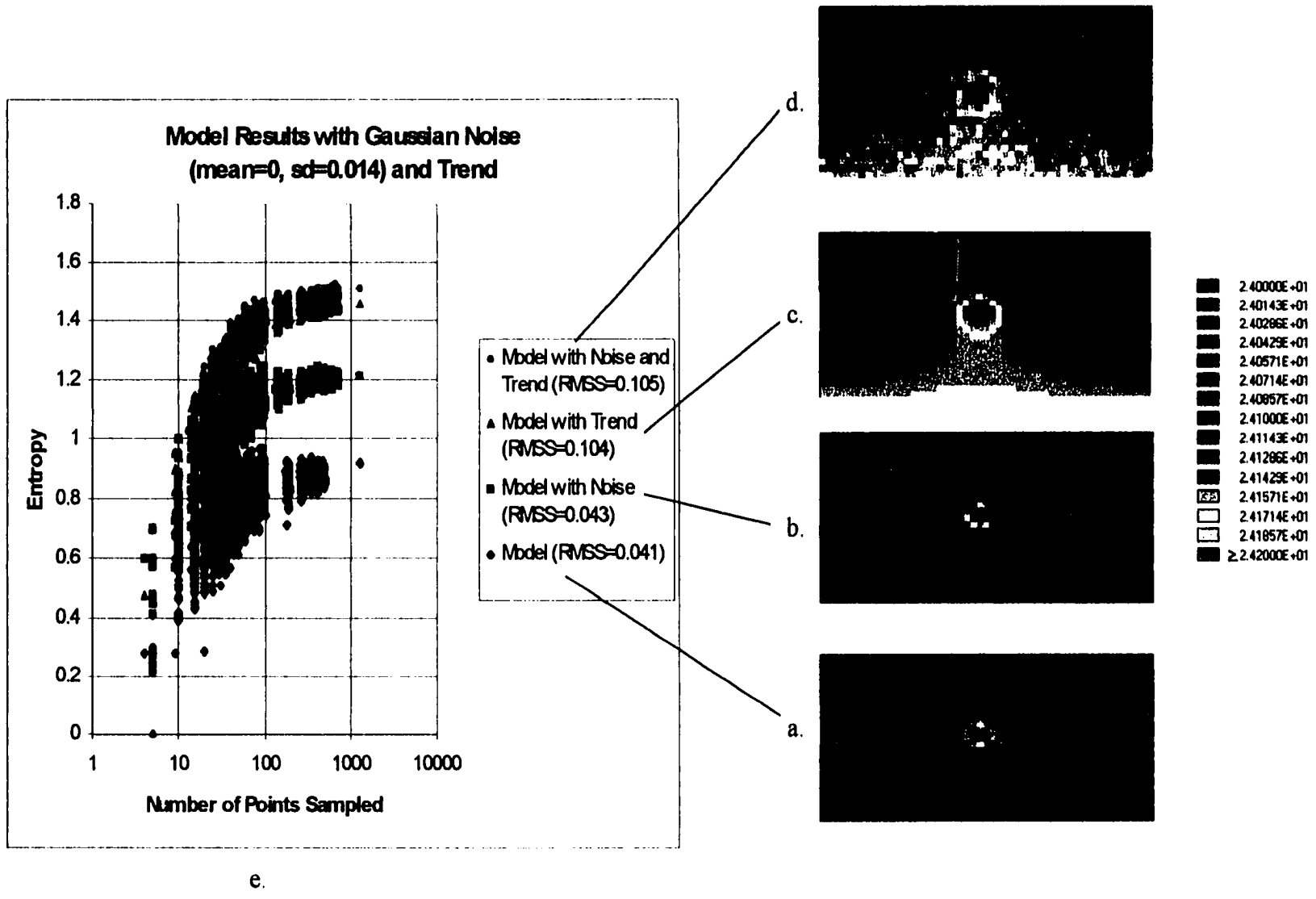

Fig. 4.6 Entropy diagram and hydraulic signatures of model results with Gaussian noise and trend surface.

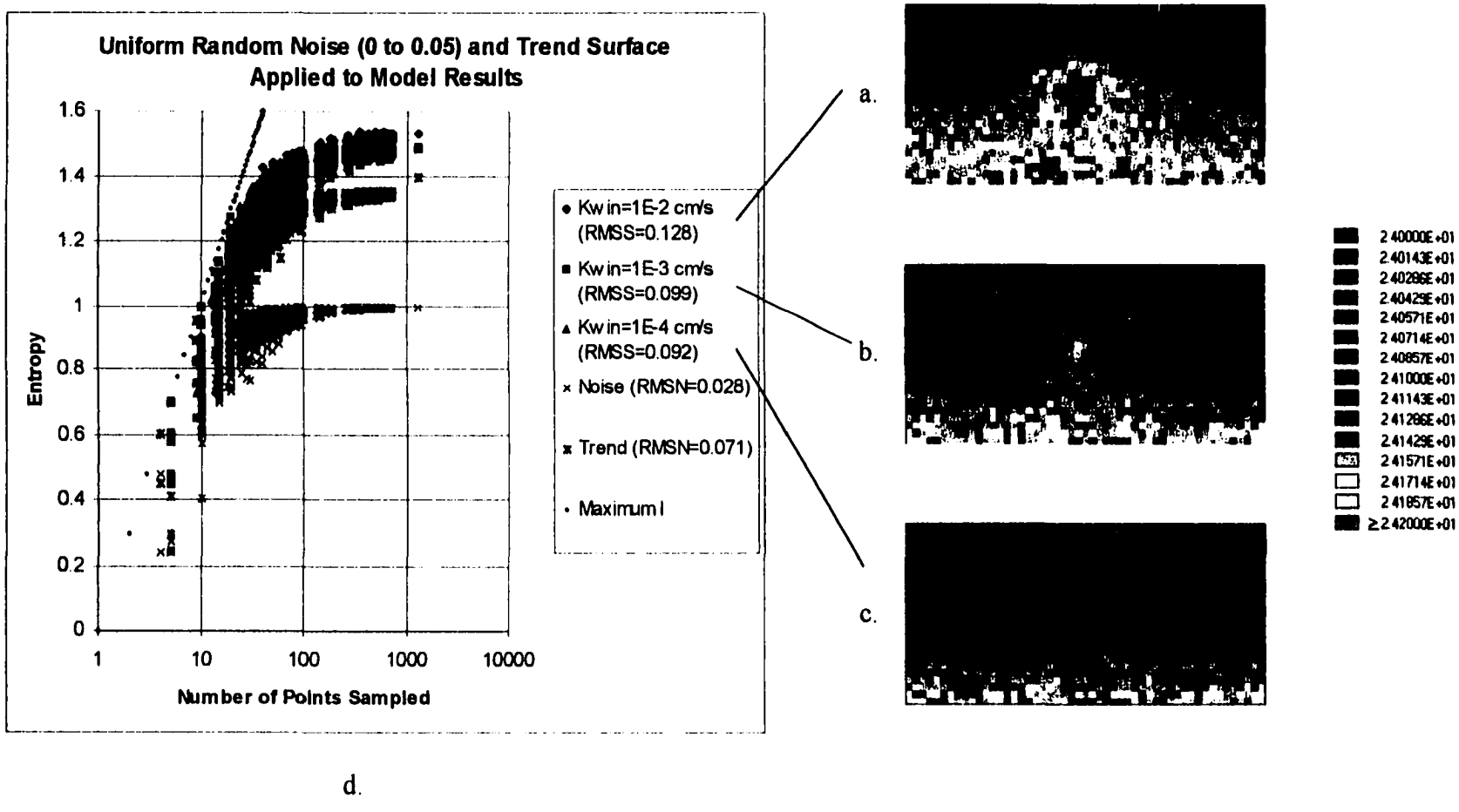

Fig. 4.7 Entropy diagram and hydraulic signatures of model results with uniform noise (0.0-0.05 m) and trend surface.

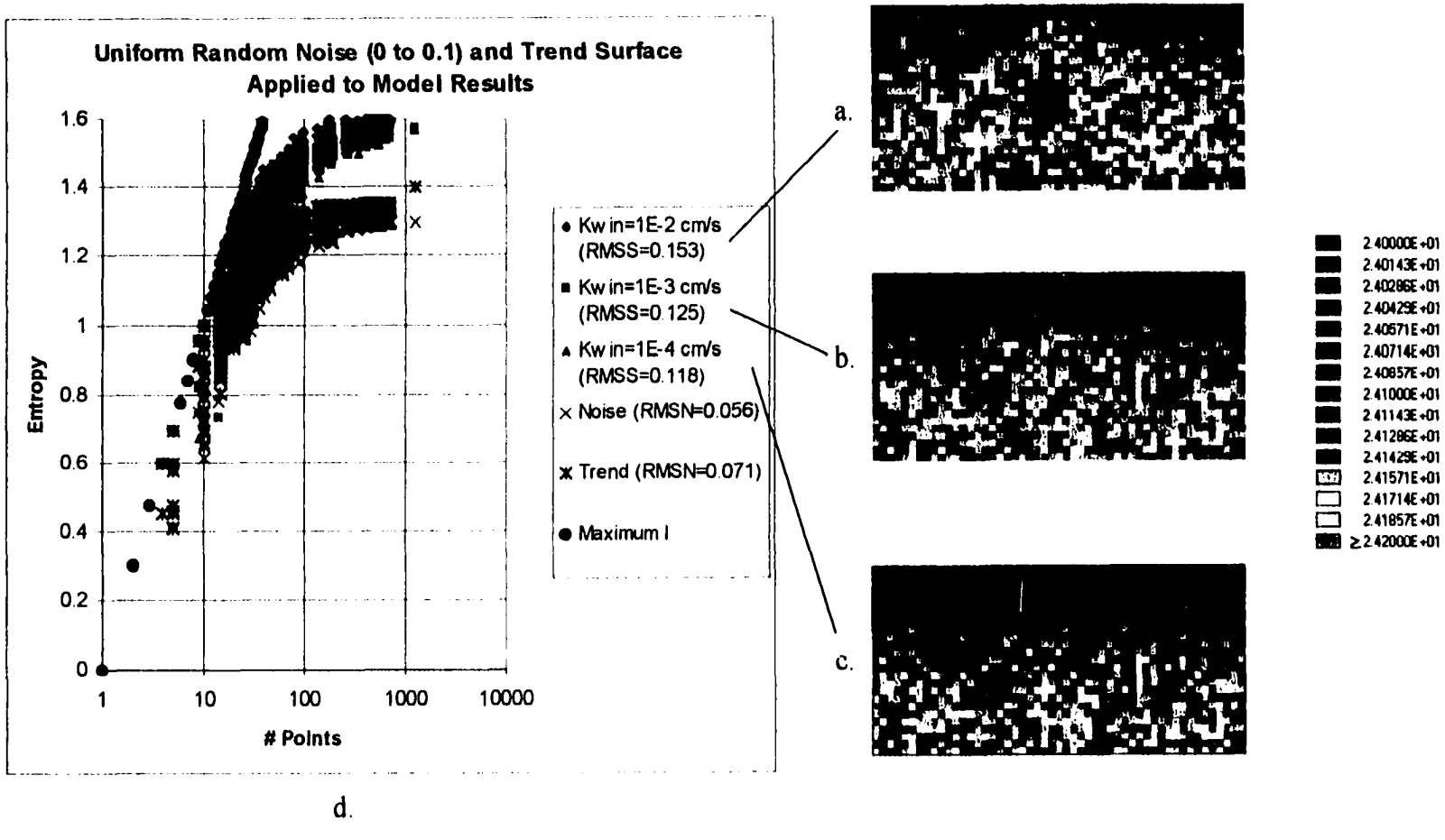

Fig. 4.8 Entropy diagram and hydraulic signatures of model results with uniform noise (0.0-0.1 m) and trend surface.

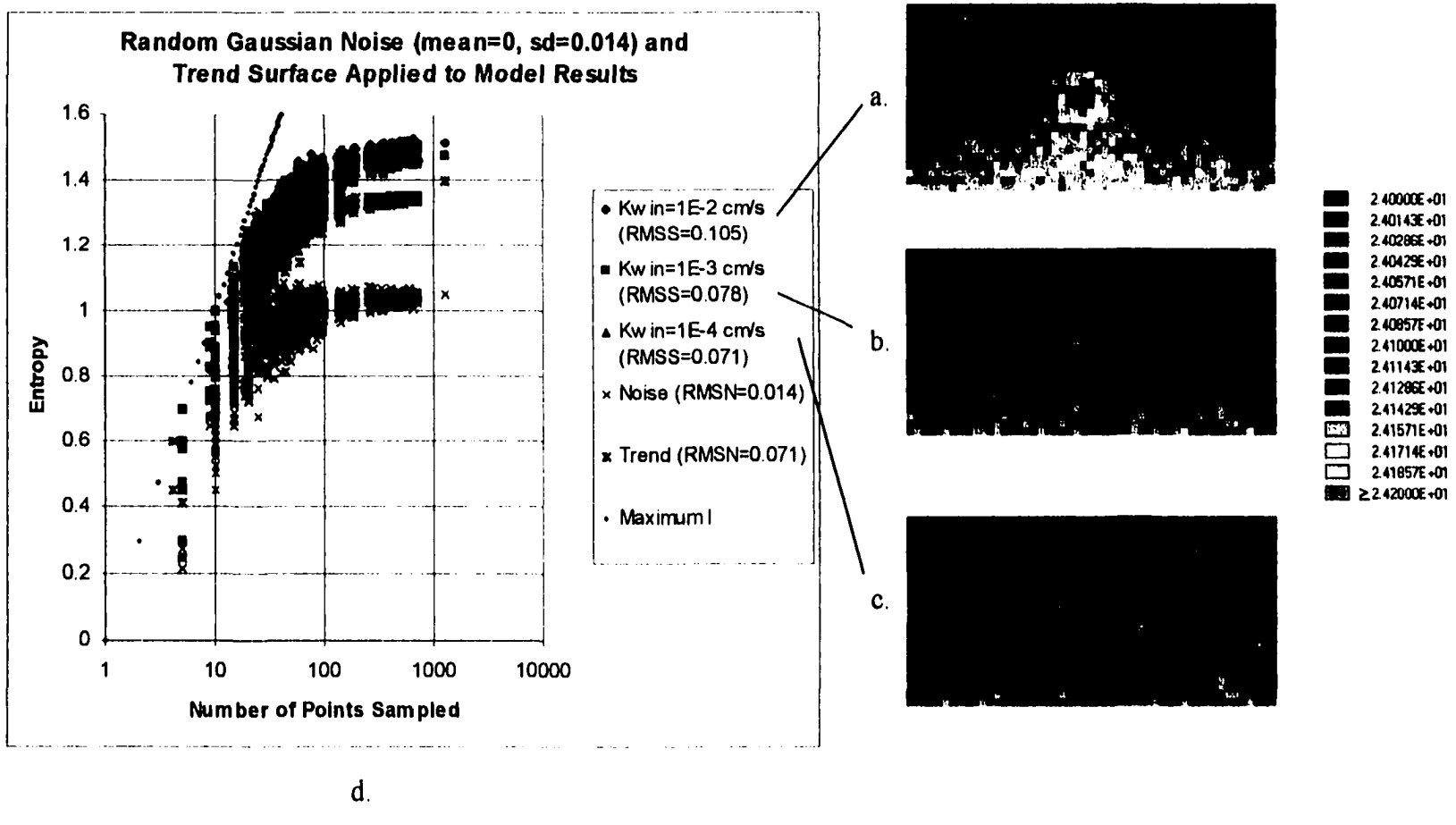

Fig. 4.9 Entropy diagram and hydraulic signatures of model results with Gaussian noise and trend surface.

4.4.3 Effects of Noise and Trend Data on Entropy

The addition of random noise and trend data to the hydraulic signature of a leak results in an increase in total entopy (I_T) of the surface, as indicated in Table 4.5. The change in entropy is a function of the nature and magnitude of noise applied to the model results. The addition of uniformly distributed random noise (Fig. 4.4e) and normally distributed random noise (Fig. 4.6e) results in similar increases in information content. The largest increase in information content resulting from the addition of a single noise overlay was observed with the trend surface (Fig. 4.4e). Similar increases were observed with the application of uniformly distributed random noise to the model data.

As the magnitude of the hydraulic signature relative to the noise decreases, the information content of the surface decreases, and approaches that of the noise. This effect is observed when the noise and trend surfaces are applied to the results of different modeling scenarios. The application of trend data and uniform random noise to the hydraulic signatures of leakage through windows results in a decrease in the total information content of the surfaces (Fig. 4.7d). Similar trends are observed when the applied uniform random noise is increased by a factor of two, in conjunction with trend data (Fig. 4.8d), and with the application of Gaussian noise and trend data to model results (Fig. 4.9d). These results indicate that as the number of sampling points increases, the information content for a surface with a small hydraulic signature relative to the noise approaches the total information content of the noise surface.

Table 4.5. Total Entropy (I_T) Values for Model Results

Kwin (cm/s)	Total Entropy
1×10^{-2}	0.923
1×10^{-3}	0.398
1×10^{-4}	0.067
1×10^{-5}	0.00

4.4.4 Discrimination of Different Magnitudes of Leakage Without Noise

The dimensions and trends of the entropy envelopes vary significantly, depending on the magnitude of leakage. The entropy envelope for leakage through a high hydraulic conductivity window generally has a wider range of values per number of points sampled than those calculated for windows with lower hydraulic conductivity values (Fig. 4.3a). The total entropy values tend to increase as the hydraulic conductivity of the windows increase (Fig. 4.3a and Table 4.5). This can be related to the spatial variability of the data sets. As the hydraulic conductivity of the windows increase, flux through the windows increase. This results in larger areas being impacted by the leakage.

The minimum number of sampling points needed to discriminate between leakage of different magnitudes may be determined from Fig. 4.3a. The discriminator (N_D) is based on the points of convergence between the upper and lower boundaries of adjacent entropy envelopes. Visual detection of the hydraulic signature of the leak becomes more difficult as the signal to noise ratio decreases.

4.4.5 Discrimination of Model Results and Noise of Similar Magnitude

The number of points necessary to discriminate model results and normally distributed random noise with similar RMSN values were evaluated. Random Gaussian noise was generated with a mean of zero and a standard deviation equal to the RMSS of the model results. This resulted in the generation of noise surfaces with RMSN values approximately equal to the RMSS of the model results.

The number of points necessary to differentiate the model results and noise of similar magnitude is delineated by the point of convergence of adjacent entropy envelope boundaries. Approximately 20 random sampling points are necessary to differentiate normally distributed random noise from the hydraulic signature of leakage through a window with a hydraulic conductivity of 1×10^{-2} cm/s (Fig. 4.10). Similarly, approximately 25 and 70 points are required to differentiate entropy envelopes of Gaussian noise and leakage through windows with hydraulic conductivity values of 1×10^{-3} cm/s (Fig. 4.11) and 1×10^{-4} cm/s (Fig. 4.12), respectively. These results suggest that more sampling points will be required to discriminate leakage from background noise of similar RMSN, as the hydraulic signature of a leak diminishes.

4.4.6 Discrimination of Hydraulic Signature with Varying Magnitudes of Noise

In order to better understand the relationship between entropy and noise, RMSS values were calculated for model results and surfaces derived from the addition of noise and trend data (Table 4.6). The number of points required to discriminate the hydraulic signature of a leak from that of a leak impacted by noise was evaluated. The discriminator is based on the convergence of adjacent entropy envelopes, as described above. Approximately 30 sampling points are indicated to discriminate between the entropy envelopes for the model, and a model with uniformly distributed random noise (Fig. 4.4e). Similarly, approximately 50 sampling points are required to discriminate between the entropy envelopes for the model with uniform noise and model with trend surface.

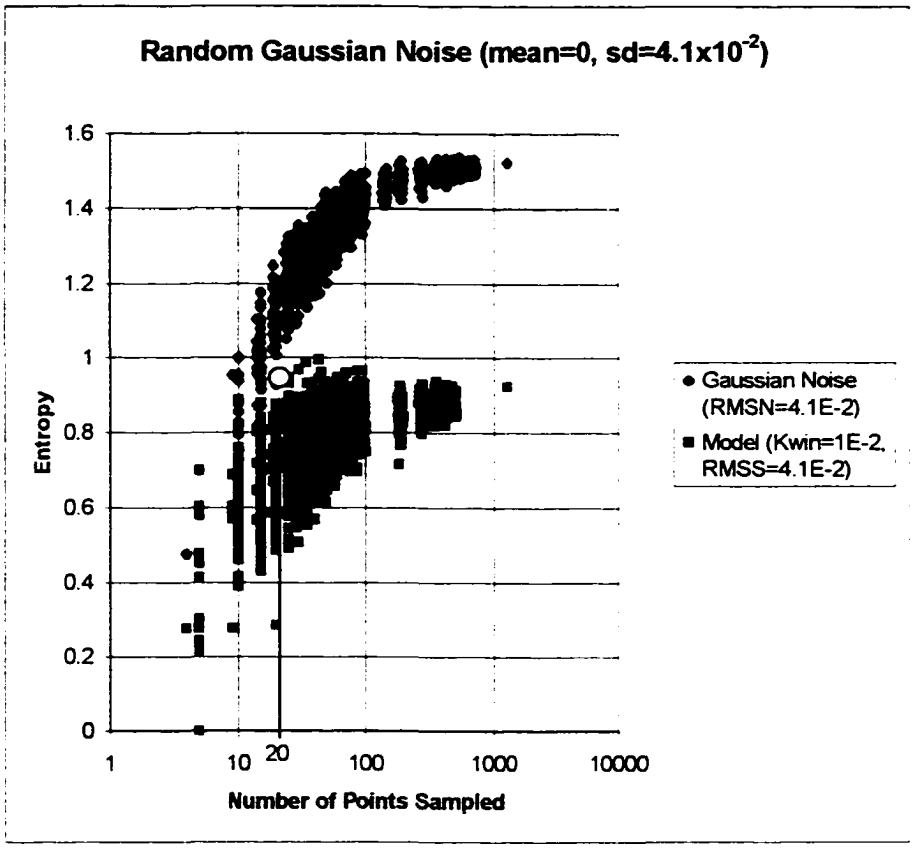

Fig. 4.10 Entropy diagram for model results (K_{win}=1x10^{-2} cm/s) and Gaussian noise with similar RMS values.

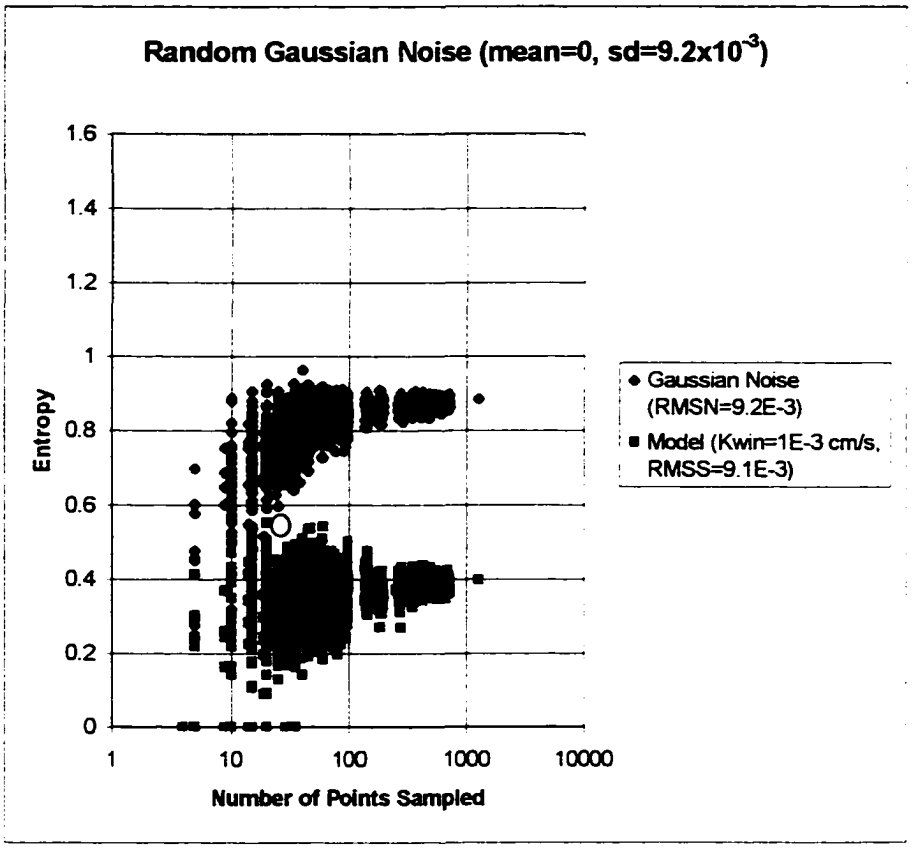

Fig. 4.11 Entropy diagram for model results (K_{wn}=1x10^{-3} cm/s) and Gaussian noise with similar RMS values.

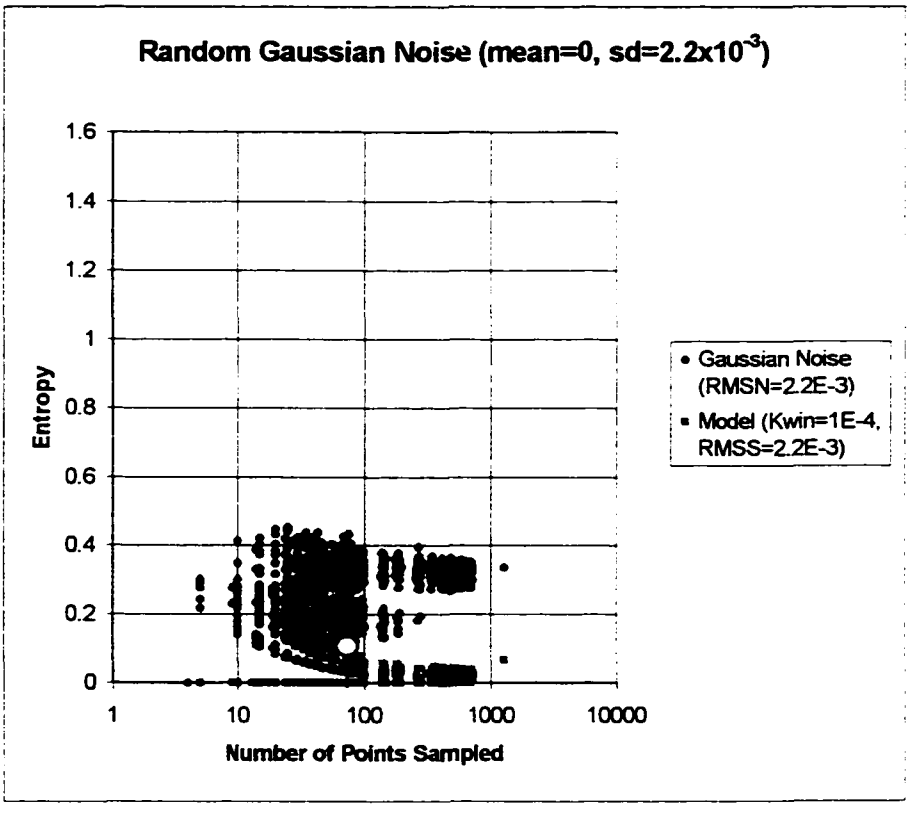

Fig. 4.12 Entropy diagram for model results (K_{win}=1x10^{-4} cm/s) and Gaussian noise with similar RMS values.

Table 4.6. Total entropy (I_T) and root mean square signalvalues for different simulations with noise and trend surface added.

	Kwin (cm/s) 1×10^{-2}		Kwin (cm/s) 1×10^{-3}		Kwin (cm/s) 1×10^{-4}	
Model and Specific Overlay	I_T	RMSS	I_T	RMSS	I_T	RMSS
Model Results Only	0.923	0.0412	0.398	0.0091	0.067	0.0022
Model with Gaussian Noise ($\bar{x} = 0$)	1.212	0.0431	1.079	0.0161	1.049	0.0138
Model with Uniform Noise (0-0.05)	1.224	0.0648	1.082	0.0344	1.014	0.0265
Model with Uniform Noise (0-0.1)	1.422	0.0911	1.336	0.0622	1.304	0.0547
Model with Trend Surface	1.463	0.1043	1.402	0.0763	1.398	0.0691
Model with Gausian Noise and Trend Surface	1.515	0.1051	1.476	0.0776	1.478	0.0705
Model with Uniform Noise (0-0.05) and Trend Surface	1.530	0.128	1.488	0.0997	1.485	0.0922
Model with Uniform Noise (0-0.1) and Trend Surface	1.609	0.1534	1.571	0.1252	1.569	0.1175

Though not as well defined, approximately 400 sampling points are required to discriminate between the model with trend surface and model with noise and trend surface.

The procedure described above was repeated for simulation results of flow through windows with $K_{win}=1\times10^{-3}$ cm/s and 1×10^{-4} cm/s with the same noise and trend data applied to the surface. Discriminator values were also selected for the model results with uniform noise (0-0.1) and trend data (Fig. 4.8e), as well as model results with Gaussian noise and trend data (Fig. 4.9e) using the procedure described above. The discriminator values for adjacent pairs of entropy envelopes for all data sets presented in Figs. 4.4e, 4.5e and 4.6e are plotted against the RMSS value for the upper most entropy envelope of the pairs (Fig. 4.13). The general trend of the data indicates that the number of points necessary to differentiate entropy envelopes increases as the magnitude of noise increases.

4.4.7 Signal To Noise Ratio

The RMSS values for model results with noise and trend surfaces are plotted against the total entropy of each surface in Fig. 4.14. The RMSN values for the noise and trend surface combinations, and their respective total entropy values, are included in the figure. Inspection of Fig. 4.14 indicates a significant relationship between the signal and noise RMS values and entropy. An increase in the RMSS is indicative of an increase in the deviation of a surface relative to a reference surface. This may result from an increase in the magnitude of leakage through the window, or the addition of noise or trend surfaces to the model data. The reference surface for this study is the hydraulic head distribution associated

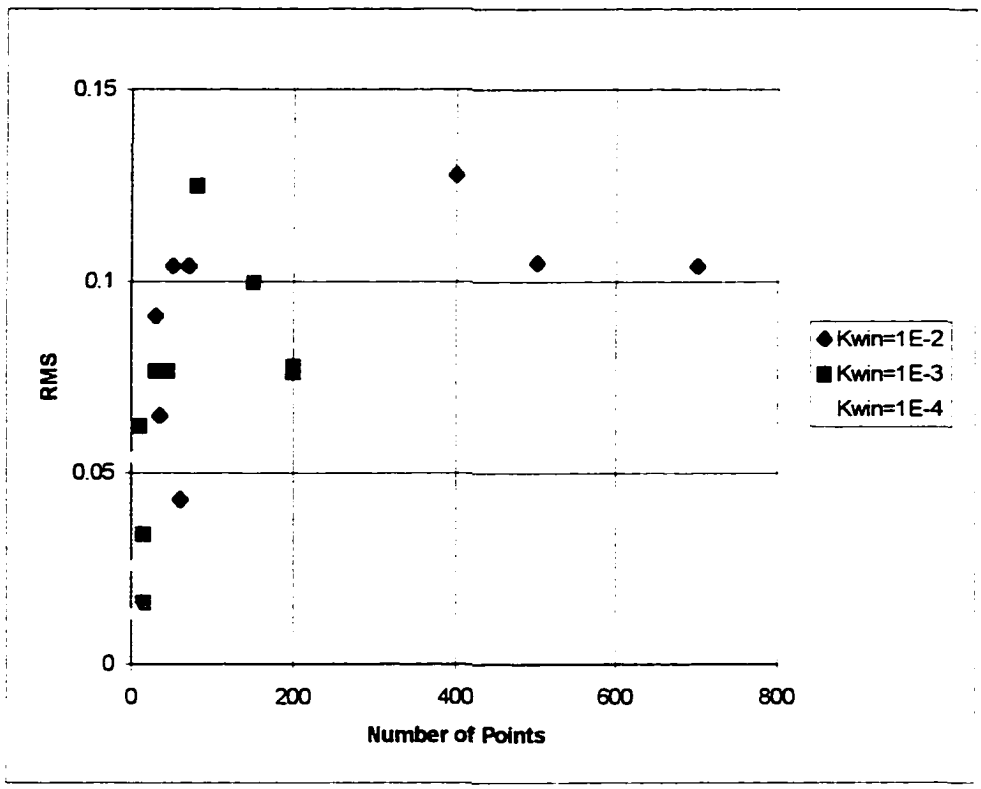

Fig. 4.13 Discriminator numbers (N_D) for all model results with random noise and trend surfaces.

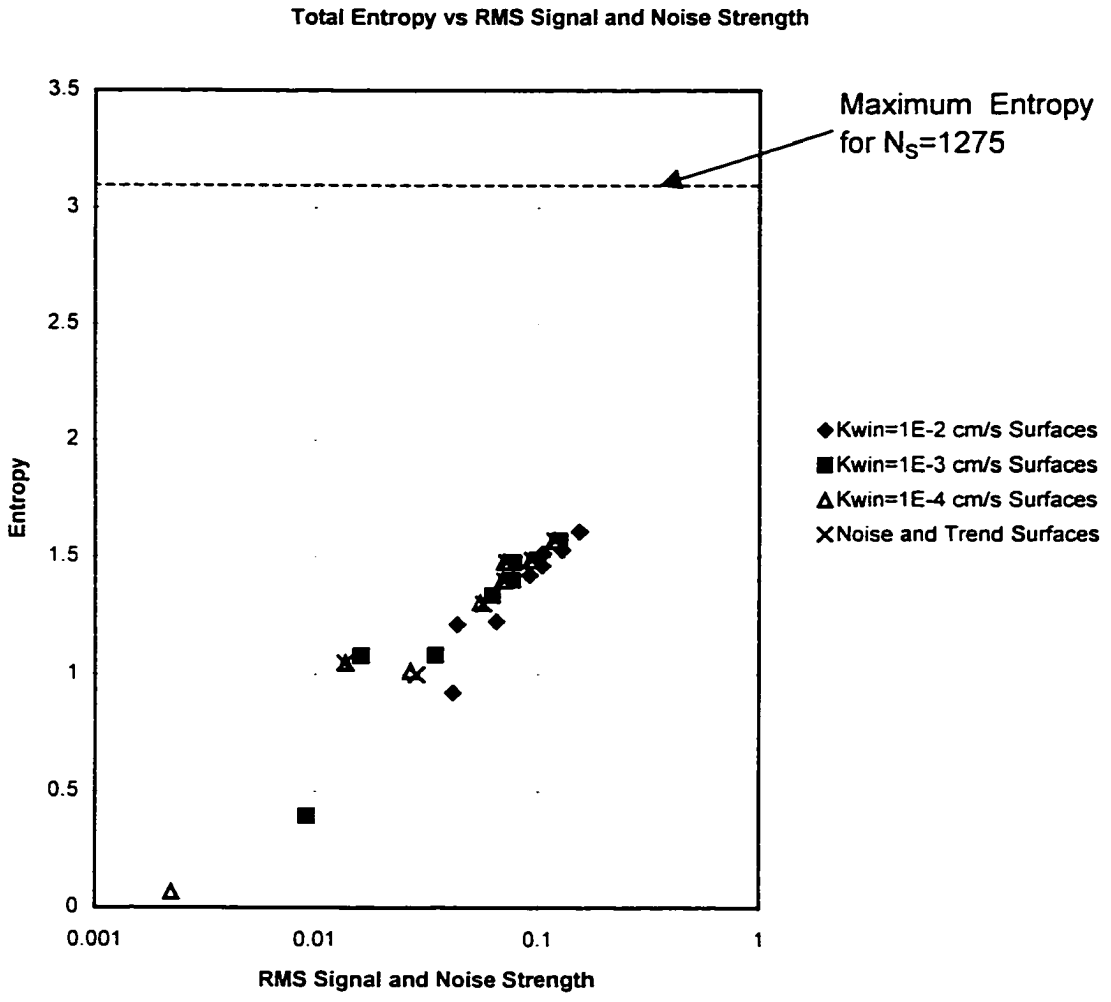

Fig. 4.14 Signal to noise strength versus the total entropy of model results and surfaces derived from the addition of noise to model results.

with a competent vertical barrier (i.e., no leak). As the variability of the surface increases, as indicated by an increase in the RMS values, the total entropy of the surface increases. This may result from the increased number of bins occupied by the hydraulic signature or noise. The theoretical maximum entropy for the surface is denoted by the dotted line in Fig. 4.14.

The relative magnitude of the RMSS of the hydraulic signature (signal) to the RMSN of the noise and/or trend surfaces is measured by the signal to noise ratio (SNR). The SNR values for all surfaces used in this study are listed in Table 4.7 and plotted in Fig. 4.15. Two mechanisms may account for an increase in the SNR - the magnitude of noise applied to a surface may be decreased, or the magnitude of the hydraulic signature may be increased. The former is best illustrated by data from the hydraulic signatures of leakage through the 1×10^{-2} cm/s hydraulic conductivity window. As the magnitude of noise increases, the resulting SNR decreases and the total entropy of the surface increases. Decreasing the magnitude of noise applied to a surface is responsible for the decrease in entropy observed in data from the hydraulic signatures of leakage through the windows with hydraulic conductivity values of 1×10^{-3} cm/s and 1×10^{-4} cm/s (Fig. 4.15). The SNR asymptotically approaches the total entropy value for each surface as it increases to the point at which no noise is present (e.g., infinite signal to noise ratio).

Table 4.7. Signal to noise ratio for model and derived surfaces

Model and Specific Overlay	Kwin 1×10^{-2} (cm/s)	Kwin 1×10^{-3} (cm/s)	Kwin 1×10^{-4} (cm/s)
Model with Gaussian Noise ($\bar{x} = 0$)	3.16	1.18	1.01
Model with Uniform Noise (0-0.05)	2.29	1.22	0.94
Model with Uniform Noise (0-0.1)	1.61	1.10	0.97
Model with Trend Surface	1.47	1.08	0.97
Model with Gausian Noise and Trend Surface	1.46	1.07	0.98
Model with Uniform Noise (0-0.05) and Trend Surface	1.36	1.06	0.98
Model with Uniform Noise (0-0.1) and Trend Surface	1.28	1.05	0.98

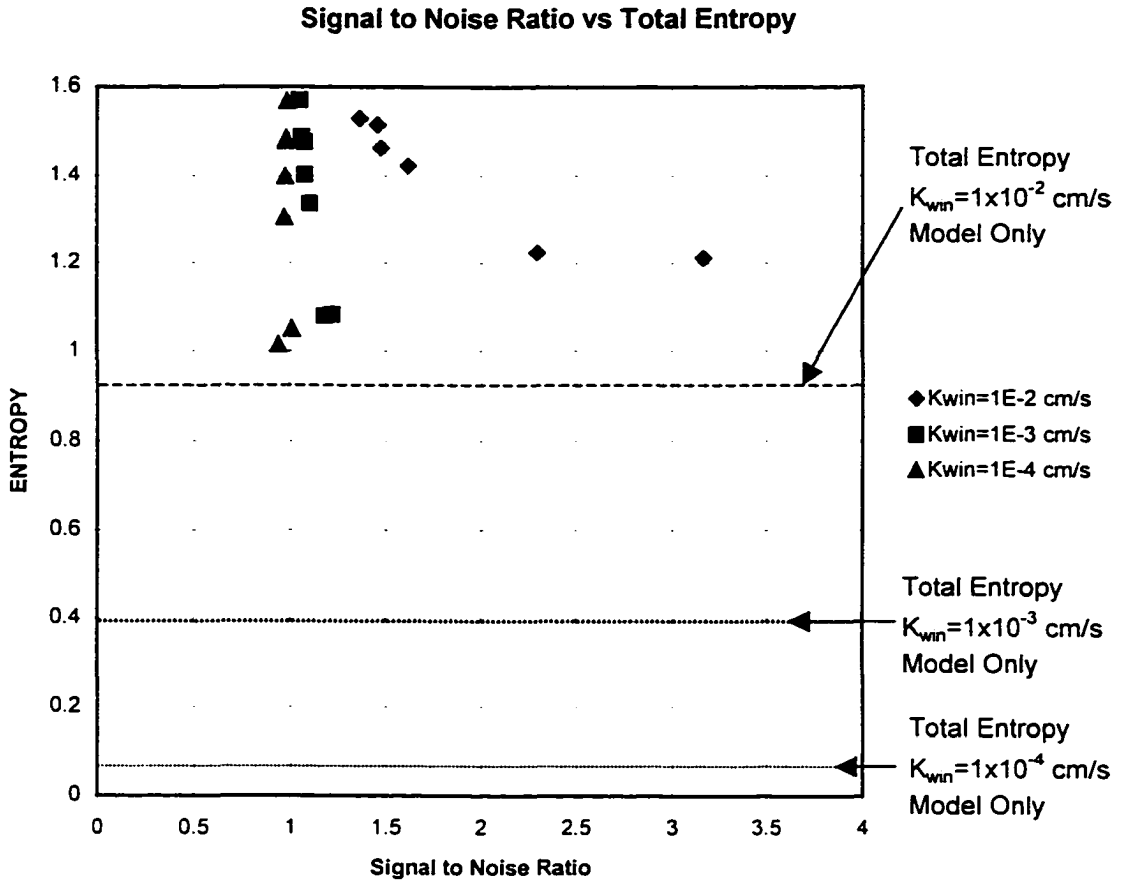

Fig. 4.15 Signal to noise ratio plotted against the total entropy (I_T) of model results and surfaces derived from the application of noise to model results.

4.4.8 Entropy Threshold Number

The minimum number of sampling points necessary to discriminate between the entropy envelopes of different hydraulic signatures and noise has been discussed. Now, the maximum number of sampling points necessary to characterize the information content of surfaces resulting from leakage is addressed. As noted previously, information content generally increases as the number of sampling points increases. The rate of increase in information content generally diminishes beyond an unspecified number of sampling points. For example, as the number of sampling points increases in Fig. 4.16 and 4.17, the entropy envelopes narrow and converge on the total entropy value.

As the number of sampling points increases, so would costs associated with installation and monitoring. The cost-effectiveness of acquiring additional data points must be evaluated against established criterium. For this study, the criteria for determining when sufficient data have been collected is based on information content. It is assumed that the information content gained by increasing the number of data points beyond that which corresponds to the ninetieth percentile of the total entropy is not necessary to adequately define a surface. Conversely, it is assumed that a loss of 10% of the total information content of a surface is acceptable.

The entropy threshold number (N_{ET}) is defined as the number of random sampling points necessary to capture 90% of the total information content of a surface, which

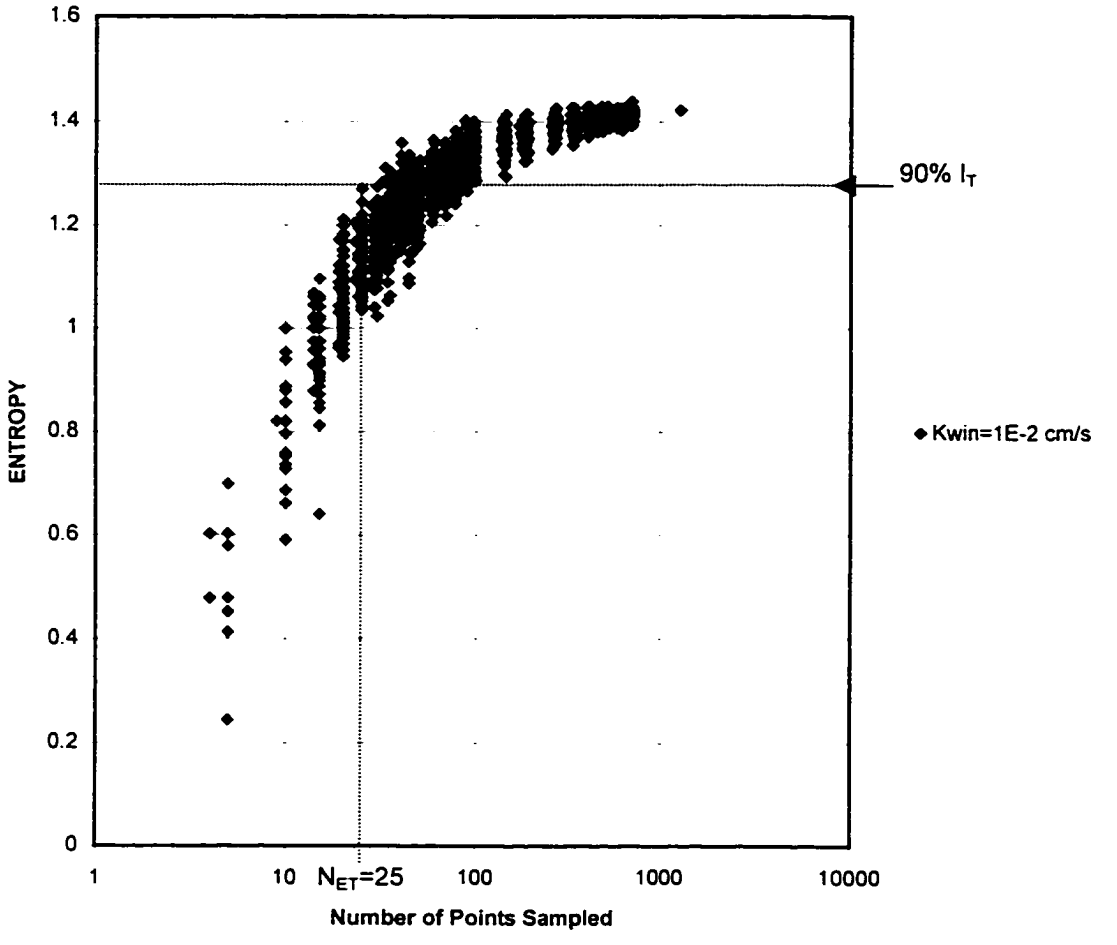

Fig. 4.16 Signal to noise ratio plotted against the total entropy (I_T) of model results and surfaces derived from the application of noise to model results.

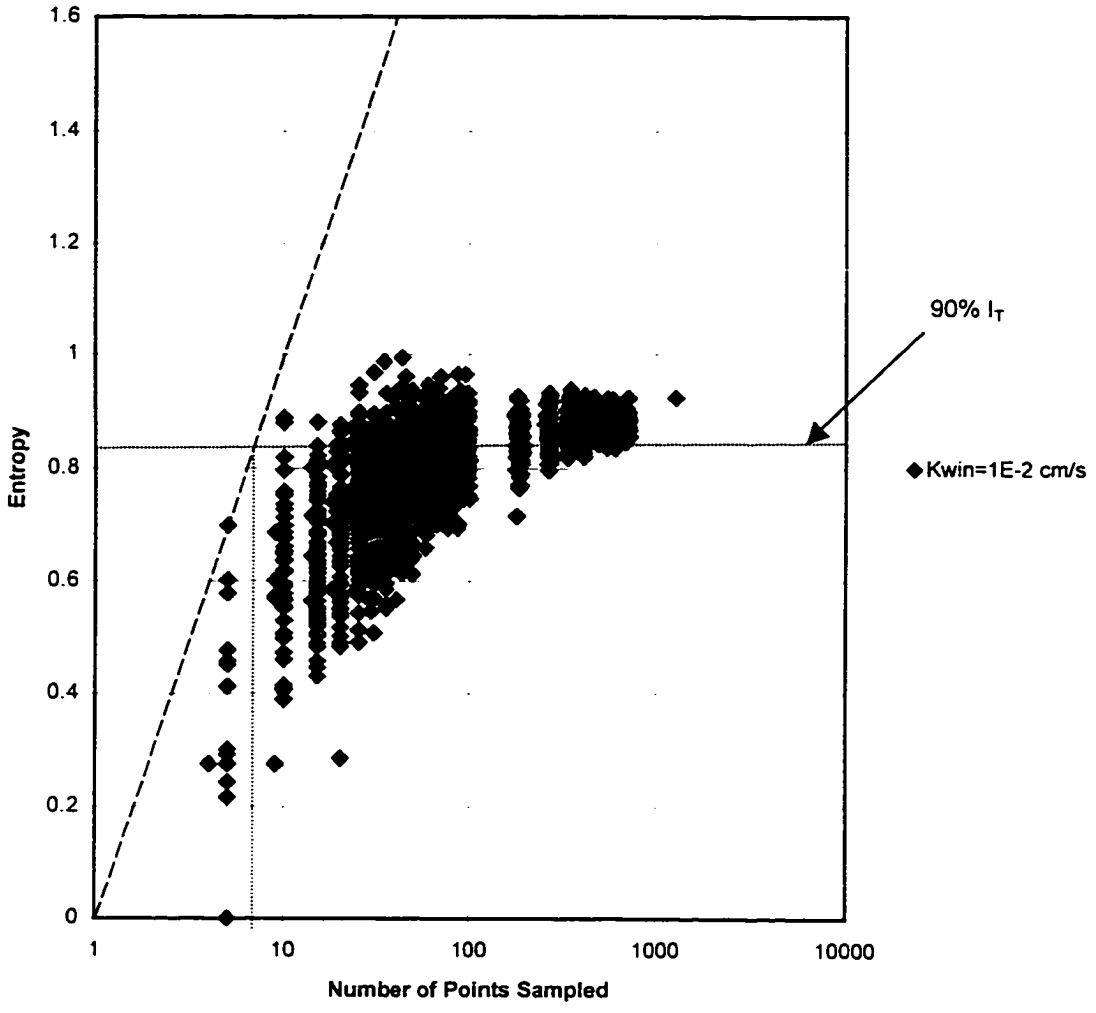

Fig. 4.17 Determination of N_{ET} for model results (K_{win}=1x10^{-2} cm/s) with ambiguous entropy envelope boundaries.

corresponds to the intersection of a line delineated by $0.9\times I_T$ and the upper boundary of the entropy envelope (Fig. 4.16). For data sets with less distinct entropy envelope boundaries (Fig. 4.17), the $0.9\times I_T$ line is extended to intersect the maximum entropy line, which corresponds to the upper entropy envelope boundary for relatively small sample sizes. The entropy threshold number for such cases can be calculated by raising the value $(0.9\times I_T)$ to the power of 10. The N_{ET} values for the previously described data sets are presented in Table 4.8.

The plot of N_{ET} versus the RMS for signal and noise strength (Fig. 4.18) reinforces the previous observation that the number of points necessary to adequately sample the surface increases with magnitude of noise. A plot of the entropy threshold number against the signal to noise ratio is presented in Fig. 4.19. This figure illustrates trends similar to Fig. 4.15. As the SNR increases the number of random sampling points necessary to adequately define the surface decreases. Conversely, the SNR may decrease if the system noise increases or if the hydraulic signature of the leak decreases. As the level of noise increases the number of points necessary to capture the 90% of the total information content of the surface increases. As the magnitude of noise increases to the point where the hydraulic signature is completely masked by noise (e.g., SNR≈1), an increase in the number of points sampled will not result in any additional gain in information content, and the leak will be undetectible, regardless of the number of points sampled.

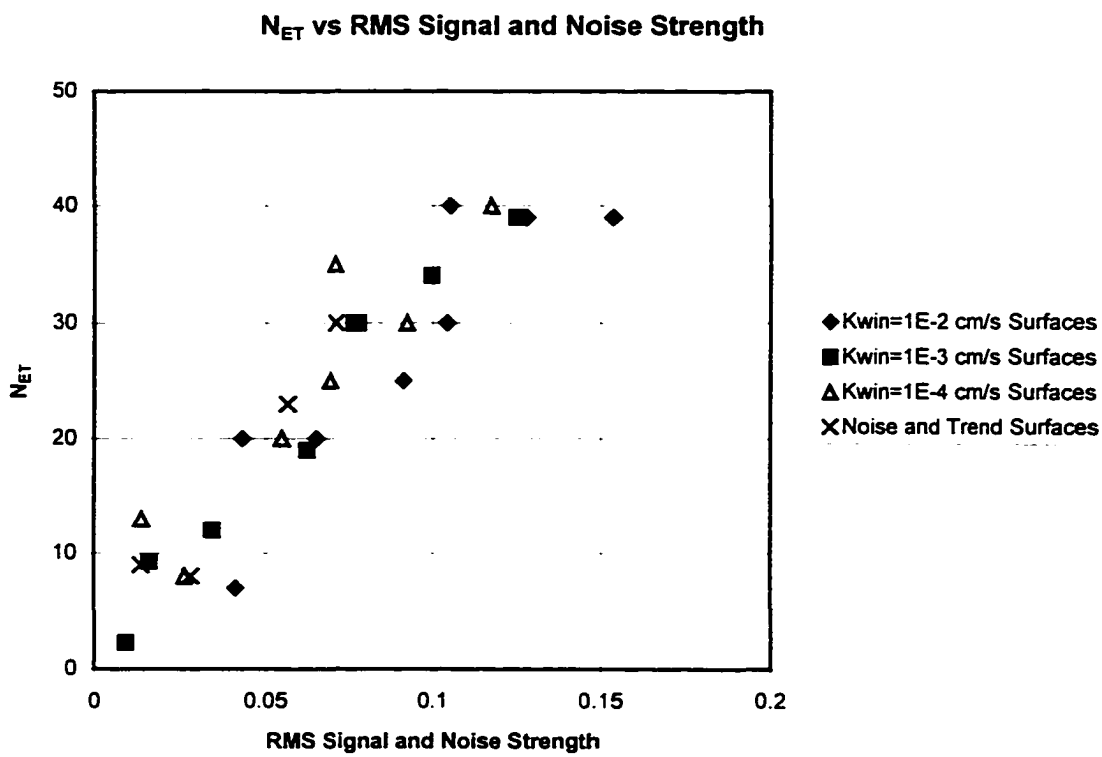

Fig. 4.18 Signal and noise strength plotted against the entropy threshold numbers for simulation results and surfaces derived from the addition of noise to model results.

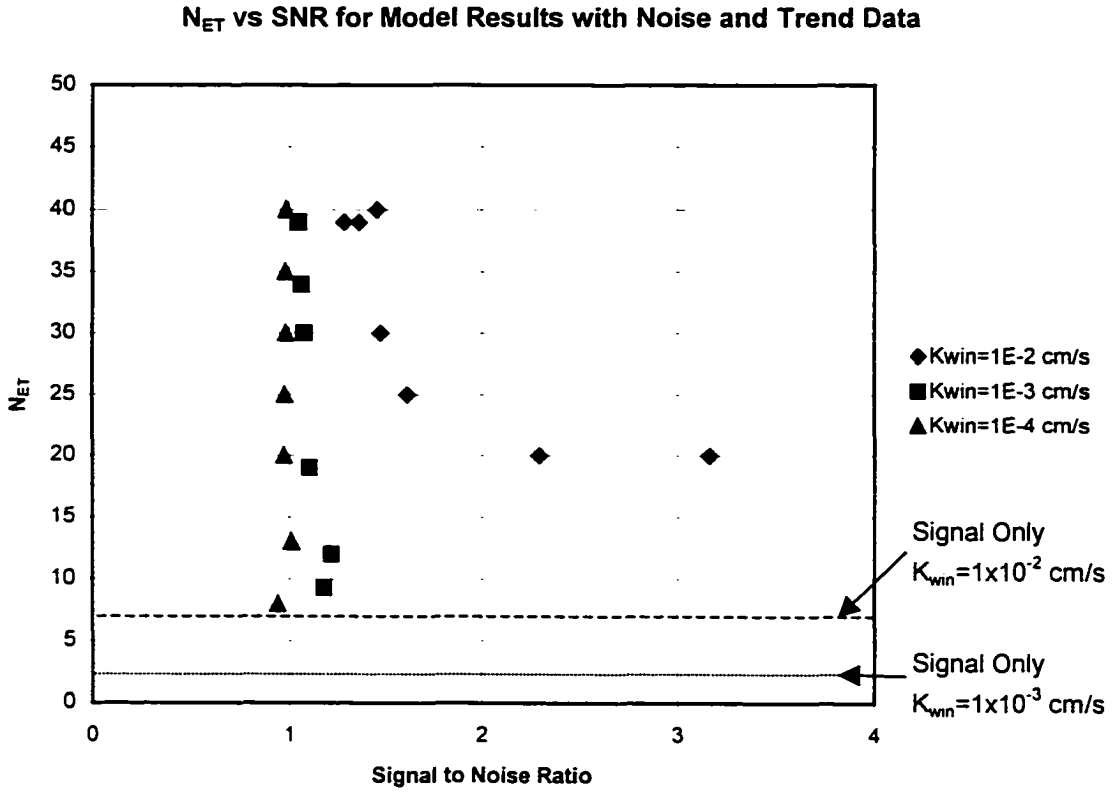

Fig. 4.19 Signal to noise ratio versus entropy threshold number for simulation results and surfaces derived from the application of noise to model results.

Table 4.8. Entropy threshold Numbers

Model and Specific Overlay	Kwin (cm/s) 1×10^{-2}	Kwin (cm/s) 1×10^{-3}	Kwin (cm/s) 1×10^{-4}
Model Results Only	7	2.3	1.1
Model with Gaussian Noise ($\bar{x} = 0$)	20	9.3	13
Model with Uniform Noise (0-0.05)	20	12	8
Model with Uniform Noise (0-0.1)	25	19	20
Model with Trend Surface	30	30	25
Model with Gausian Noise and Trend Surface	40	30	35
Model with Uniform Noise (0-0.05) and Trend Surface	39	34	30
Model with Uniform Noise (0-0.1) and Trend Surface	39	39	40

The values for N_{ET} may be related to a dimensionless box ratio (r) using a method presented by Barnsley, and others (1988), by

$$\left(\frac{L_{\max}}{L_{box}}\right)^{D} = \frac{1}{r^{D}} \qquad [11]$$

where D is the fractal dimension (assumed to equal 2.0), L_{max} is equal to the square root of N_T, and L_{box} is equal to the square root of N_{ET}. By solving for r, the dimensionless box ratio may be obtained which, when multiplied by 100, yields the percentage of area that must be sampled to capture the specified information content of a surface. The results presented in Table 4.9 reinforce the observation that the number of sampling points must increase as the level of noise increases in order to adequately describe a surface.

In Figs. 4.20, 4.21 and 4.22, the values for N_{ET}, SNR and N_D are listed below the appropriate hydraulic signatures. The disriminator numbers (N_D) represent the number of sampling points necessary to differentiate between surfaces of increasing noise, derived from the same model results. Several general trends, consistent with previously stated observations, are visible in these figures. As the noise level increases for a specific model result, the SNR decreases and the N_{ET} increases. This trend is consistent for the three noise overlays evalutated in this study. As the leak becomes progressively weaker, an increased number of points, N_D, is necessary to discriminate between a leak and noise of equal RMS strength.

Table 4.9. Box ratio numbers (r) derived from N_{ET} values.

Model and Specific Overlay	Kwin (cm/s) 1×10^{-2}	Kwin (cm/s) 1×10^{-3}	Kwin (cm/s) 1×10^{-4}
Model Results Only	0.074	0.042	1.0291.1
Model with Gaussian Noise ($\bar{x} = 0$)	0.125	0.085	0.101
Model with Uniform Noise (0-0.05)	0.125	0.097	0.079
Model with Uniform Noise (0-0.1)	0.14	0.122	0.125
Model with Trend Surface	0.153	0.153	0.14
Model with Gausian Noise and Trend Surface	0.177	0.153	0.166
Model with Uniform Noise (0-0.05) and Trend Surface	0.175	0.163	0.153
Model with Uniform Noise (0-0.1) and Trend Surface	0.175	0.175	0.177

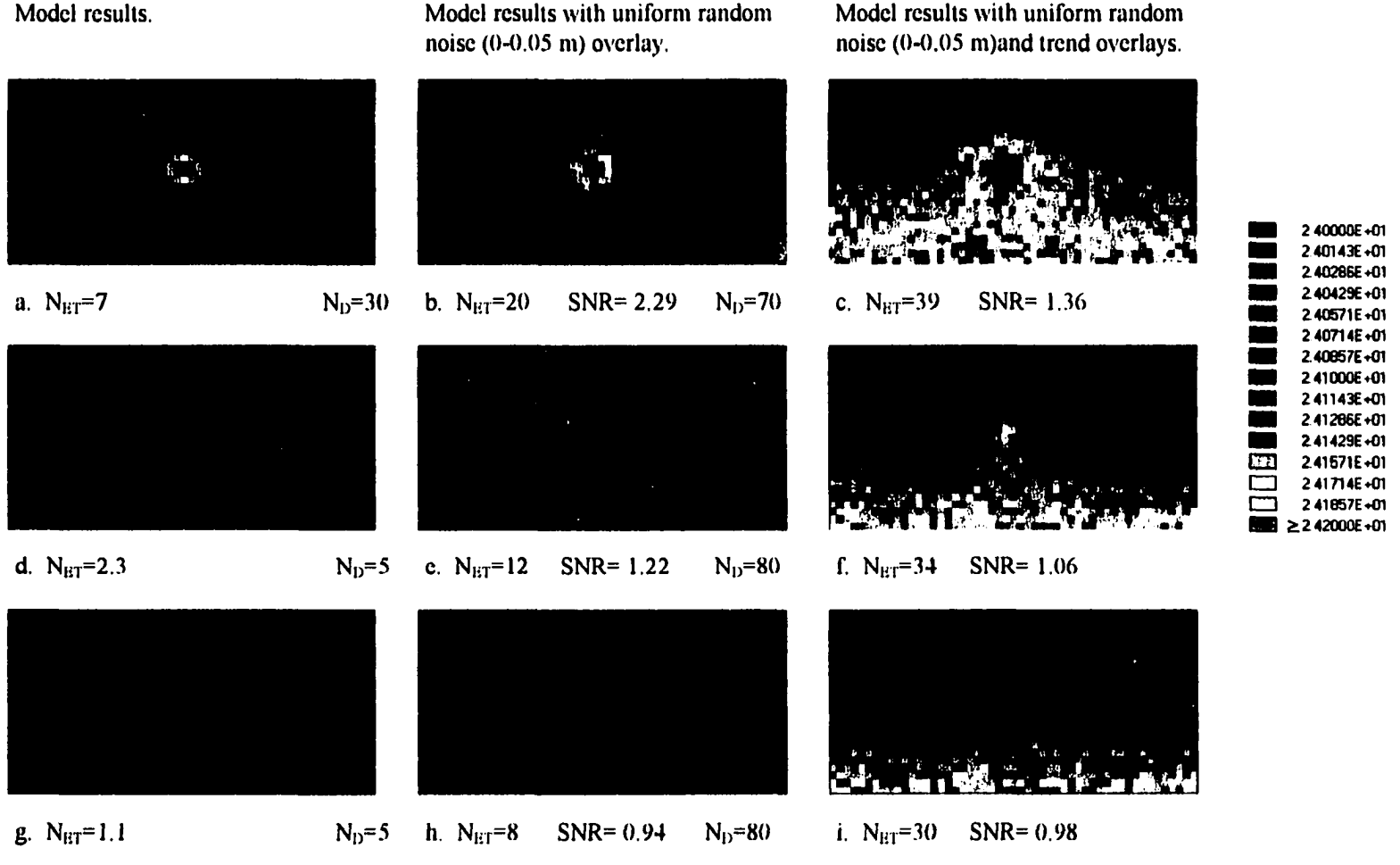

Fig. 4.20. Hydraulic signatures of leakage through windows with hydraulic conductivities of $K_{win}=1x10^{-2}$ cm/s (a., b., and c.), $K_{win}=1x10^{-3}$ cm/s (d., e., and f.) and $K_{win}=1x10^{-4}$ cm/s (g., h., and i.) and applications of uniform random noise (0-0.05 m) and trend data.

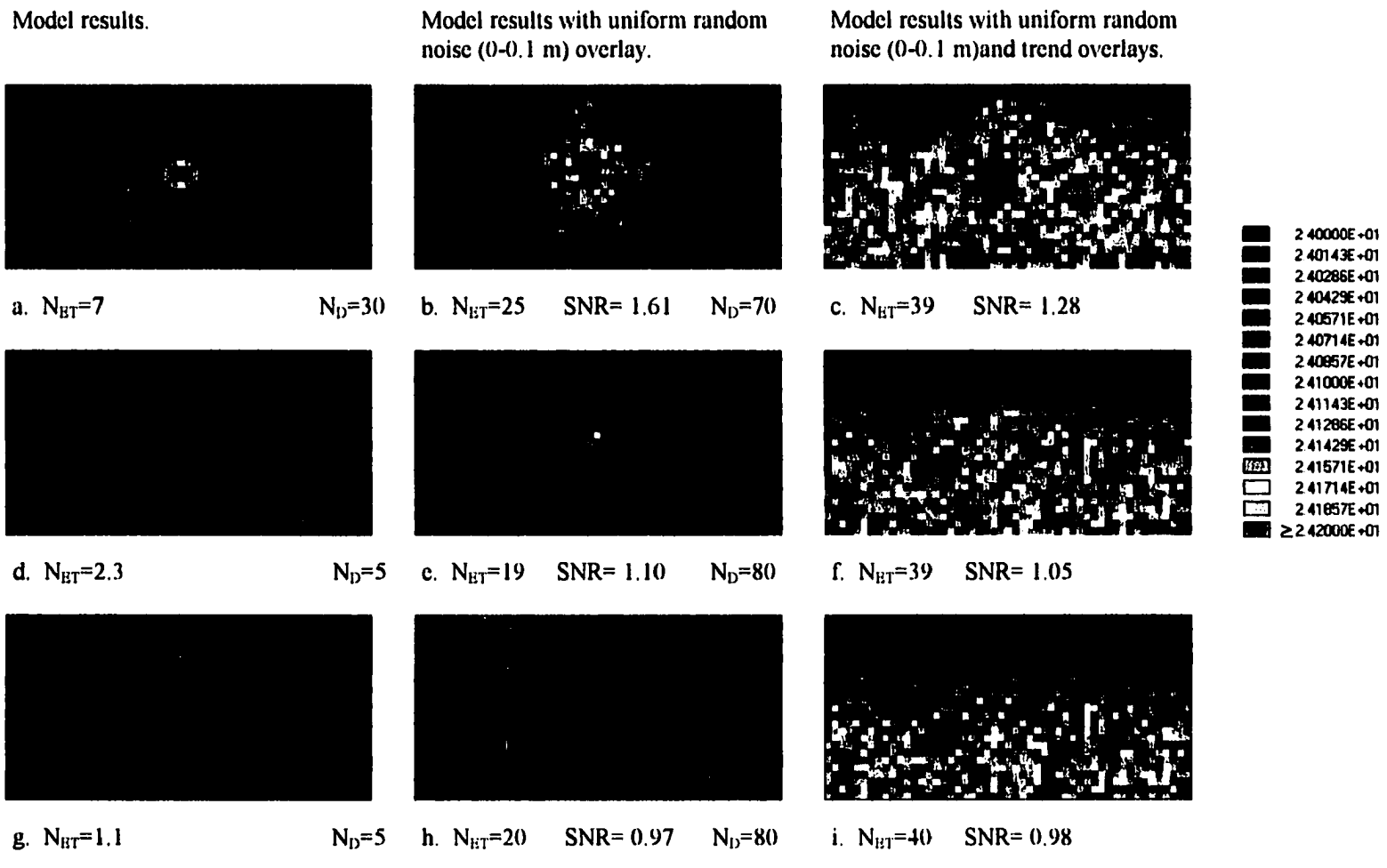

Fig. 4.21. Hydraulic signatures of leakage through windows with hydraulic conductivities of $K_{win}=1x10^{-2}$ cm/s (a., b., and c.), $K_{win}=1x10^{-3}$ cm/s (d., e., and f.) and $K_{win}=1x10^{-4}$ cm/s (g., h., and i.) and applications of uniform random noise (0-0.1 m) and trend data.

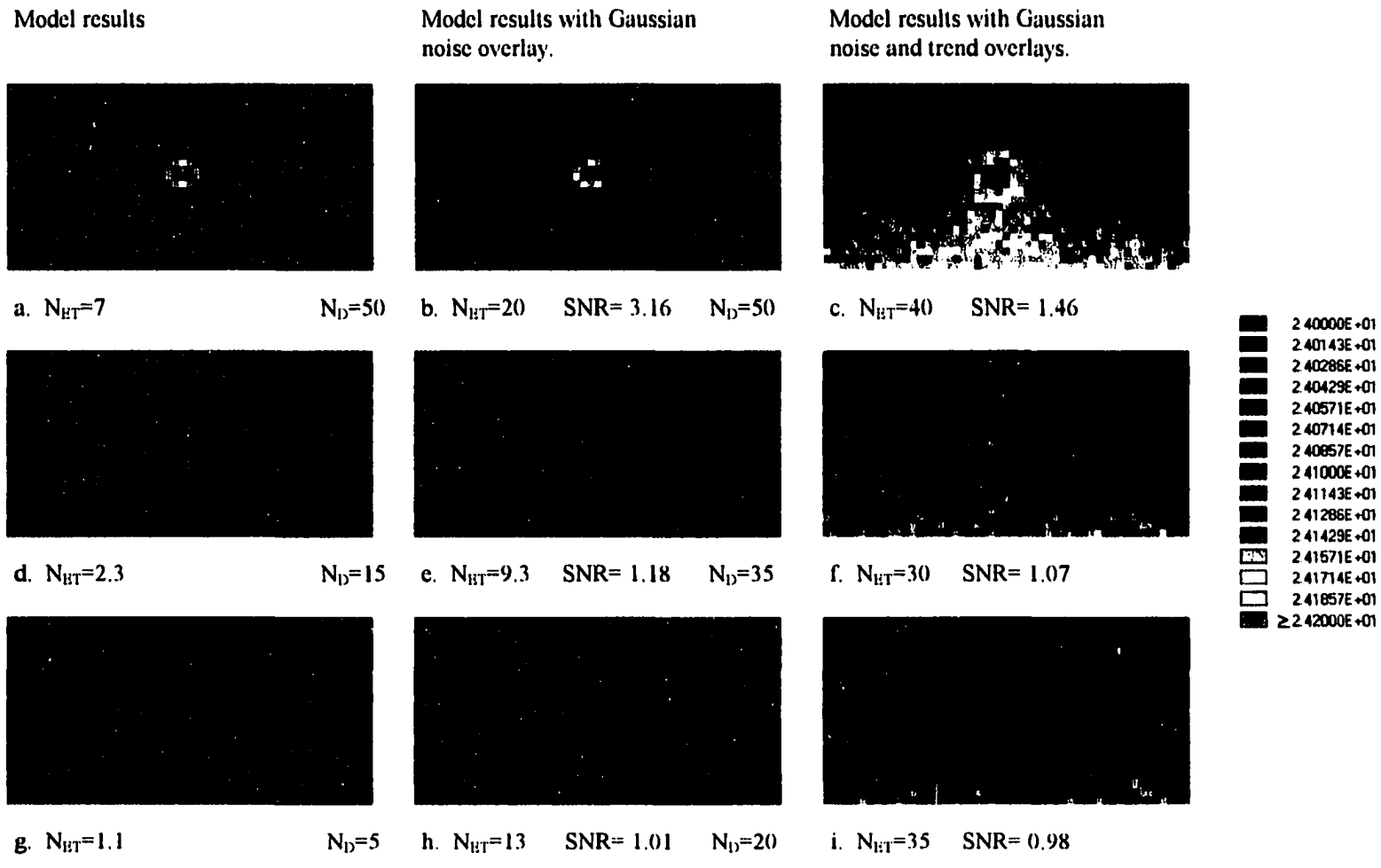

Fig. 4.22. Hydraulic signatures of leakage through windows with hydraulic conductivities of K_{win}=1x10^{-2} cm/s (a., b., and c.), K_{win}=1x10^{-3} cm/s (d., e., and f.) and K_{win}=1x10^{-4} cm/s (g., h., and i.) and applications of Gaussian noise and trend data.

4.5 CONCLUSIONS

A new method is presented to discriminate between leakage from a containment system of different orders of magnitude and to discriminate leakage from noise and trend surfaces. The proposed method represents a potential tool for evaluating the adequacy of monitoring systems at existing and proposed hazardous waste containment systems. Based on the results presented above, the following conclusions are made:

- The effect of increasing the number of random sampling points used to calculate information content is dependant on the magnitude of the hydraulic signature and the nature and magnitude of noise applied to the model results;
- As the number of sampling points increases for a surface characterized by a small RMSS relative to the noise RMSN, the total information content approaches that of the noise.
- As the number of sampling points increases, the range of entropy values becomes progressively smaller, resulting in less uncertainty in the estimation of informational entropy of a surface;
- The informational content of a sample points will approximate the total entropy of the surface as the sample PDF approaches that of the surface;
- As the magnitude of noise increases relative to the hydraulic signature, the entropy values increase. Conversely, as the magnitude of the noise decreases relative to that of the hydraulic signature, information content decreases. This trend agrees

favorably with the observations of Shannon (1948) and Jaynes (1957). This is especially evident when comparing the total entropy (I_T)values of the surfaces.

- Informational entropy can discriminate between hydraulic signatures and noise with similar RMS values.
- Informational entropy can discriminate between hydraulic signature of leakage of different orders of magnitude.
- Informational entropy can discriminate between hydraulic signature of leaks and leaks with differing magnitudes of noise.
- Entropy calculations are relatively sensitive to the selection of histogram intervals and the location of the histogram origin (i.e., minimum value). This is significant in that entropy values may vary, depending on what value used as the origin (minimum) for the histogram. This appears to be most significant for the sample sets in which the majority of values are distributed over a narrow range. In such cases, the entropy values may vary significantly as the origin of the histogram is shifted.
- The histogram intervals used to calculate information content should be large enough to capture the spatial variability of the surfaces in question. However, the bin widths should not be smaller than the precision of the instruments used to acquire the data.
- As the magnitude of noise increases to the point where the hydraulic signature is completely masked (e.g., SNR<1), no additional information content is gained with an increase in the number of sampling points.

4.6 REFERENCES

American Petroleum Institute (1993). *Pump and Treat: The Petroleum Industry Perspective*. API, Washington, D.C.

Amorocho, J. and B. Espildora (1973). Entropy in the assessment of uncertainty in hydrologic systems and models. Water Resources Research, 9(6):1511-1522.

Barnsley, M.R., Devaney, R.L., Mandelbrot, B.B., Peitgen, H., Saupe, D. and Voss, R.F. (1988). *The Science of Fractal Images*. eds. H. Peitgen and D. Saupe, Springer-Varlag, New York, 58-63 pp.

Bartels, J.H.M., Janse, T.A.H.M., Pijpers, F.W., and P.C. Thijssen (1985). Improvement of the representation of water quality by application of information theory, Analytica Chimica Acta, 177:47-55.

Bodocsi, A., McCandless, R.M., and Ling, K.W. (1990). "Detection of Macro Defects in Soil-Bentonite Cutoff Walls," Remedial Action, Treatment and Disposal of Hazardous Waste, Proceedings of the Fifteenth Annual Research Symposium, Cincinnati, OH, April 10-12, 1989. EPA/600/9-90/006.

Chapman, T.G. (1986). "Entropy as a measure of hydrologic data uncertainty and model performance," Journal of Hydrology, 85:111-126.

Chiu, C. (1986). "Entropy and Probability concepts in hydrology," Journal of Hydraulic Engineering, 113(5):583-600.

Eastman, J.R. (1993). *IDRISI Technical Reference*, Version 4.0, Revision 3, Clark University, Worchester, MA..

Eastman, J.R. (1995). *IDRISI for Windows: User's Guide*, Version 1.0, Clark University, Worchester, MA.

Englehardt, J.D. and Lund, J.R. (1992). "Information theory in risk analysis," Journal of Environmental Engineering, 118(6):890-903.

Farajalla, N.S. and Vieux, B.E. (1995). "Capturing the Essential Spatial Variability in Distributed Hydrological Modeling: Infiltration Parameters," Journal of Hydrological Processes, 9(1):55-68.

Fetter, C.W. (1993). *Contaminant Hydrogeology*, Macmillan Publishing Company, New York, N.Y.

Gilham, R.W. and Burris, D.R. (1992). "In Situ Treatment Walls - Chemical Degradation, Denitrification, and Bioaugmentation." *Subsurface Restoration Conference Proceedings*, Dallas, TX, June 21-24, 1992.

Guiger, N. and Franz, T. (1995). *VISUAL MODFLOW, The Integrated Modelling Environment for MODFLOW and MODPATH, Version 1.1*, Waterloo Hydrogeologic, Ontario, Canada.

Isaaks, E.H., and Srivastava, R.M. (1989). *Applied Geostatistics*, Oxford University Press, New York, 561 pp.

Jaynes, E.T. (1957). *Papers on Probability, Statistics and Statistical Physics*, ed. R.D. Rosenkrantz, Kluwer Academic Publishers, Boston..

Johnson, M.W. (1992). "The Information Content of Continuous Functions and the Geodesic Principle," Rutherford Appleton Laboratory, Science and Engineering Research Council, Chilton, England, RAL-92-042.

Krstanovic, P.F. and Singh, V.P. (1992). "Evaluation of rainfall networks using entropy: I. Theoretical Development," Water Resources Management, 6:279-293.

Leopold, L.B. and Langbein, W.B. (1962). "The Concept of Entropy in Landscape Evolution," U.S. Geological Survey Professional Paper 500-a, U.S. Printing Office, Washington, D.C..

McDonald, M.G., and Harbuagh, A.W. (1988). "A Modular Three-Dimensional Finite-Difference Ground-Water Flow Model (MODFLOW)," U.S. Geological Survey Techniques of Water-Resources Investigation, Book 6, Chapter A1.

National Research Council (1994). *Alternatives To Ground Water Cleanup*, National Academy Press, Washington, D.C., 315 pp.

Papoulis, A., 1984. Probability, Random Variables and Stochastic Processes, McGraw-Hill, New York, 2nd ed., 500-567 pp.

Ross, R.R. and Beljin, M.S. (1995). "MODRISI: A PC Approach to GIS and Ground-Water Modeling," Proceedings, National Conference on Environmental Problem-Solving with Geographic Information Systems, Cincinnati, OH, September 21-23, 1994. EPA/625/R-95/004.

Ross, R.R. and Beljin, M.S. (1996). "Evaluation of Containment Systems Using Hydraulic Head Data," Journal of Environmental Engineering, 124(6): 575-578.

Shannon, C.E. (1948). "A Mathematical Theory of Communication," The Bell System Technical Journal, 27(3):379

Shannon, C.E. and Weaver, W. (1964). "The Mathematical Theory of Communication," University of Illinois Press, Urbana, 1964.

Tetra Tech (1997). *Evaluation of Subsurface Engineered Barriers at Waste Sites, Volume 1*. Prepared by Tetra Tech EM, Inc., for U.S. Environmental Protection Agency, Office of Solid Waste and Emergency Response, Washington, DC, September 30, 1997.

Thompson, S.K., 1992. Sampling. John Wiley & Sons, Inc., New York, 343 pp.

U.S. EPA (1994). "Methods for Monitoring Pump-and-Treat Performance," Office of Research and Development, R.S. Kerr Environmental Research Laboratory, Ada, OK, EPA/600/R-94/123.

Vieux, B.E. (1993). "DEM Aggregation and Smoothing Effects on Surface Runoff modeling," Journal of Computing in Civil Engineering, 7(3):310-338.

Vieux, B.E., Farajalla, N.S. (1994). "Capturing the essential spatial variability in distributed Hydrological Modeling: Hydrauiic Roughness," Journal of Hydrological Processes, 8(3):221-236.

Woodbury, A.D. and Ulrych, T.J. (1993). "Minimum relative entropy: Forward probabilistic modeling," Water Resources Research, 29(8):2847-2860.

Woodbury, A., Render, F. and Ulrych, T. (1995). "Practical probabilistic ground-water modeling," Ground Water, 33(4):532-538.

CHAPTER 5

SUMMARY, CONCLUSIONS AND RECOMMENDATIONS FOR FURTHER RESEARCH

5.1 SUMMARY AND CONCLUSIONS

The determination as to whether a physical containment system is functioning as designed may be made using the concepts presented in Chapter 1. The rate of leakage from the system may be estimated using the equations in Chapter 2. The calculated leakage rates may be compared to that deemed acceptable based on design criteria, at which time stake holders must determine if the leakage is significant and poses a risk to human health and the environment. Detecting and locating discrete zones of leakage from containment systems using hydraulic head data is problematic.

The hydraulic signature assessment method presented in Chapter 3 can estimate the grid spacing necessary to detect the hydraulic signatures of leakage from containment systems, with a specified confidence and specific constraints (i.e., dimensions and shape of hydraulic feature). The method assumes that criteria have been established that positively identify the hydraulic anomalies associated with leakage. For this study,

hydraulic head values of 0.05 and 0.1 m greater than the average head of the surface were identified as critical values indicating the presence of a leak. The hydraulic assessment method indicated that between 40 and approximately 300 monitoring points would be necessary to identify the hydraulic signature of leaks of varying magnitude.

A new approach to applying informational entropy to hydraulic head distributions is presented in Chapter 4. The method uses informational entropy to determine the minimum number of points necessary to capture 90% of the total information content of a hydraulic signature of a leak in the presence of different noise levels. The results indicate that the number of points necessary to capture the bulk of the information content is dependant on the strength of the hydraulic signature, relative to that of the noise. Very few samples are required to capture the spatial variability quiescent surfaces characterized by relatively small hydraulic signatures and no noise, while a significantly larger sample size will be required to capture the variability of relatively strong hydraulic signatures, especially in the presence of noise. If the SNR is less than 1, then no amount of sampling will detect the leak.

The proposed methods represent potential tools for evaluating the adequacy of existing and proposed hazardous waste containment systems in terms of their potential for detecting leakage in the presence of background noise. The major findings of this dissertation are as follows:

- The hydraulic signature associated with a minor leak in a vertical barrier may be difficult to detect;
- By using the nomographs, the probability of failing to detect the hydraulic signature of a leak can be estimated for a given monitoring well spacing and specified constraints;.
- The dimensions of the smallest hydraulic signature detectable with a given monitoring spacing can be estimated, given the appropriate constraints and specified confidence;
- The monitoring point spacing used at many hazardous waste sites is likely inadequate to detect the hydraulic signatures of all but the largest leaks;
- The effect of increasing the number of random sampling points to calculate the information content of vertical cross-sections of ground-water flow modeling results is dependant upon several factors, including the magnitude of the hydraulic signature and the nature and magnitude of noise applied to the model results;
- As the number of sampling points increases for a surface characterized by a relatively small RMSS for the hydraulic signature, relative to the noise RMSN, the total information content approaches that of the noise.
- As the number of sampling points increases, the range of entropy values becomes progressively smaller, resulting in less uncertainty in the estimation of informational entropy of a surface;
- The informational content of a sample points will approximate the total entropy of the surface as the sample PDF approaches that of the surface;

- As the magnitude of noise increases relative to the hydraulic signature, the entropy values increase. Conversely, as the magnitude of the noise decreases relative to that of the hydraulic signature, information content decreases. This trend agrees favorably with the observations of Shannon (1948) and Jaynes (1957), that as the uncertainty increases (in the form of increasing noise), so does the entropy. This is especially evident when comparing the total entropy (I_T)values of the surfaces.
- Informational entropy can discriminate between hydraulic signatures and noise with similar RMS values.
- Informational entropy can discriminate between hydraulic signature of leakage of different orders of magnitude.
- Informational entropy can discriminate between hydraulic signature of leaks and leaks with differing magnitudes of noise.
- Entropy calculations are relatively sensitive to the selection of histogram intervals and the location of the histogram origin (i.e., minimum value). The is significant in that entropy values may vary, depending on what value used as the origin (minimum) for the histogram. This appears to be most significant for the sample sets in which the majority of values are distributed over a narrow range. In such cases the entropy values may vary significantly as the origin of the histogram is shifted.
- The histogram intervals used to calculate information content should be large enough to capture the spatial variability of the surfaces in question. However, the

bin widths should not be smaller than the precision of the instruments used to acquire the data.

- As the magnitude of noise increases to the point where the hydraulic signature is completely masked by the noise (e.g., SNR<1), an increase in the number of points sampled will not result in the gain of additional information content of the surface;
- The informational entropy approach is more robust in that it accounts for random noise;
- For a simulation where $K^*=1\times10^5$ and no noise is present, $N_{ET}=7$, which means that only 7 sampling points are necessary to capture 90% of the total information content of the 1275 m^2 surface. Other surfaces would require sampling of approximately 7% of the surface area, or a box ratio of r=0.074.

5.2 RECOMMENDATIONS FOR FURTHER RESEARCH

The work presented in this dissertation represents advancements in the identification of hydraulic signatures associated with leakage from hazardous waste containment systems. Based on these findings, it is recommended that additional research address the following.

- Field evaluation of the proposed methodologies;

- Development of a computer code to allow the accurate calculation of the grid spacing necessary to identify the hydraulic signature of containment system leakage, given specific constraints. This should include the incorporation of basic ground-water flow equations to allow the estimation of hydraulic signature dimensions using a range different hydrogeologic assumptions;
- Modify the hydraulic signature assessment methodology for use with non-elliptical hydraulic signatures. For example, the hydraulic signature associated with leakage at the interface between the vertical barrier and cap will produce a asymmetrical hydraulic signature. Similar asymmetric hydraulic signatures are expected for leakage under a vertical barrier;
- Extend the hydraulic signature assessment methodology to predict the necessary spacing of monitoring wells for the detection of tracers, based on the calculated dimensions of the capture zone of each well;
- Apply the hydraulic signature assessment methodology to model surfaces with different statistical distributions of random noise;
- Evaluate the possibility of applying hydraulic signature assessment method for identification of improperly abandoned wells.

CHAPTER 6

BIBLIOGRAPHY

American Petroleum Institute (1993). *Pump and Treat: The Petroleum Industry Perspective*, API, Washington, D.C.

Amorocho, J. and B. Espildora (1973). Entropy in the assessment of uncertainty in hydrologic systems and models, Wat. Res. Res., 9(6):1511-1522.

Bakr, A.A.M (1976). Stochastic Analysis of the Effect of Spatial Variations of Hydraulic Conductivity on Groundwater Flow, Ph.D. Dissertation, New Mexico Institute of Mining and Technology, 243 pp.

Barnsley, M.R., Devaney, R.L., Mandelbrot, B.B., Peitgen, H., Saupe, D. and Voss, R.F. (1988). *The Science of Fractal Images*. eds. H. Peitgen and D. Saupe, Springer-Varlag, New York, 58-63 pp.

Bartels, J.H.M., Janse, T.A.H.M., Pijpers, F.W., and P.C. Thijssen (1985). "Improvement of the representation of water quality by application of information theory," Analytica Chimica Acta, 177:47-55.

Bear, J., Beljin, M.S., and Ross, R., (1992). *Fundamentals of Ground-Water Modeling, Ground Water Issue*, U.S. Environmental Protection Agency, Office of Research and Development, R.S. Kerr Environmental Research Laboratory, Ada, OK, EPA/540/S-92/005.

Bodocsi, A., McCandless, R.M., and Ling, K.W. (1990). "Detection of Macro Defects in Soil-Bentonite Cutoff Walls," Remedial Action, Treatment and Disposal of Hazardous Waste, Proceedings of the Fifteenth Annual Research Symposium, Cincinnati, OH, April 10-12, 1989. EPA/600/9-90/006.

Canter, L.W., and Knox, R.C. (1986). *Ground Water Pollution Control*, Lewis Publishers, Boca Raton, FL. 526 pp.

Chapman, T.G. (1986). "Entropy as a measure of hydrologic data uncertainty and model performance," J. Hydrol., 85:111-126.

Chiu, C. (1986). "Entropy and Probability concepts in hydrology," J. Hydr. Eng, 113(5):583-600.

Conover, W.J. (1980). *Practical Nonparametric Statistics*, John Wiley & Sons, New York, 493 pp.

D'Appolonia, D.J. (1980). "Soil-bentonite slurry trench cutoff," J. Geotech. Eng.., ASCE, 106(4):399-417.

Eastman, J.R. (1993). *IDRISI Technical Reference*, Version 4.0, Revision 3, Clark University, Worchester, MA..

Eastman, J.R. (1995). *IDRISI for Windows: User's Guide*, Version 1.0, Clark University, Worchester, MA.

Englehardt, J.D. and Lund, J.R. (1992). "Information theory in risk analysis," J. Envir. Eng., 118(6):890-903.

Evans, J.C. (1991).,"Geotechnics of Hazardous Waste Control Systems," Chapter 20, Foundation Engineering Handbook, 2nd ed., (H.Y. Fang, Ed.), Van Nostrand Reinhold , New York..

Farajalla, N.S. and Vieux, B.E. (1995). "Capturing the Essential Spatial Variability in Distributed Hydrological Modeling: Infiltration Parameters," J. Hydrol. Proc., 9(1):55-68.

Fetter, C.W. (1993). *Contaminant Hydrogeology*, Macmillan Publishing Company, New York, N.Y.

Freeze, R.A. (1975). "A Stochastic-Conceptual Analysis of One-Dimensional Groundwater Flow in Nonuniform Homogeneous Media," Water Resour. Res., 11(5):725-741.

Freeze, R.A. and Cherry, J.A. (1979). Groundwater. Prentice-Hall. 604 pp.

Gilbert, R.O. (1987). *Statistical Methods for Environmental Pollution Monitoring*, Van Nostrand Reinhold, New York., 320 pp.

Gilham, R.W. and Burris, D.R. (1992). "In Situ Treatment Walls - Chemical Degradation, Denitrification, and Bioaugmentation." *Subsurface Restoration Conference Proceedings*, Dallas, TX, June 21-24, 1992.

Grube, W.E., Jr. (1992). "Slurry Trench Cut-Off Walls for Environmental Pollution Control," Slurry Walls: Design, Construction and Quality Control. ASTM STP 1129, David B. Paul, Richard R. Davidson, and Nicholas J. Cavalli, Eds., American Society for Testing and Materials, Philadelphia.

Guiger, N. and Franz, T. (1995). *VISUAL MODFLOW, The Integrated Modelling Environment for MODFLOW and MODPATH, Version 1.1*. Waterloo Hydrogeologic, Ontario, Canada.

Inyang, H. I., and Tumay, M.T. (1995). "Containment Systems for Contaminants in the Subsurface", Chapter 5 in Encyclopedia of Environmental Control Technology, Gulf Publishing, Houston, TX, pp. 175-215.

Isaaks, E.H., and Srivastava, R.M. (1989). *Applied Geostatistics*, Oxford University Press, New York, 561 pp.

Jaynes, E.T. (1957). *Papers on Probability, Statistics and Statistical Physics*, Ed. R.D. Rosenkrantz, Kluwer, Boston..

Johnson, M.W. (1992). "The Information Content of Continuous Functions and the Geodesic Principle," Rutherford Appleton Laboratory, Science and Engineering Research Council, Chilton, England, RAL-92-042.

Koerner, R.M. and Lord, A.E. (1985). "Microwave System for Locating Faults in Hazardous Material Dikes," U.S. Environmental Protection Agency, Hazardous Waste Engineering Research Laboratory, Cincinnati, OH, EPA/600/2-85/014.

Krstanovic, P.F. and Singh, V.P. (1992). "Evaluation of rainfall networks using entropy: I. Theoretical Development," Wat. Res. Man., 6:279-293.

LaGrega, M., Buchingham, P. and Evans, J. (1994). *Hazardous Waste Management* McGraw-Hill New York..

Leopold, L.B. and Langbein, W.B. (1962). "The Concept of Entropy in Landscape Evolution," U.S. Geological Survey Professional Paper 500-a, U.S. Printing Office, Washington, D.C.

Ling, K., (1995b). *Windows Development and Detection in Soil-Bentonite Cutoff Walls*, Ph.D. Dissertation, University of Cincinnati.

McDonald, M.G., and Harbuagh, A.W. (1988). "A Modular Three-Dimensional Finite-Difference Ground-Water Flow Model (MODFLOW)," U.S. Geological Survey Techniques of Water-Resources Investigation, Book 6, Chapter A1.

Mott, H.V., and Weber, W.J., Jr. (1991). "Diffusion of organic contaminants through soil-bentonite cut-off barriers," *Res. J. Water Pollut. Control Fed.*, 63:166-176.

National Research Council (1994). *Alternatives To Ground Water Cleanup*, National Academy Press, Washington, D.C., 315 pp.

Papoulis, A., 1984. *Probability, Random Variables and Stochastic Processes*, McGraw-Hill, New York, 2nd ed., 500-567 pp.

Ross, R.R. and Beljin, M.S. (1995). "MODRISI: A PC Approach to GIS and Ground-Water Modeling," Proceedings, National Conference on Environmental Problem-Solving with Geographic Information Systems, Cincinnati, OH, September 21-23, 1994. EPA/625/R-95/004.

Ross, R.R. and Beljin, M.S. (1998). "Evaluation of Containment Systems Using Hydraulic Head Data," J. Env. Eng., 124(6): 575-578.

Rumer, R.R., and Ryan, M.E., eds. (1995). *Barrier Containment Technologies For Environmental Remediation Applications*, John Wiley & Sons, New York., 170 pp.

Savinskii, J.D. (1965). *Probability Tables for Locating Elliptical Underground Masses with a Rectangular Grid*, Consultants Bureau, New York, 110 pp.

Shannon, C.E. (1948). "A Mathematical Theory of Communication," The Bell System Technical Journal, 27(3):379.

Shannon, C.E. and Weaver, W. (1964). *The Mathematical Theory of Communication*, University of Illinois Press, Urbana, 1964.

Shih, S.R., Doolittle, J.A., Myhre, D.L. and Schellentrager, G.W. (1986). "Using Radar for Groundwater Investigation," J. Irrig. .Drain. Eng., 112(2):110-118.

Singer, D.A., (1972). "ELIPGRID, a Fortran IV program for calculating the probability of success in locating elliptical targets with square, rectangular and hexagonal grids," Geocon Prog., 4(1):1-16.

Singer, D.A., and Wickman, F.E. (1969). "Probability Tables for Locating Elliptical Targets with Square, Rectangular and Hexagonal Point-Nets," Mineral Sciences Experiment Station Special Publication 1-69, Pennsylvania State University, University Park Pennsylvania, 100 pp.

Tetra Tech (1997). *Evaluation of Subsurface Engineered Barriers at Waste Sites, Volume 1*. Prepared by Tetra Tech EM, Inc., for U.S. Environmental Protection Agency, Office of Solid Waste and Emergency Response, Washington, DC, September 30, 1997.

Thompson, S.K., 1992. *Sampling*. John Wiley & Sons, New York, 343 pp.

Todd, D.K. (1980). *Groundwater Hydrology*. John Wiley & Sons, New York, 560 pp.

U.S. EPA (1984). "Slurry Trench Construction for Pollution Migration Control," Municipal Environmental Research Laboratory, Office of research and Development, Cincinnati, OH, EPA-540/2-84-001.

U.S. EPA (1987). "Construction Quality Control and Post-Construction Performance Verification for the Gilson Road Hazardous Waste Site Cutoff Wall," Hazardous Waste Engineering Research Laboratory, Office of Research and Development, Cincinnati, OH, EPA/600/2-87/065.

U.S. EPA (1994). "Methods for Monitoring Pump-and-Treat Performance," Office of Research and Development, R.S. Kerr Environmental Research Laboratory, Ada, OK, EPA/600/R-94/123.

Vieux, B.E. (1993). "DEM Aggregation and Smoothing Effects on Surface Runoff modeling," J. Comp. Civ. Eng., 7(3):310-338.

Vieux, B.E., Farajalla, N.S. (1994). "Capturing the essential spatial variability in distributed Hydrological Modeling: Hydraulic Roughness," J.Hydrol. Proc., 8(3):221-236.

Woodbury, A.D. and Ulrych, T.J. (1993). "Minimum relative entropy: Forward probabilistic modeling," Wat. Resour. Res., 29(8):2847-2860.

Woodbury, A., Render, F. and Ulrych, T. (1995). "Practical probabilistic ground-water modeling," Ground Water, 33(4):532-538.

IMAGE EVALUATION
TEST TARGET (QA-3)

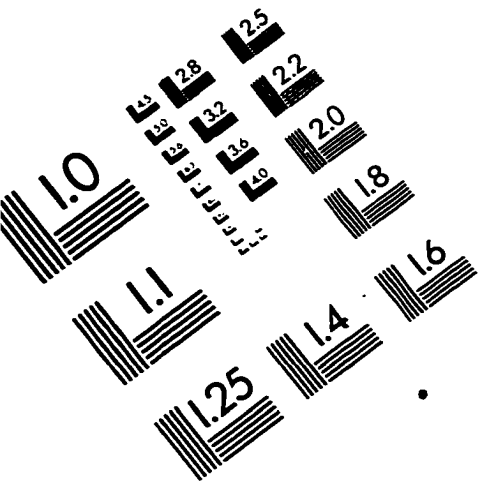

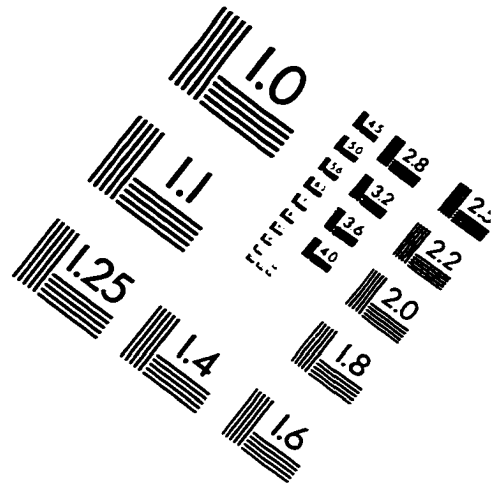

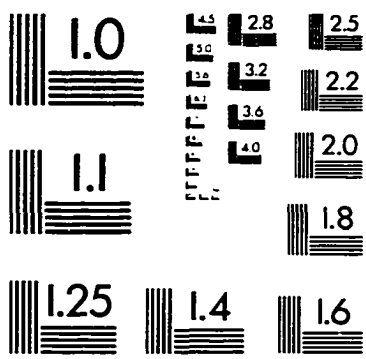

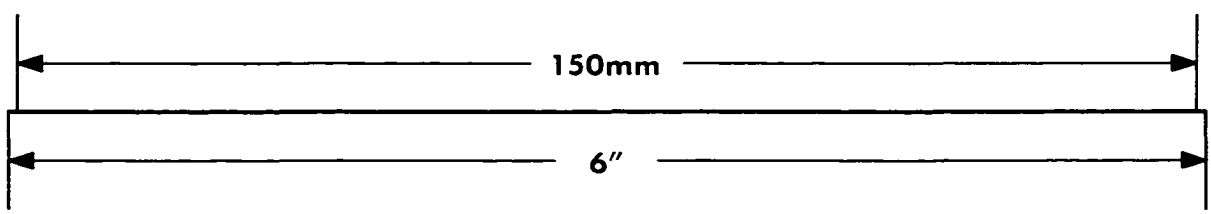

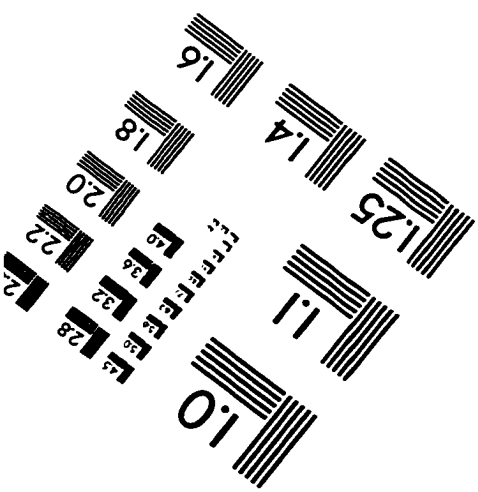

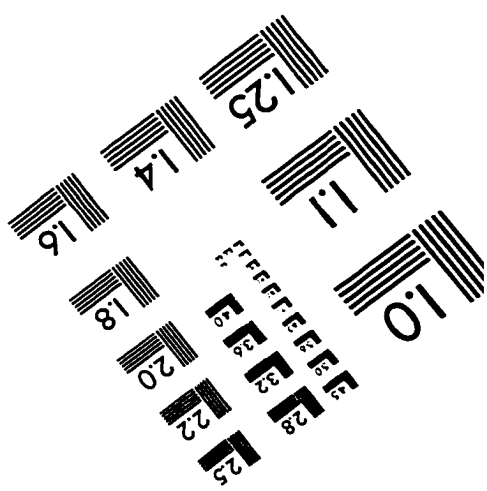

APPLIED IMAGE, Inc
1653 East Main Street
Rochester, NY 14609 USA
Phone: 716/482-0300
Fax: 716/288-5989

© 1993, Applied Image, Inc., All Rights Reserved